For Reference

NOT TO BE TAKEN FROM THIS ROOM

Ex libris
universitatis
albertaensis

BRUCE PEEL SPECIAL COLLECTIONS LIBRARY
University of Alberta

REQUEST FOR DUPLICATION

I wish a photocopy of the thesis by_____

entitled_____

The copy is for the sole purpose of private scholarly or scientific study and research. I will not reproduce, sell or distribute the copy I request, and I will not copy any substantial part of it in my own work without

Address_____

List pages copied_____

Date_____ Signature_____

Name_____

Address_____

List pages copied_____

Date_____ **Signature**_____

Digitized by the Internet Archive
in 2026 with funding from
University of Alberta Library

https://archive.org/details/0162005679616

THE UNIVERSITY OF ALBERTA

RELEASE FORM

NAME OF AUTHOR GILLES RIVARD

TITLE OF THESIS **DOCUMENTATION AND ANALYSIS OF AN ICE JAM, MACKENZIE RIVER AT NORMAN WELLS, N.W.T.**

DEGREE FOR WHICH THESIS WAS PRESENTED MASTER OF SCIENCE

YEAR THIS DEGREE GRANTED SPRING 1985

Permission is hereby granted to THE UNIVERSITY OF ALBERTA LIBRARY to reproduce single copies of this thesis and to lend or sell such copies for private, scholarly or scientific research purposes only.

The author reserves other publication rights, and neither the thesis nor extensive extracts from it may be printed or otherwise reproduced without the author's written permission.

THE UNIVERSITY OF ALBERTA

DOCUMENTATION AND ANALYSIS OF AN ICE JAM, MACKENZIE RIVER AT NORMAN WELLS, N.W.T.

by

© GILLES RIVARD

A THESIS

SUBMITTED TO THE FACULTY OF GRADUATE STUDIES AND RESEARCH

IN PARTIAL FULFILMENT OF THE REQUIREMENTS FOR THE DEGREE

OF MASTER OF SCIENCE

DEPARTMENT OF CIVIL ENGINEERING

EDMONTON, ALBERTA

SPRING 1985

THE UNIVERSITY OF ALBERTA

FACULTY OF GRADUATE STUDIES AND RESEARCH

The undersigned certify that they have read, and recommend to the Faculty of Graduate Studies and Research, for acceptance, a thesis entitled **DOCUMENTATION AND ANALYSIS OF AN ICE JAM, MACKENZIE RIVER AT NORMAN WELLS, N.W.T.** submitted by GILLES RIVARD in partial fulfilment of the requirements for the degree of MASTER OF SCIENCE.

ABSTRACT

Analytical models of the mechanics of ice jams are reviewed. The quantitative assessment of these models is limited by the impossibility of directly measuring the thickness of the accumulation. Different approaches to determine this parameter by indirect methods are presented and discussed critically. Most of these studies have concentrated on the equilibrium reach of the jam without a closer examination of the transition reaches at the head and toe regions region of the jam. The goal of this study was to simulate, using gradually varied flow calculations, the complete water level profile through an ice jam and to investigate the thickness and roughness variation along the jam.

The documentation of the water level profile along an ice jam at Norman Wells on the Mackenzie River, N.W.T., provided the opportunity to assess the analytical models, which describe equilibrium conditions, on a very large river. The analysis was extended to the non-uniform regions upstream and downstream, to evaluate the thickness and roughness variation along and across the jam. This non-uniform flow analysis was accomplished using the backwater model HEC-2. The 'closure' problem caused by the absence of thickness measurements was overcome by estimating the hydraulic roughness of the accumulation independently. By observing the ice jam surface appearance and by assuming that the underside had a similar configuration, a roughness estimate could be determined from backwater simulations as

field evidence suggests that the absolute hydraulic roughness is somewhere between 1 and 3 times the larger roughness projections. The resultant average value of the accumulation parameter μ was 1.6.

In the investigation carried out in the toe region, it was shown that the steep water level increases characteristic of this region could be simulated adequately by regular non-uniform flow calculations and that there was nothing particularly unusual about the toe region in this instance. An important aspect that contributed to the success of the calculations in the toe region was the use of the absolute roughness with the semi-logarithmic expression to describe the flow rather than the usual Manning's equation. When dealing with ice jams, the latter can be very misleading as it is more dependent on the stage and has been found to poorly define the flow against very rough boundaries.

ACKNOWLEDGEMENTS

The author wishes to sincerely thank his supervisor, Dr. R. Gerard, who suggested this research topic and provided valuable guidance, continual support and encouragement throughout the study.

Other individuals contributed willingly of their time and expertise. Mr. Terry Kemp, of Esso Resources Canada Ltd., provided much appreciated help during the field measurement periods as well as welcome discussions at various stages of the investigation. The author would like to express his gratitude to Mr. Darryl Calkins, of USACRREL, who proposed the use of the HEC-2 model with the ice option and agreed kindly to provide a copy of the source program. Also acknowledged is the contribution of Mr. Peter Stagg and Mr. Jim Moir, of Esso Resources Canada Ltd., who assisted with the field documentation and provided valuable discussion on the simulations. Special thanks are finally extended to Mr. Gordon Putz who gave freely his time and field expertise during the summer survey.

Appreciation is expressed to Esso Resources Canada Ltd., the Natural Sciences and Engineering Research Council and the Department of Civil Engineering for providing financial support for this investigation.

Table of Contents

Chapter Page

ABSTRACT iv

ACKNOWLEDGEMENTS vi

List of Tables xi

List of Figures xii

List of Appendices xvi

Nomenclature xvii

1. INTRODUCTION 1

1.1 General 1

1.2 Background to the problem 2

1.2.1 General 2

1.2.2 Classification of ice jams 2

1.2.3 Initiation of ice jams 6

1.2.4 Need for case studies 7

1.3 Purpose and scope 8

2. ICE JAM MECHANICS AND ANALYSIS 10

2.1 General 10

2.2 Composite roughness 11

2.3 Ice jam resistance 13

2.3.1 Status of information 13

2.3.2 Expression for flow resistance of ice jams 14

2.3.3 Field data on ice jam resistance 17

2.4 Ice jam theories 21

2.4.1 General 21

2.4.2 Kennedy (1959) 24

2.4.3 Pariset et al. (1961,1966) 25

2.4.4 Michel (1965, 1971) 30

2.4.5 Uzuner and Kennedy (1976) 31

2.4.6 Beltaos (1983) 33

2.4.7 Calkins (1983) 33

2.4.8 Comparison of theories 35

2.4.9 Limitations of theoretical models 35

2.5 Ice jam analysis 36

2.5.1 General 36

2.5.2 Pariset et al. (1966), Calkins (1983) 38

2.5.3 Beltaos (1978) 38

2.5.4 Michel (1980) 39

2.5.5 Andres (1980) 40

2.5.6 Limitations of past approaches 40

3. BACKGROUND INFORMATION ON THE MACKENZIE RIVER 42

3.1 General description of the Mackenzie River system 42

3.2 Geomorphological features 44

3.3 Discharge 44

3.4 General ice conditions 46

3.5 Past studies of ice conditions 47

3.5.1 General 47

3.5.2 MacKay and MacKay (1960 - 1973) 48

3.5.3 Public Agencies Reports (1977 - 1981) 50

3.5.4 Parkinson (1981, 1982) 52

3.5.5 Kamphuis and Moir (1983) 52

3.5.6 Kemp (1983) 53

3.5.7 Stagg et al (1983) 54

3.6 Field data collection: techniques and results 56

3.6.1 General 56

3.6.2 1983 breakup 57

3.6.3 Summer 1983 survey 72

3.6.4 1984 breakup 78

4. CASE STUDY: ICE JAM AT NORMAN WELLS 85

4.1 Method 85

4.1.1 General 85

4.1.2 HEC-2 model 86

4.2 Open water calibration 89

4.2.1 Background 89

4.2.2 HEC-2 simulation 90

4.3 Ice jam analysis 95

4.3.1 General background 95

4.3.2 Discharge estimation 97

4.3.3 Constant thickness simulations 102

4.3.4 Equilibrium thickness and internal friction coefficient 108

4.3.5 Longitudinal variation of ice jam thickness 111

4.3.6 Special conditions at ice jam toe 113

4.4 Discussion of 1983 ice jam analysis 122

4.4.1 Final ice jam simulation 122

4.4.2 Effect of discharge 122

4.4.3 Internal friction coefficient, equilibrium thickness, and stage 129

4.4.4 Thickness and roughness variation along and across the jam 135

4.4.5 Limitations of analysis 137

4.5 General implications for analysis of ice jams at Norman Wells 140

5. CONCLUSIONS 144

6. RECOMMENDATIONS 146

List of references 148

APPENDIX A 156

APPENDIX B 160

APPENDIX C 162

APPENDIX D 166

APPENDIX E 170

APPENDIX F 175

APPENDIX G 179

List of Tables

Table	Description	page
1.	Relation between roughness and thickness for ice accumulations at freeze-up (Nezhikhovskyi, 1964)	18
2.	Peak water levels at Norman Wells, 1973-1983 (Stagg et al., 1983)	55
3.	Summary of HEC-2 simulations for Q = 12 000 m^3/s (constant thickness)	105
4.	Computed variation of Manning's "n" in the toe region	119
5.	Summary of HEC-2 simulations for Q = 14 700 m^3/s (constant thickness)	127
6.	Computed values of μ for a Q = 14 700 m^3/s	126
7.	Computed hydraulic parameters in equilibrium reach (Q = 12 000 m/s)	134

APPENDIX TABLES

A-1	Summary of aerial observations, 1983 breakup	157
B-1	Bench mark locations and open water profile between Fort Norman (km 828) and km 935	161
C-1	1983 ice jam water profile	163
D-1	Summary of aerial observations, 1984 breakup	167

List of Figures

Figure	Description	page
1.	Effect of an ice cover on the hydraulic radius for a wide channel	10
2.	Flow in a wide ice-covered channel	12
3.	Variation of $n/R^{1/6}$ in open channels (Beltaos, 1979)	16
4.	Comparison of freeze-up roughness measurements (Gerard and Andres, 1981)	20
5.	Evolution of fragmented ice covers (Uzuner and Kennedy, 1974)	22
6.	Schematic illustration of an equilibrium ice jam (Beltaos, 1983)	23
7.	Dimensionless ice jam stability diagram (Pariset et al., 1966)	28
8.	Dimensionless ice jam stability diagram (Michel, 1966)	29
9.	Dimensionless depth versus dimensionless discharge for floating breakup jams (Beltaos, 1983)	34
10.	Location map for the Mackenzie River	43
11.	Longitudinal profile for Mackenzie River system	45
12.	Dates of break-up and freeze-up for Mackenzie River (Allen, 1977)	51

Figure	Description	page
13.	Break-up progression, 1983.....	59
14.	General view of 1983 ice jam at Fort Norman	60
15.	General view of the ice jam at Norman Wells, May 23 1983.....	61
16.	Close-up view of the toe region of the ice jam at Norman Wells, May 23, 1983.....	62
17.	Surface appearance of running ice pack just after ice jam failure at Fort Norman, May 23, 1983.....	66
18.	Ice conditions at Norman Wells after ice movement, as observed from the ground, May 23 1983.....	67
19.	Typical ice sheet composition, Norman Wells, May 23 1983.....	68
20.	Temporary bench mark locations, Norman Wells.....	70
21.	Thawing degree-days and water levels during breakup, Norman Wells, 1983.....	71
22.	Open water and 1983 ice jam profiles.....	75
23.	Aerial view of the ice conditions at Norman Wells, May 23 1983.....	76
24.	Aerial view of the ice conditions at Norman Wells, May 23 1983.....	77
25.	Breakup progression, 1984.....	81

Figure Description page

26. General view of the 1984 ice jam at Old Fort Point (km 770)..... 82

27. General view of the 1984 ice jam at Fort Norman..... 83

28. Thawing degree-days and water levels during break-up, Norman Wells, 1984..... 84

29. Cross-section locations between Fort Norman (km 828) and km 935..... 92

30. Comparison of measured cross-section and cross-section obtained from the hydrographic charts (km 904)..... 93

31. HEC-2 model: open water calibration..... 94

32. General ice conditions during the 1983 ice jam and river bed data..... 96

33. Open water, rising stage and falling stage rating curves at Norman Wells.....100

34. Intact ice sheet roughness.....101

35. Toe conditions for the 1983 ice jam at Norman Wells.106

36. View of ice accumulation in equilibrium reach.....107

37. Variation of μ along the 1983 ice jam in the Norman Wells area.....110

38. Computed ice thickness profile for the 1983 ice jam 114

Figure Description page

39. Bathymetry of the Mackenzie River in the Norman Wells area..... 115

40. Variation of hydraulic roughness with the thickness at the toe..... 121

41. Complete simulated water profile for the ice jam at Norman Wells..... 123

42. Complete simulated ice thickness profile for the ice jam at Norman Wells.....124

43. Effect of discharge on water levels at Norman Wells.....128

44. Probability distribution of peak water levels at Norman Wells, 1973-1983 (Stagg et al., 1983).....143

APPENDIX FIGURES

E-1 Typical cross-sections.....171

F-1 Cross-section downstream of the ice jam at km 935.5 178

G-1 Simulation of ice conditions before the ice jam release at Fort Norman.....188

Nomenclature

A = cross-sectional area (m^2);

B = channel width (m);

b = suffix denoting parameters pertaining to the river bed;

C_o = (dimensionless) shear strength coefficient;

C_i = cohesion of an ice jam;

d = uniform sand grain roughness elements;

e = ice jam porosity;

f = friction factor;

g = acceleration of gravity (m/s^2);

H = water stage (m);

h_j = depth of flow under a jam (m);

i = suffix denoting parameters pertaining to an ice jam;

K = (dimensionless) compressive strength coefficient;

k = absolute hydraulic roughness (m);

n = Manning roughness coefficient;

o = suffix denoting composite roughness flow parameters;

Q = flow discharge (m^3/s);

q = unit discharge (m^2/s);

R = hydraulic radius (m);

S = channel slope;

s_i = specific gravity of ice;

t = ice jam thickness (m);

V = average flow velocity (m/s);

Δ = equivalent diameter of larger roughness projection;

η = (dimensionless) jam depth;

ϕ = angle of internal friction;

μ = (dimensionless) coefficient depending on the angle of internal friction and porosity;

ξ = dimensionless flow discharge;

ρ, ρ_i = densities of water and ice;

σ_x = normal stress in downstream direction;

σ_z = normal stress perpendicular to the water surface;

τ_i = fluid shear stresses on ice jam (Pa);

1. INTRODUCTION

1.1 General

In cold regions, ice jams are an important aspect of river engineering because they can cause unusually high water levels due to both the restriction of the flow area by the ice accumulation and the increased resistance to flow. Ice jams can also cause operational problems for river structures and be a major concern for hydro-power installations. Another problem is interference with navigation by the formation of a large ice jam. This is well illustrated by the St. Clair River between Lake Huron and Lake St. Clair in southern Ontario. The river is used intensively as a navigation waterway and when an ice jam forced the closure of the route in the spring of 1984, approximately $1.5 million were estimated to be lost each day by the shipping industry.

Probably the most apparent consequence of ice jams is the property damage caused by high water levels. According to a U.S. Army Corps of Engineers survey quoted by Uzuner and Kennedy (1976), the reported average annual loss due to ice jams in the United States was $16.6 million for the period between 1963 and 1973. In Canada, Atkinson (1973) placed the average annual loss at $10 million. It is evident that much can be gained from systematic research to enhance our understanding of ice jam behaviour.

1.2 Background to the problem

1.2.1 General

An ice jam is a complex phenomenon. Anyone who has witnessed the formation, the evolution and the sometimes disastrous consequences of a major ice jam can but agree with Uzuner and Kennedy (1976) when they remarked that "large natural ice jams are, at best, chaotic, disordely, untidy affairs". Nevertheless, engineers and researchers have, over the years, developed some theoretical models and gathered field measurements to validate these models. Despite the complexity of the problem, the information accumulated in the literature can at least be used to evaluate the global or general features of an ice jam. This may be sufficient in practical applications.

The salient features of ice jams, as they are presently understood, are discussed in the following and the contributions of past work to this understanding briefly reviewed. A good summary of the research prior to 1968 can be found in a comprehensive literature review compiled by Bolsenga (1968). In a more recent paper, Beltaos (1983) reevaluated the past work and analysed recent field measurements.

1.2.2 Classification of ice jams

Ice jams can be classified according to several characteristic features. The following summarizes briefly

the most common criteria.

Season. Ice jams characteristics and significance are different according to the season in which they form.

(i) Freeze-up jams. These jams are generally less severe in consequence than at spring as breakup discharges are usually much larger than the ones prevailing during freeze-up. They are usually initiated when frazil (or pancake ice) is stopped at a location where the open water width is restricted by border ice and the concentration of frazil ice is beyond a critical limit.

(ii) Winter jams. Ice jams can form due to a warm spell during the winter season. An important feature of these jams is that they can refreeze in place and produce a greater obstruction for the subsequent spring breakup.

(iii) Breakup jams. This is usually the most common type of ice jam and the one that can cause the most serious damage due to its sudden and dramatic nature. Consequently, most of the available literature on ice jams deals with spring ice jams. It is usually assumed that these ice jams are not significantly affected by cohesion.

Vertical extent. Ice jams have been further classified according to the portion of the waterway they occupy (Barnes, 1928).

(i) Floating (or simple) jams. Theoretical work accumulated

to date on ice jams has concentrated on this type of jam in which the ice obstructs a definite portion of the waterway but still permits unobstructed flow beneath it. Flow through the voids is usually neglected.

(ii) Grounded jams. As the name implies, a grounded jam blocks a large portion of the waterway as the ice accumulation extends to the stream bed over a considerable portion of the width at the toe of the jam. Much of the flow in this situation is then of the seepage type as it must pass through the voids. Therefore, "resistance" to flow must be defined in terms of the permeability of the accumulation, which is different from the resistance caused by tangential forces due to flow past a boundary. Although grounded jams seem to be less common, they may be produced by the dynamic release of a floating jam and the subsequent sudden stoppage of the surge of ice and water against a natural or man-made obstacle. Barnes (1928) and Frankenstein and Assur (1972) reported on two ice jams on the Allegheny and Israel Rivers respectively that were known to be grounded. The information provided is, however, only qualitative and as pointed out by many investigators, virtually nothing is known quantitatively about grounded jams. As Michel (1971) states, "it has been impossible to determine losses in a general manner because of the seemingly fortuitous length of grounding in each case and the variable solidarity of the accumulation of the floes".

Evolving and "steady-state" jams. Although ice jams formation is an unsteady phenomena, very little is known about the transient aspects of ice jams, i.e. the factors affecting their initiation, evolution, and release. Research to date has concentrated on the description of the jam which has attained a "quasi-steady" state.

"Narrow" and "wide" channel jams. Although the terms "narrow" and "wide" channel jams will be discussed in more detail in a subsequent section, they are included here as they have become an essential feature to characterize an ice jam. The terms were first proposed by Pariset et al. (1966) to distinguish between two different modes of ice jam formation. In a "narrow" channel jam, the thickness of the accumulation is governed by the hydraulic constraint at the upstream edge. If velocity at this location is low enough, simple accumulation of a single layer of incoming ice floes will result and the accumulation will progress in the upstream direction. If the velocity is beyond a certain limit, the ice floes will be entrained and moved under the cover until sufficient backwater is created to lower the velocity under the critical limit. The cover will then again progress in the upstream direction. On the other hand, in the "wide" channel case, the thickness will be the result of structural adjustments (shoving) of the cover. This is the only way for the jam to increase its strength to compensate for the downstream thrust which, in this case, increases with distance in the downstream direction. The ice jam

studied herein is of the "wide" channel floating type.

1.2.3 Initiation of ice jams

Although the determining factors for a jam formation at a given location have yet to be expressed in a quantitative way (Frankenstein and Assur, 1972), a number of qualitative observations over the years have allowed the main parameters influencing the initiation of an ice jam to be isolated. They can be divided into two categories: physical obstructions or specific hydraulic features.

Obviously, the morphology of a river at a given location will often be the main factor governing the initiation of an ice jam. Islands, bars, shoals and pronounced bends are some morphological features which can act as a physical obstruction to the passage of ice. A common obstruction is the intact ice sheet. The mainstream ice cover is a frequent cause of ice jamming at the mouth of tributaries. Finally, man-made obstructions like bridge piers can facilitate the formation of ice jams.

Ice jams can also form at locations where specific hydraulic characteristics are met. Locations where the slope changes from steep to flat are prone to ice jamming. Headwater of reservoirs have also been shown to be a common place for ice jams (Donchenko, 1975).

1.2.4 Need for case studies

Theoretical models describing the hydromechanics of floating ice jams have been developed since the early 1960's. Pariset et al. (1961,1966) were among the first investigators in North America to formulate theoretically the problem of a floating ice jam. For a "wide" channel ice jam, which is the type of jam analysed in the present study, they developed an equation which relates the forces acting (mainly the shear force of the flow underneath the ice cover and the ice jam weight component in the direction of flow) and the resisting forces (the shear at the banks, which is a function of the accumulation thickness and the friction developed between the ice floes). When, after successive collapses the ice jam reaches a stable or "static" condition, i.e. when the resisting forces counteract the acting forces, the corresponding thickness is referred to as the equilibrium thickness. If a jam is long enough, it can contain an "equilibrium" reach along which the jam thickness and flow depth are approximately uniform. From uniform flow, the energy slope line in that reach should then be approximately parallel to the open water surface slope. The internal strength of the accumulation, which significantly affects the resulting equilibrium thickness, is described by a coefficient, μ, which must be quantified empirically, from field and laboratory experiments.

Although the above cited theory provides an analytical framework to study ice jams, few prototype verifications of

the model have been reported. This is mainly due to the difficulties in obtaining pertinent data during breakup and, more specifically, to the impossibilty to this day of adequately measuring either the thickness or the roughness of an ice jam. A supplementary assumption has therefore to be made to get an estimate of the thickness to perform the analysis. Hence, there is a need for systematic field measurements to assess the validity of the various assumptions involved in the application of the theory.

1.3 Purpose and scope

The purpose of this study was to document in situ the characteristics of an ice jam and, as previous studies have considered only the uniform flow equilibrium section, to investigate whether the complete measured water profile could be simulated using standard gradually varied flow calculations coupled with the available theory describing the mechanics of ice jams. In 1983 an ice jam was documented on the Mackenzie River in the Norman Wells area. This provided the opportunity to test the applicability of the ice jam theory on an unusually large river.

The study consisted of collecting and reviewing the available literature, planning and conducting the field investigations, and analysing the documented ice jam. Although emphasis in the study was put on the analysis of the "static" ice jam condition, information on the surge created by the release of an ice jam was documented. It is

presented in appendix G. Breakup was also monitored in 1984 but no significant ice jams formed in the reach of interest.

2. ICE JAM MECHANICS AND ANALYSIS

2.1 General

From a hydraulic point of view, the addition of an ice cover on a river almost doubles the wetted perimeter as shown in Figure 1. For a wide channel, the hydraulic radius will therefore be approximately half what it is for an open channel of the same depth.

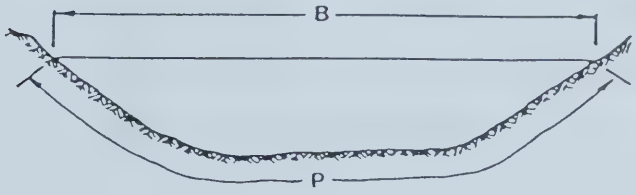

Open water $R = A/P \cong A/B$

Ice-covered $R = A/(P + B) \cong A/2B$

Figure 1. Effect of an ice cover on the hydraulic radius for a wide channel.

Hence, for the same discharge, the water level in an ice-covered river will be higher than under open water conditions for two reasons:

(i) ice floats with approximately 0.92 of its thickness submerged (0.92 being the specific gravity of ice) so that this depth of flow is removed from the waterway area, and

(ii) the water is flowing against another solid boundary, which provides additional resistance to the flow.

For an ice jam condition, these two factors can dramatically affect the water level because an ice jam is usually much thicker and rougher than the normal ice cover.

The following sections will consider the available information on the composite roughness of an ice-covered river and on ice jam hydraulic resistance, parameters that are very important in ice jam analysis.

2.2 Composite roughness

The flow under an ice cover in a wide channel is analogous to flow between two parallel plates having different roughnesses. The resistance coefficients (such as n or f) or the hydraulic roughness k must therefore reflect the overall or composite roughness obtained by combining the roughness of the ice cover with that of the river bed. The situation in a wide channel will then be as is illustrated in Figure 2.

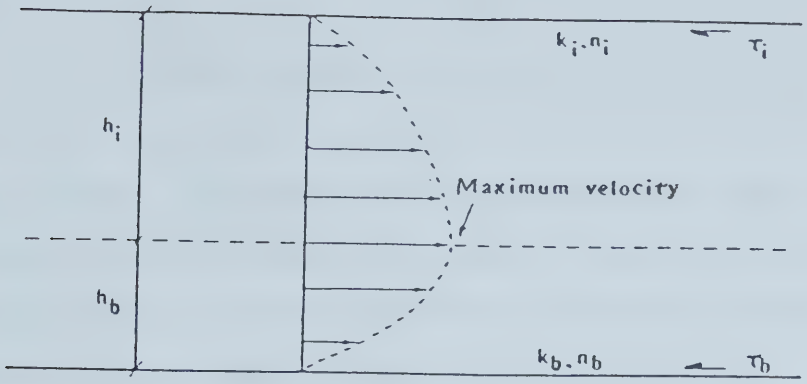

Figure 2. Flow in a wide channel

Uzuner (1975) presented a comprehensive literature review of the composite roughness of ice-covered streams and recommended the use of Larsen's (1969) or Hancu's (see Uzuner, 1975) methods because of their rigour. Larsen's analysis considers two-dimensional flow and shows n_o to depend on n_i, n_b and the ratio h_i/h_b. The latter ratio was found by Larsen to depend on n_i, n_b and the respective relative roughnesses. In practice, much use has been made of the simple Sabaneev equation (see Michel, 1971):

$$n_o = ((n_b^{1.5} + n_i^{1.5})/2)^{2/3}) \qquad (1)$$

The above equation can be derived if it is assumed that the average velocity in the regions associated to each

boundary are approximately equal. Furthermore, this assumption implies that:

$$R_b/R_i = (n_b/n_i)^{3/2} \quad (2)$$

Beltaos (1983) discussed the above assumption and reported that examination of field data showed V_i and V_b to be within 10 percent of each other. Tatinclaux and Gogus (1983), using the point of zero shear rather than the point of maximum velocity to approach the problem, found that the predicted ice jam characteristics for a case study showed a variation of 10 percent. Beltaos (1979) used the above equations but stressed the fact that jams often act as "extremely rough" boundaries and that these two equations might not be valid.

2.3 Ice jam resistance

2.3.1 Status of information

There is very little experimental information on ice jam resistance, especially under natural conditions, due to the obvious difficulties in collecting the data. Moreover, there have been questions raised recently regarding the applicability to ice jams of the ice cover resistance data compiled by Nezhikhoskiy (1964). On the other hand, as the flow under fragmented ice covers is frequently of the "extreme" roughness type, a theoretical approach to the problem must also be used with caution as the detailed fluid

mechanics of that type of flow have not yet been fully investigated.

2.3.2 Expression for flow resistance of ice jams

There are many different flow resistance equations that have been used when dealing with rivers and, more specifically, with ice-covered streams. They are:

Chezy $V = C\, R^{1/2}\, S^{1/2}$ (3)

Manning $V = (R^{2/3} S^{1/2})/\, n \quad (SI)$ (4)

Darcy-Weissbach $V = (8g/f)^{1/2}\, R^{1/2} S^{1/2}$ (5)

Power law $V/V_* = 8.0\, (R/k)^{1/6}$ (6)

Semi-log law $V/V_* = 2.5 \ln (R/k) + 6.2$ (7)

where V is the average velocity (Q/A), C is the Chezy coefficient, R the hydraulic radius (A/P), S the slope of the energy line, n the Manning coefficient, f the Darcy-Weissbach friction factor, V_* the average shear velocity over the section boundary ($\sqrt{gRS}$), and k the average boundary hydraulic roughness.

Although the tradition in river hydraulics has been to use the Manning's 'n' coefficient to express the flow resistance, it is well known that this parameter has some

limitations. Ice jamming conditions usually produce a situation where 'n' cannot be assumed to be independent of the flow. First of all, although jam stages are generally high, a large portion of the water depth is due to the accumulation thickness so that the depth of flow under the accumulation is shallow enough to make 'n' strongly stage-dependent. Moreover, unlike for an open channel, there is no accrued experience to assist in judging appropriate values of 'n' in this situation. In fact, the only actual field data on 'n' values that could be relevant to ice jam roughnesses are the ones reported by Nezhikhovskyi (1964).

In view of the foregoing discussion, it seems preferable to deal with ice jam hydraulic resistance by using a relation involving a resistance parameter that is more independent of the flow and that has some background in field and laboratory validations. Such a relation is the standard semi-logarithmic expression, Eq. 7.

In order to establish a relationship between n and the measured bed roughness in natural streams, Limerinos (1970) compiled the results of several field studies and computed the quantity $n/R^{1/6}$ for many different streams. Plotting this parameter versus R/d_{84}, d_{84} being the intermediate particle diameter that is not exceeded by 84 % of the streambed particles, he found that the resulting regression equation was

$$n/R^{1/6} = 0.129/\ln(4R/d_{84}) \qquad (8)$$

Now, by comparing the Manning expression with the semi-log equation, it can be shown that

$$n/R^{1/6} = 0.128\ (\ln\ (12R/k)) \qquad (9)$$

which indicates that the equivalent sand roughness k is equal to $3d_{84}$ for non-uniform roughness elements. For uniform sand grain roughness elements, k = d by definition. Therefore, this would suggest that $\Delta < k < 3\Delta$ where Δ is the equivalent diameter of the larger projections. As shown in Figure 3, taken from Beltaos (1979), the equation proposed by Limerinos provides a reasonable fit down to about R/d_{84} = 0.45, or $R/k \cong 0,15$.

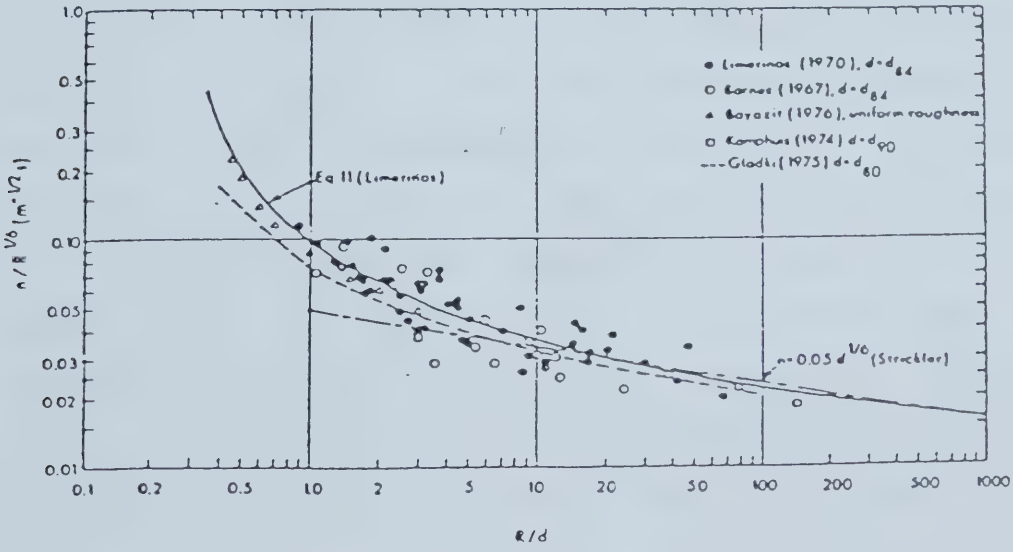

Figure 3. Variation of $n/R^{1/6}$ with R/d in open channels (after Beltaos, 1979).

As pointed out by Gerard (1984), the use of the semi-log equation when dealing with ice jams has some

obvious advantages. The first one is that the equation has been shown by Limerinos to provide good estimates for low values of R/k. Secondly, from a practical point of view, the use of k enables an observer to evaluate the hydraulic roughness of a surface directly as the parameter has a simple, direct and easily visualized relation to the size of the boundary roughness elements. Reasonable bounds on k can therefore be estimated without the need for considerable experience.

2.3.3 Field data on ice jam resistance

There is very little information in the literature regarding field measurements of the roughness coefficient for the underside of floating ice jams. The data compiled by Nezhikhovskyi (1964) is the only comprehensive account of relevant field data. Computations of ice cover resistance were made from hydrological data obtained in the U.S.S.R. for the period 1936-1959. Nezhikhovskyi classified his results, shown in Table 1, into three general types of accumulation and found a relationship between the thickness of the accumulation and its roughness. The data for ice floes are thought to be the most relevant to ice jams.

Thickness of accumulation (m)	Type of accumulation		
	Loose Slush	Dense Slush	Ice Floes
0.1	-	-	0.015
0.3	0.010	0.013	0.04
0.5	0.01	0.02	0.05
0.7	0.02	0.03	0.06
1.0	0.03	0.04	0.07
1.5	0.04	0.06	0.08
2.0	0.04	0.07	0.09
3.0	0.05	0.08	0.10
5.0	0.06	0.09	-

Table 1. Values of n_i for ice accumulations at the beginning of freeze-up (after Nezhikhovskyi, 1964).

There are many reasons why Nezhikhovskyi's data is not very appropriate for an ice jam analysis. First, the data were collected mainly during freeze-up with very few points at breakup and may therefore not be directly applicable to spring ice jams. Secondly, the simple relation between the thickness of an accumulation and its roughness has to be taken with reserve. As pointed out by Michel (1980), "the ice grown by thermal exchange for thin ice cover is always smooth at the interface whereas the covers made by packing of slush as well as ice jams are much rougher and correspond to thicker covers." Therefore, on the average, thick covers will tend to be rougher than thin ones and any "curve smoothing of data will produce a relation where roughness increases with thickness". In fact, the hydraulic roughness should depend more on the size and character of the ice floes than on the accumulation thickness. Nezhikhovskyi's

data is also presented in terms of Manning 'n'. As discussed earlier, this parameter is very sensitive to the flow depth and may in fact be dramatically affected in range of R/k (generally lower than 3) produced by an ice jam. Nezhikhovskyi gives little information about the range of R_i. Finally, values of 'n' were deduced from the hydraulic geometry of only one section, whereas, as even Nezhikhovskyi remarked, "it should have been determined (from) the average area for the entire reach between slope stations". The above discussion therefore suggests that Nezhikhovskyi's data has severe limitations and that it should only be used to give a broad indication of magnitude for ice cover roughnesses.

Pariset et al. (1966) showed that 'n_i' for the St-Lawrence River was in the range 0.05 - 0.06 at the formation stage of the ice cover and between 0.033 - 0.043 during the later stage of a later cover. Finally, Gerard and Andres (1982) reported on roughness measurements carried out during the freeze up period. Figure 4 taken from their paper presents the results. They concluded "that the roughness of freeze-up accumulations is best estimated from the expected pan size and state of the accumulation, rather than from generalized trends with accumulation thickness. Further, power-law average velocity relations should be used with caution in situations with such low R/k values".

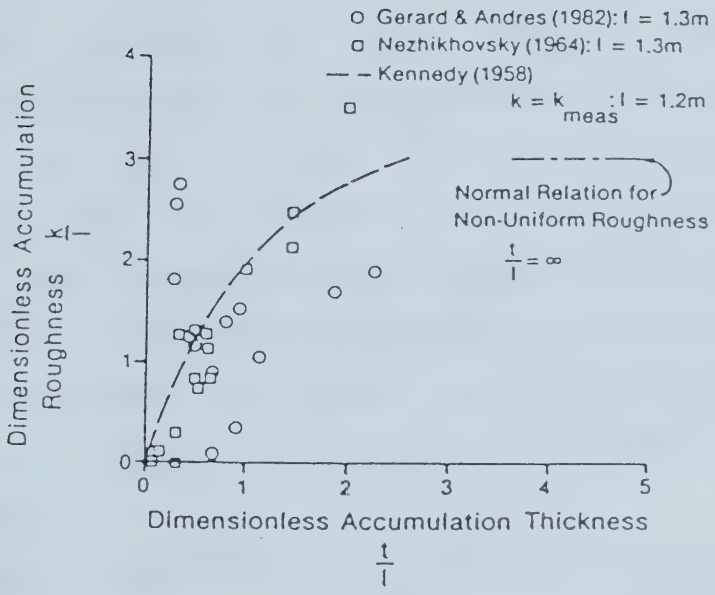

Figure 4. Comparison of freeze-up roughness measurements (Gerard and Andres, 1981).

2.4 Ice jam theories

2.4.1 General

Figure 5, reproduced from Uzuner and Kennedy (1974), gives a schematic summary of the evolution of fragmented ice covers. The mode of formation noted "A", characterized by a high velocity, is probably the one most common for ice jams forming at breakup. As noted earlier, research has concentrated over the years on the problem of equilibrium jams, i.e. jams that no longer evolve. Theoretical work has resulted in a model for floating ice jams in equilibrium that has been tested with some success. As pointed out by Beltaos (1983), this "has considerable practical merit since it can be argued that, under certain circumstances, the highest water stages occur when a jam has attained equilibrium."

Figure 6, reproduced from Beltaos (1983), provides a schematic illustration of an equilibrium jam. There are typically three regions within the length of such a jam:

(i) **Upstream transition:** For a certain distance below the head of the jam, the thickness increases and approaches an asymptotic value.

(ii) **Equilibrium thickness reach:** In this portion, the flow under the jam can be considered uniform The thickness of the jam stays relatively constant

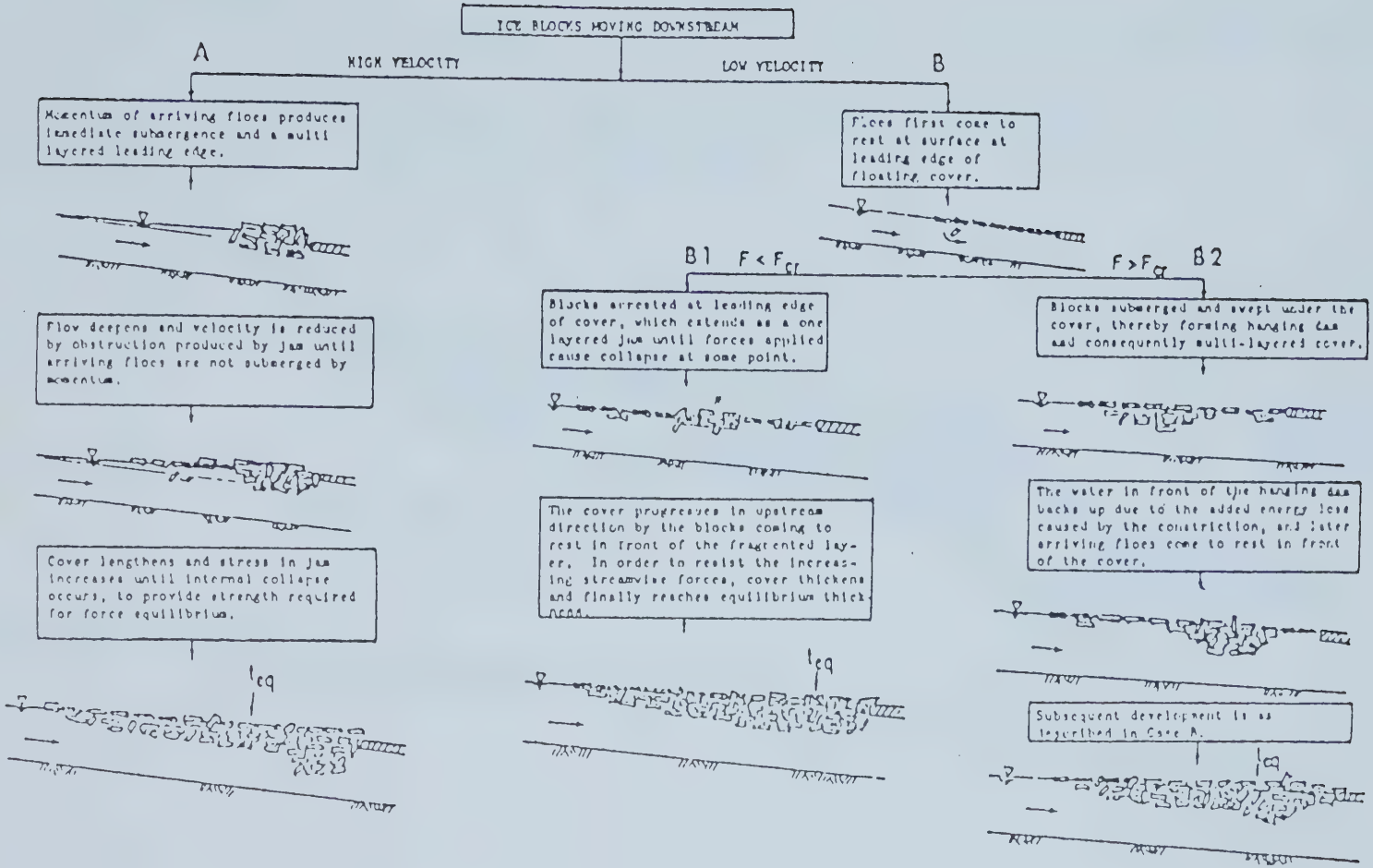

Figure 5. Evolution of fragmented ice covers (Uzuner and Kennedy, 1974)

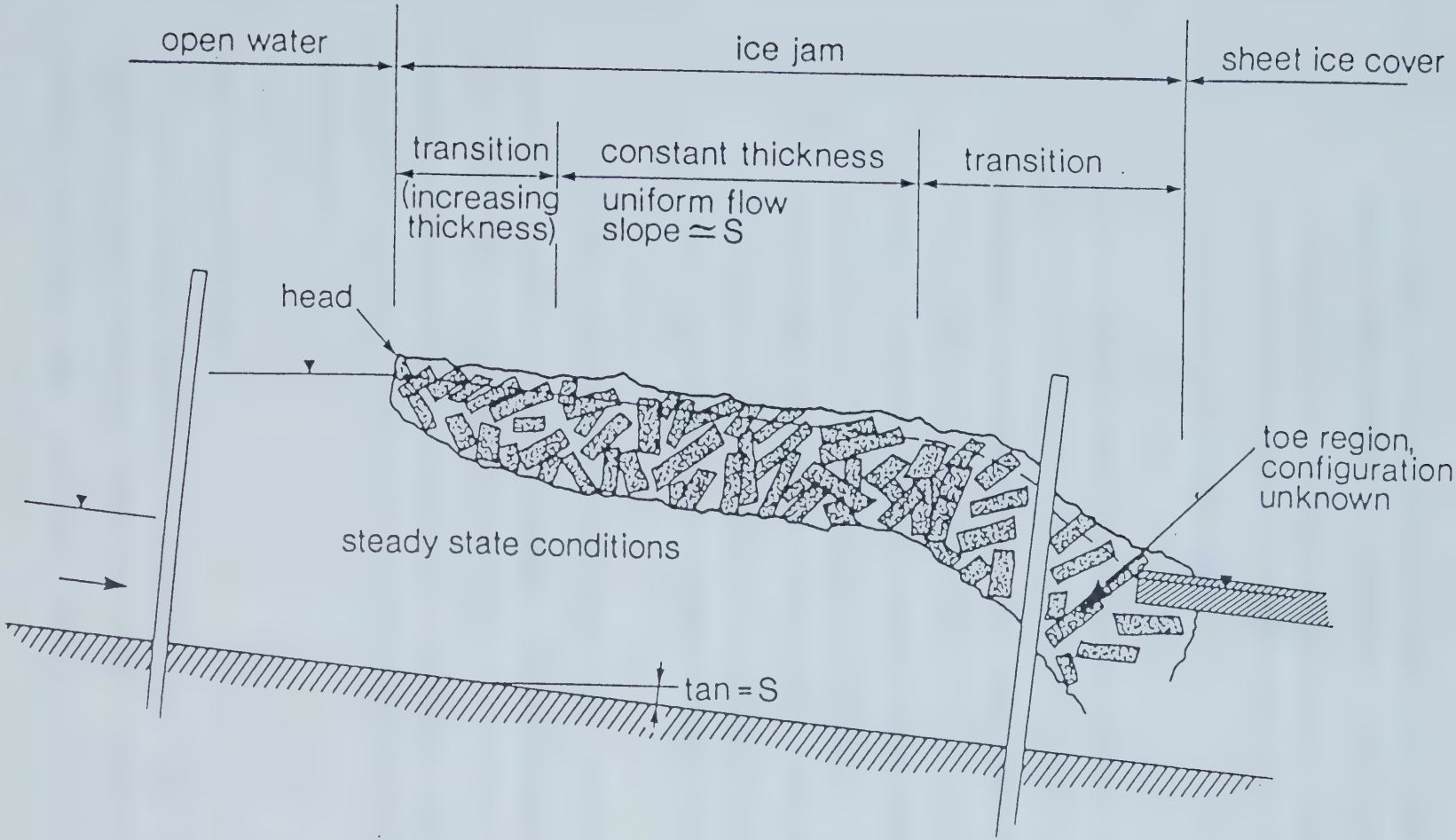

Figure 6. Schematic illustration of an equilibrium ice jam (Beltaos, 1983).

and approximately equal to what has been called the "equilibrium" thickness. As pointed out previously, theoretical models have concentrated in deriving equations to calculate this thickness, using force balance analysis.

(iii) **Downstream transition:** Finally, below the equilibrium reach, the water surface profile steepens progressively to meet the lower water stage prevailing at the toe. The shape of the water surface in this region roughly approximates an M2 curve. It is however difficult to assess precisely what occurs at the toe: the flow configuration could vary in each case depending on local conditions and on mode of jam initiation.

Existing ice jam theories have been reviewed by a number of authors (see Bolsenga, 1968; Beltaos, 1983). A brief overview of the most significant theories is given below to put each one in perpective. The final sections will present a comparison of the theories and discuss their limitations.

2.4.2 Kennedy (1959)

The earliest quantitative treatment of jams is the one reported by R.J. Kennedy (1959) and deals with the forces exerted by log jams. Kennedy based his analysis on "the

analogy between pulpwood in a river and granular material contained between two parallel walls". He also noted that "it was subsequently discovered that Janssen had developed the same relation in connection with the design of grain elevators". Using a force balance analysis, Kennedy derived an expression for the force equilibrium of the jam. As pointed out later by Uzuner and Kennedy (1976), the early analysis had two major shortcomings. Firstly, the streamwise component of the aggregate weight of the jam was neglected and it was implicitly assumed that the thickness is independent of the distance and that the flow depth under the jam is constant. The other debatable point is that he assumed a boundary condition at the head of the jam (upstream end, at $x = 0$) of $T = 0$ (T being the upstream force acting on the accumulation).

2.4.3 Pariset et al. (1961,1966)

In a series of papers during the early 60's, Pariset and others built upon Kennedy's approach to develop a more comprehensive theory. The streamwise component of the jam weight was accounted for but the jam thickness was again assumed to be independent of the distance. The upstream boundary condition was generalized by putting $T = T_o$ at $x = 0$ (the upstream end of the jam). The resistance to shear at the sides of the jam was assumed to consist of a cohesive term and a frictional term.

As discussed earlier, an important contribution was the distinction between what Pariset et al. (1966) called "narrow" and "wide" channels. In the so-called "narrow" channel, the thickness of the ice jam is governed by the hydro-dynamic constraint at the upstream edge. Many authors have subsequently derived different equations describing the hydraulic conditions at the edge which could be used to assess if a floe coming to rest at this location will be entrained underneath the cover or not. Ashton (1978) gives a review of the relevant studies for this type of ice jam formation. Beltaos (1975) pointed out that of ice jams at breakup rarely form according to the hydraulic constraint. They are rather of the "wide" type as the thickness of the accumulation is governed by a structural constraint. The jam will shove and thicken as it lengthens so that it can sustain the additional load to be transferred. By increasing its thickness, the accumulation will be provided with additional shear at the banks so that the drag added by an advance of the front can be compensated.

This "equilibrium" thickness is given by (Pariset et al., 1966):

$$\mu \rho_i (1 - s_i) g t^2 - (g\rho_i S - 2C_i/B)B \; t - \tau_i B = 0 \qquad (10)$$

where μ is a dimensionless parameter reflecting the internal friction and porosity of the accumulation, s_i is the specific gravity of the ice, t is the equilibrium thickness,

ρ_i is the ice density (usually taken as 0.92), S is the channel slope, C_i is a cohesion parameter, B is the channel width at the bottom of the accumulation, and τ_i is the shear stress of the water on the bottom of the accumulation.

In the "wide" channel case then, which is the case studied herein, the thickness of the jam will depend mainly on μ and C_i. Values of μ have been determined from field measurements (Pariset and Hausser, 1966) and although values ranging from 0.9 to well above 2 have been reported, an average value of 1.2 has been proposed (Beltaos, 1983). Little is known about the cohesive parameter C_i, except that its effect seems to be small in breakup jams. It has become accepted to neglect it completely when dealing with breakup ice jams.

Assuming that jams at breakup are cohesionless, Pariset et al. rewrote their general expression for equilibrium as:

$$X = Q^2/BC^2H^4 = BV^2/C^2H^2 = \mu(1 - s_i)s_i(t/H)^2((1 - s_i(t/H))^3/(1 + s_i(t/H))) \quad (11)$$

where C is the Chezy coefficient, t the thickness of the accumulation and H the depth of flow upstream of the accumulation. Taking a value of 1.28 for μ (as suggested by their field measurements) and assuming that s_i = 0.92, Pariset et al. produced the dimensionless stability diagram given in Figure 7. The plot defines regions of stability (inside the curve) and instability (anywhere outside).

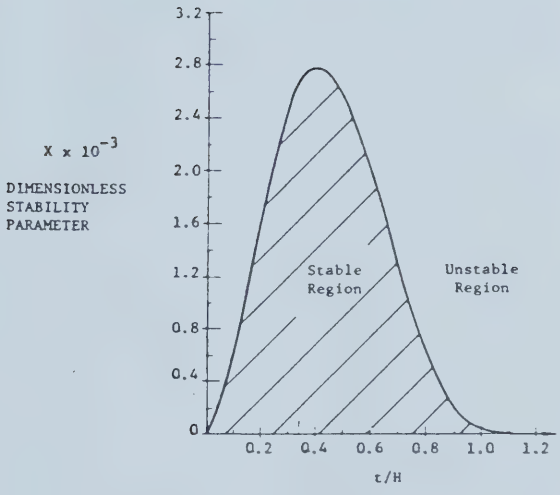

Figure 7. Dimensionless ice jam stability diagram (Pariset et al., 1966)

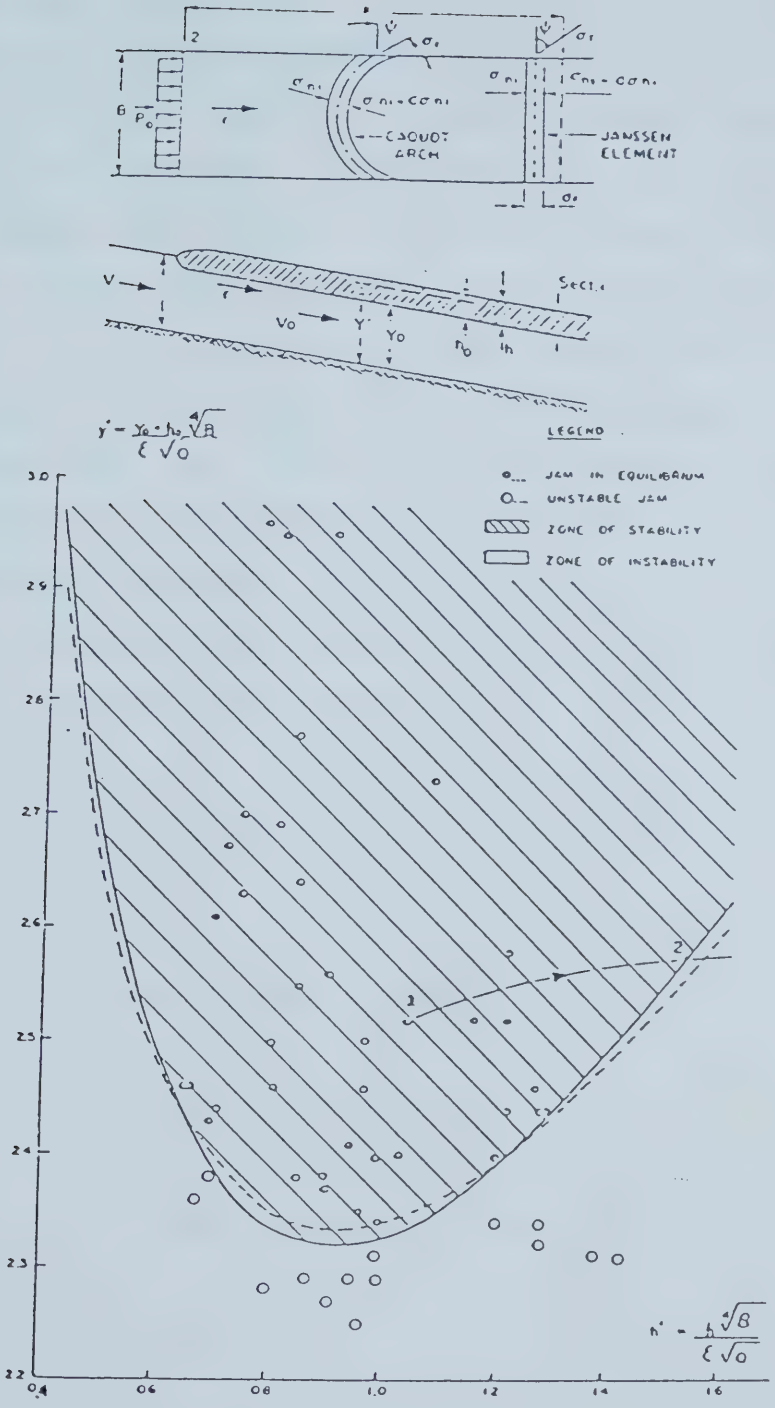

Figure 8. Dimensionless ice jam stability diagram (Michel, 1966)

2.4.4 Michel (1965, 1971)

Michel's work has somewhat paralleled that of Pariset et al. (1966) and, although he used a different approach, he derived a similar equation. The main difference lies in the basic element used by each investigator to perform the force balance analysis: Pariset et al. (1966) used a unit linear element of length dx (the older Janssen theory for grain elevators) whereas Michel used a natural parabolic arch that corresponds to the direction of the principal stresses in the accumulation as suggested by the more recent Caquot theory (see Figure 8).

The final equilibrium equation obtained is (refer to Figure 8 for symbol definitions):

$$(y'-h')^3(h')^2 - \beta y' - h'(1-e-\beta) = 0 \qquad (12)$$

with

$$y' = (Y_o + h_o)B^{1/4}/\ \xi\sqrt{Q}$$

$$h' = (h_o B^{1/4})/(\xi\sqrt{Q})$$

$$\xi = (2.28\gamma n_o^2)/(\sin 2\psi(1-e)(\gamma-\gamma)Y_o^{1/3})^{1/4}$$

$$\beta = 1/2(n_i/n_o)^{3/2}$$

Michel (1965) further notes that for an ice jam, the roughness underneath the accumulation is predominant and

$\beta \rightarrow 1$. Figure 8, reproduced from Michel (1966), shows the resulting equation of equilibrium and represents the limit of stability of an ice jam. The limiting condition implied by the equation is:

$$h'/y' = h_o/(Y_o + h_o) \cong 0,41 \qquad (13)$$

$$y' = ((Y_o + h_o)/(\xi\sqrt{Q}))B^{1/4} \cong 2.36 \qquad (14)$$

The results of laboratory tests are shown in Figure 8. Polyethylene blocks of density 0,92, porosity 0,4 were used to test the above limiting condition. Also shown on the figure in a dotted line is the curve obtained with the Janssen theory (Pariset et al., 1966).

2.4.5 Uzuner and Kennedy (1976)

Uzuner and Kennedy have formulated the time-dependent differential equations describing the force equilibrium within, and the flow hydraulics beneath, an ice jam. These equations are too complex to permit a general analytical solution but it was shown that after an evolutionary period, the jam attains a quasi-steady condition. Although the original paper discussed in some detail the velocity of upstream propagation of jams and the time required for evolution of jams to equilibrium, the following will focus on the equations describing the quasi-steady (equilibrium) conditions and the streamwise distribution of flow depth and

jam thickness and on the quasi-steady (equilibrium) conditions.

To express the shear stress that can be developed at the banks, it was assumed that the Mohr-Coulomb relation could be used:

$$|\tau| = C_o\sigma_z + C_i \qquad (15)$$

where C_i represents the cohesion, C_o is a dimensionless coefficient, and σ_z is the thickness-averaged normal stress in the direction perpendicular to the water surface (= $0.5(1-s_i)(1-e)\rho_i gt$). The strength of the accumulation was assumed to be

$$\sigma_x = K\,\sigma_z \qquad (16)$$

where K is a dimensionless coefficient equal to $\tan^2(45 + \phi/2)$, where ϕ is the angle of internal friction.
Finally, using a force balance analysis, they obtained:

$$\partial(K\gamma t^2)/\partial x + 2\,((C_o\gamma t + C_i)/B)t - (\rho_i gSt + \tau_i) = 0 \qquad (17)$$

Equation 17 can be integrated to find the variation of the accumulation thickness with distance. Setting $dt/dx = 0$ in Eq. 17 gives an expression for the equilibrium thickness comparable to the one given by Pariset et al. (1966):

$$(C_o(1-e)\rho_i(1-s_i)g)\ t^2 - (g\rho_i S - 2C_i/B)Bt - \tau_i B = 0 \qquad (18)$$

2.4.6 Beltaos (1983)

Beltaos (1983) rearranged the analysis of Pariset et al. (1966) and Uzuner and Kennedy (1976) and derived an equation with dimensionless parameters that are more convenient for interpreting the available field data. The resulting expression relates a dimensionless depth η to a dimensionless discharge ξ

$$\eta = H/BS = F(f_o, f_i/f_o, \mu, \xi)$$

where $\xi = (q^2/gS)^{1/3}/BS$ with q being the unit discharge (Q/B). Figure 9, taken from Beltaos (1980) shows this relation.

2.4.7 Calkins (1983)

Calkins (1983) also rearranged the equilibrium ice jam thickness expression given by Pariset et al. (1966) to a more convenient form that shows the relationship between the uniform flow hydraulics beneath the ice cover and the ice cover thickness. He used it to analyse ice jams in shallow rivers with floodplain flow.

2.4.8 Comparison of theories

The theories should not be too different in their results as they all basically use the same approach, i.e. they all provide an equation expressing the equilibrium conditions of the forces acting on and within the cover.

Comparing Eqs. 10 and 18, Beltaos (1978) noted that the internal friction parameter μ used by Pariset (1961) is directly related to the parameters used by Uzuner and Kennedy viz.:

$$\mu = C_o(1-e) \tag{19}$$

Assuming that $\mu \cong 1.3$ based on field measurements reported by Pariset et al.(1966) and taking $e = 0.4$, we obtain a value for C_o of 2.2. On the other hand, Uzuner and Kennedy (1976) found in laboratory tests that

$$2 < C_o < 100$$

and that C_i was approximately equal to 96 Pa.

2.4.9 Limitations of theoretical models

Before reviewing the approaches used in the past to analyse ice jams, it may be appropriate to point out the inherent limitations of the theory. As given by Beltaos (1983), these limitations are:

(i) The theory assumes a wide prismatic channel. For the purpose of ice jam calculations, a natural stream may be replaced by a prismatic channel of equivalent average dimensions.

(ii) Theoretical prediction depends partly on the evaluation of the hydraulic resistance of the jam's underside.

(iii) The theory does not take into account special constraints that may be present such as existence of low flood plains, by-pass channels, possible effects of bridge piers on jamming frequency, etc.

2.5 Ice jam analysis

2.5.1 General

Referring to the equations discussed earlier, the equations required for the analysis of the equilibrium portion of an ice jam are

(1) The equilibrium thickness equation (Eqs. 10 or 18).

(2) The expression for the shear stress under the ice accumulation as used in the equilibrium

thickness equation:

$$\tau_i = \rho g S R_i \qquad (20)$$

where S is the energy slope and R_i the hydraulic radius associated with the ice cover (actually the average depth for a wide channel).

(3) An expression for the composite roughness.

(4) An expression relating the depths of flow associated with each boundary (ice and river bed) to their respective roughnesses.

(5) The expression for the maximum stage, H, of a floating jam

$$H = R_i + R_b + s_i t \qquad (21)$$

where R_i and R_b are respectively the depths of flow associated with the ice cover and the river bed.

(6) A resistance flow equation.

Combining (1) and (2) produces an equation with μ, t and R_i as the three unknowns. Combining (3), (4), (5) with (6) provides another equation with t and R_i as unknowns. This results in a closure problem as the number of unknowns exceeds the number of available equations by one. What is needed is a safe and sufficiently accurate method to measure

the jam thickness directly. Unfortunately, even with recent improvements in radar technology, this has so far proved elusive for spring jams. Therefore, a supplementary assumption must be made. The following section will present briefly the approaches used in the past to effect closure of the system.

2.5.2 Pariset et al. (1966), Calkins (1983)

To complete their analysis of ice jams respectively on the St-Lawrence River and for steep shallow rivers in Vermont (U.S.A.), Pariset et al. (1966) and Calkins (1983) assumed that the roughness of the jam was approximately the same as the roughness of the river bed.

2.5.3 Beltaos (1978)

To obtain an estimate of the average value of t, Beltaos made use of the data provided by Nezhikhovskyi (1964) to derive a relation between the roughness and the thickness of the accumulation. As discussed earlier, Nezhikhovskyi found that the jam roughness increased with the jam thickness and he established empirical relationship between n_i and t. Using the data for ice floes (see Table 1 given previously), Beltaos noted that, for the very rough boundaries of ice jams, n_i should depend on R_i as well as t and attributed Nezhikhovskyi's findings to a restricted range of values for R_i (1 to 1.5 m). He then derived the following equation:

$$n_i = 0.072\ R_i^{-0.23}\ t^{0.4} \qquad (22)$$

or

$$f_i = 0.4\ (t/R_i)^{0.8}$$

in which $0.5 \leq t/R_i \leq 3$ and $t \leq 3$ m. Beltaos suggested that equation (22) could be used to obtain an estimate for the thickness of the jam.

2.5.4 Michel (1980)

Using the theory he derived during the sixties (Michel, 1965), Michel (1980) analysed field data for ice jams collected in Alberta. Putting the ratio $t/H = 0.41$ as implied by his theory, he derived a dimensionless coefficient that he called the jam number:

$$J = H/(BS) = 122f \qquad (24)$$

where H is the water stage, B the river width, S the energy slope and f the coefficient, in Michel's notation (1980), which represents the internal friction of the ice accumulation. The jam number can then be obtained directly from field measurements. Knowing the river bed roughness from summer data computations, the "exact roughness of the ice cover can be obtained from the measurements giving the jam number".

2.5.5 Andres (1980)

Andres proposed another approach which does not necessitate any assumptions regarding the ice jam thickness. He simply assumed that the jam thickness and the roughness did not change appreciably for a short period of time following establishment of equilibrium conditions. Therefore, by documenting the water stage profile for the ice jam for two different discharges, the closure problem is solved as the second documentation provides one extra equation.

2.5.6 Limitations of past approaches

It is easy to realize that all the previously discussed methods to estimate the jam thickness have shortcomings. First, there is no reason to assume, like Pariset et al. (1966) did that $n_i = n_b = n_o$ for all jams in all rivers. Calkins (1983) also used this assumption arguing that for the small shallow streams he was studying, the value of the roughness coefficients had only a small influence on the total stage as compared to the influence of the ice thickness. In large flat river like the one studied herein, it is more likely that the importance of the roughness is increased. Secondly, the idea of fixing the ratio t/H (Michel, 1980) has not been tested extensively against laboratory or field data. In fact, as pointed out by Beltaos (1980), " there may be grounds for reservation regarding the physical plausibility of the theoretical development that

leads to t/H = constant. For example, a major result of this theory is that H/BS = constant = 41.2; on the other hand, application of the conventional theory as given by Pariset et al. (1966) or Uzuner and Kennedy (1976) indicates that H/BS should depend on Q, B and S as well as on hydraulic resistance coefficients of the channel bed and the jam underside." By looking at the dimensionless plot proposed by Beltaos (1980) (see Figure 9), it can be seen that H/BS does in fact vary strongly with these parameters. Beltaos' approach (1978), using Nezhikhovskyi's data, is also subject to objections due to the many weaknesses of the data discussed earlier and the fact that the relationship obtained by Nezhikhovskyi has not been duplicated in the literature. Finally, Andres' suggestion (1980) provides a good and sound alternative but it is obviously not always possible to obtain two documentation of the water profile for the same jam.

In view of the foregoing discussion, the present study will approach the problem of assessing the thickness and roughness of the accumulation by yet another method, because none of the above was considered satisfactory or applicable in the present case. The following chapter will describe the site of investigation, detail the method used for the analysis and discuss the implications of the results for that specific case study.

3. BACKGROUND INFORMATION ON THE MACKENZIE RIVER

3.1 General description of the Mackenzie River system

The Mackenzie River, located in the Northwest Territories, is a large river that flows approximately 1700 km northwestward from its source at Great Slave Lake to the Beaufort Sea. The entire river system is shown on Figure 10. Great Slave Lake is the fifth largest in North America and covers an area of 28 438 km^2. It is 80 km wide and 460 km in length from Old Fort Reliance at the northeastern extremity to its outlet, the Mackenzie River, at the southwesterly end.

There are many tributaries along the river within the reach of interest for this study, i.e. from Fort Simpson (km 338)[1] to Fort Good Hope (km 1100). The larger ones are the Liard River at Fort Simpson, which more than doubles the flow of the Mackenzie River at this location, and the Redstone and Keele Rivers (km 715 and 738 respectively) which together significantly increase the flow in the Mackenzie. The entire system drains a basin of about 1 813 000 km^2 which represents approximately 1/4 the area of mainland Canada.

---

[1] Distances are measured from head of the Mackenzie River at Great Slave Lake (as given on the hydrographic charts published by the Canadian Hydrographic Service, Department of Fisheries and Oceans, Ottawa, 1983).

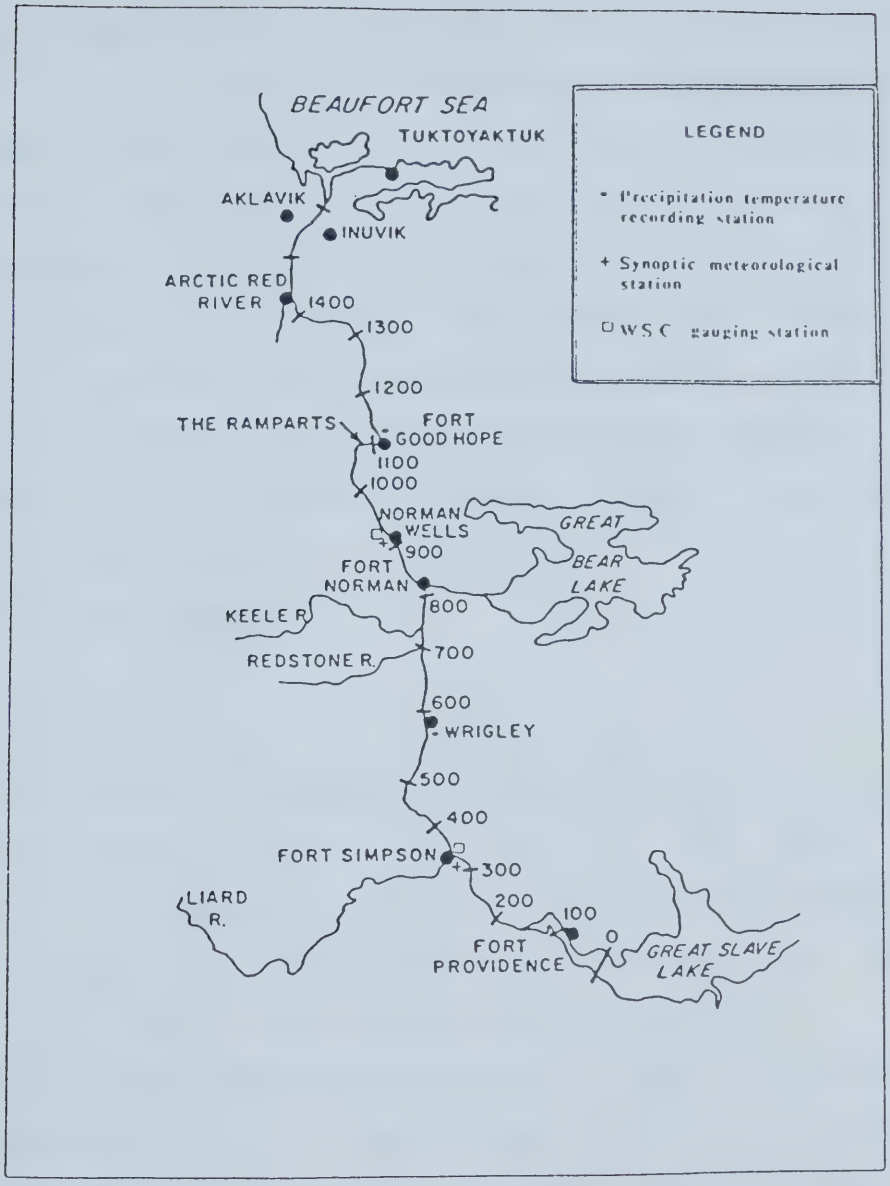

Figure 10. Location map for the Mackenzie River.

3.2 Geomorphological features

The Mackenzie River system lies in the Mackenzie lowlands between the Canadian Shield to the east and the Mackenzie section of the Rocky Mountains to the west. The river bed is quite varied along the river, varying from a silty sand at some locations to medium-sized cobbles in other reaches (see Mackenzie River Investigation, Public Works of Canada, Vol. 3, 1976). Although the mean width of the river is around 2.5 km, in reaches like that in the Fort Norman area (km 828) and the Norman Wells area (km 905), it can attain 3.5 km. Many islands are present in the wider reaches. Figure 11 shows a longitudinal profile of the Mackenzie River system.

3.3 Discharge

Water Survey of Canada measures the discharge at three locations along the Mackenzie River in the reach of interest: Fort Simpson (#10GC001), Norman Wells (#10KA001) and above Arctic Red River (#10LA003). There are two other stations that record only stages. They are Wrigley (#10HC001) and Fort Good Hope (#10LD001). Some tributaries of the Mackenzie River are also gauged: Liard River near the mouth (#10ED002), Root River near the mouth (#10GA001), Martin River near the mouth (#10GC003), Wrigley River near the mouth (#10HB003) and Redstone River near the mouth (#10HB001).

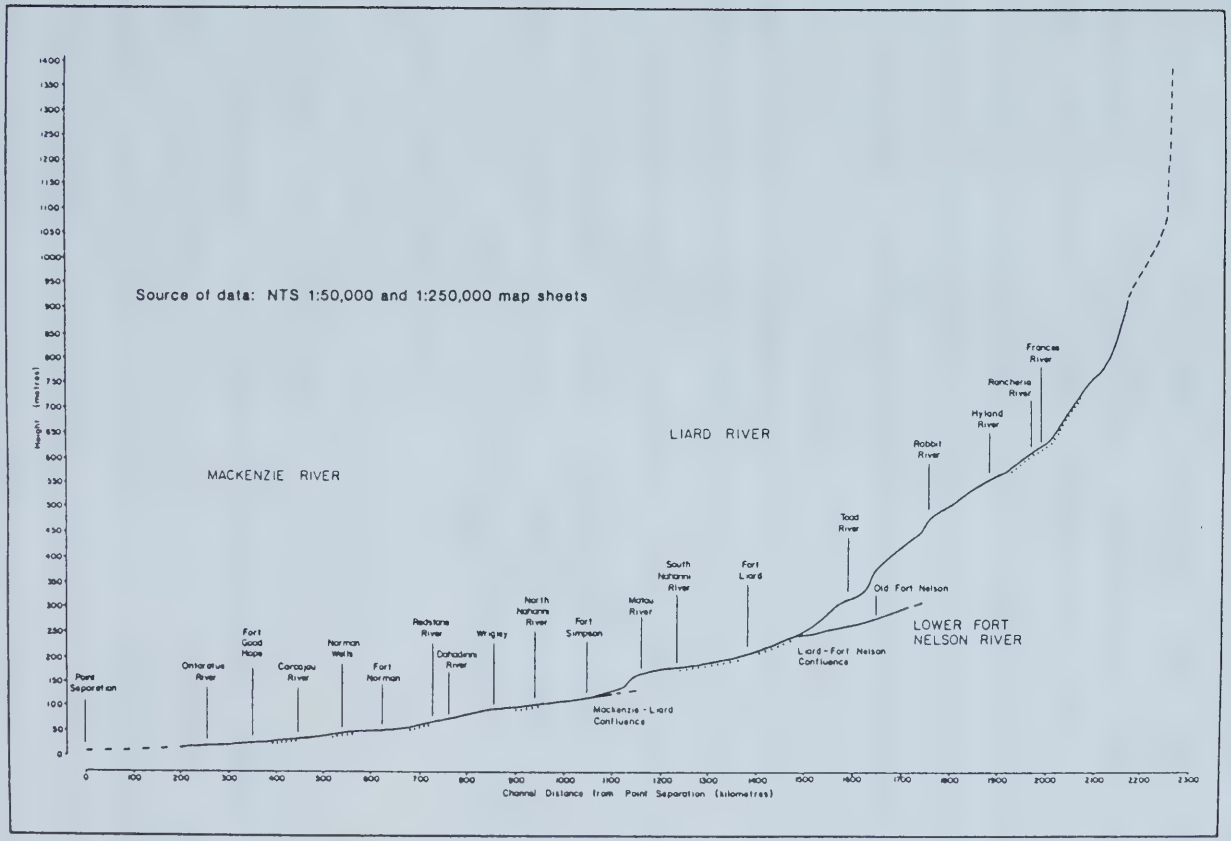

Figure 11. Longitudinal profile for Mackenzie River system (After Vol. 3, Mackenzie River Basin Committee, 1981).

The minimum discharge in the Mackenzie River occurs during late winter due to a lack of run-off and low levels on Great Slave Lake. The peak discharge is usually reached in July and high flows are maintained through the summer by outflow from Great Slave Lake, which serves as a reservoir for the river. At Fort Simpson (km 338), immediately downstream of the Liard River confluence, the open water range of monthly flows is between 6 000 and 15 000 m^3/s, with a long term mean flow of 10 340 m^3/s. In late winter, the minimum monthly flow can fall to 1 700 m^3/s. The flow at Fort Simpson is greatly affected by inflow from the Liard River, the main tributary of the Mackenzie. Monthly mean flows in the Liard range from 300 to about 6 000 m^3/s. The recorded maximum daily discharge is 16 450 m^3/s.

At Norman Wells (km 905), the Mackenzie River mean monthly discharge ranges between 9100 m^3/s and 17 800 m^3/s during the open water season, with a maximum daily discharge of over 22 000 m^3/s having been recorded. The late winter low is about 2 300 m^3/s.

3.4 General ice conditions

In general, ice covers the Mackenzie River completely from late November to the last days of April. Freeze-up and breakup usually occupy 2 1/2 months, leaving about 4 months of open water for navigation. Beginning at Inuvik (km 1560), where the ice forms during about the second week of October, the Mackenzie River freezes southward. By the end of the

second week of November, it is normally ice covered as far south as Fort Norman (Km 828), and at Fort Simpson (km 338) just downstream of the mouth of the Liard River by the end of the month. The thickness of the ice varies along the river. At the end of winter (late March), the ice thickness at Norman Wells (km 905) has a long-term average of 1.6 m whereas it can easily attain 2 m in the Delta.

Spring breakup on the Mackenzie River usually begins during the first week of May at the mouth of the Liard River, just upstream of Fort Simpson (km 338). The breakup front then progresses downstream at a rate depending on, among other things, the formation and release of ice jams along the river. Normally, breakup upstream is complete to Fort Providence (km 90) by the third week of May and downstream to Inuvik (km 1560) by the end of the month.

3.5 Past studies of ice conditions

3.5.1 General

Although some early studies dealing with ice conditions along the Mackenzie River have been reported (McConnel, 1890; Preble, 1908; Keefe, 1910; Kindle, 1920; Voorhis, 1930; Kidd, 1931), they provide, in general, only a qualitative description of the more dramatic events at a given location. Actual research into the Mackenzie River and the Delta ice regime began during the 1950's and extended until the mid-70's when oil and gas exploration in the Delta

region slowed down. In the late 1970's, the possibility of hydro-electric development of the Liard River and the oil exploitation program initiated by Esso Resources Canada Ltd. in the Norman Wells area (km 905), provided the impetus for further investigations.

3.5.2 MacKay and MacKay (1960 - 1973)

Following a paper by Brown (1957) describing general breakup observations on the Mackenzie River and its Delta in 1954, MacKay and MacKay wrote a series of papers from 1960 to 1973 dealing in great detail with freeze-up and breakup conditions along the river and in the Delta (see, for a complete list, MacKay and MacKay, 1973a, 1973b). Mackay (1963) gives mean dates of freeze-up and breakup at specific locations. For the period 1946-1955, the mean freeze-up and breakup date for Norman Wells is Nov. 11 and May 15 respectively.

Some time later, Mackay (1965, 1966) described the 1964 and 1965 breakup on the basis of aerial and ground observations and compared its timing with that of former years. After a paper by MacKay which dealt more specifically with ice conditions in the Delta region (Mackay, 1969), MacKay and MacKay (1973a) indicated that the breakup of the Mackenzie River is not a completely sequential process. The reach between Fort Simpson (km 338) and Fort Good Hope (km 1100) is generally the first one to break up, the major factor being the Liard River which acts as a trigger,

initiating the breakup sequence. Downstream of Fort Good Hope, the river breaks up at a later date due, in part, to its northerly position, the formation of ice jams upstream, and the absence of larger tributary inflows which normally tend to facilitate breakup on the mainstem. MacKay and MacKay also conclude in the same study (1973a) that the duration of the annual breakup period tends to be dependent upon the river stage, with high levels favouring a rapid clearance.

In an other study (1973b), MacKay and MacKay discussed the locations of ice jams along the river. They found that ice jams had a tendency to occur at or just below major tributary confluences (e.g. the Liard and Great Bear Rivers) and at channel constrictions such as at mid-channel islands, shoal areas, and narrow reaches. Ice jams locations were observed to be fairly consistent from year to year provided that river discharges were comparable. Jams tend to increase in size but decrease in number in high water years; conversely, they are smaller but more numerous during years with low water. The authors also pointed out that there is a considerable difference between the ice jamming characteristics from Great Slave Lake to the junction with the Liard River (km 338) and below this junction. In the 333 km reach above the Liard, the Mackenzie flow is relatively stable, somewhat late into the breakup period, and has low ice shove-driftwood limits with few major jam sites. At and below the Liard junction, the Mackenzie River breaks up

generally earlier on a more rapidly rising stage with significantly higher levels of ice shove-driftwood and numerous ice jams.

3.5.3 Public Agencies Reports (1977 - 1981)

Data on freeze-up and breakup dates, as well as ice thicknesses for selected sites within the Delta and along the Mackenzie River are given by Allen (1977). Figure 12 is based on that source and shows statistical information on freezeup and breakup.

The Mackenzie River Basin Committee (1981) conducted a study to investigate ice thickness variation in the Delta channels prior to breakup. Also, the progress and timing of the 1980 freeze-up and breakup on the lower Mackenzie River (below Fort Good Hope) and in the Delta region was recorded and studied. This study also compares the 1980 breakup with the average or historical data and recommend that more intensive, site specific investigation be undertaken to obtain information relating to ice jamming and water level conditions. The Committee concluded that the 1980 field observations confirmed the findings of former studies of ice thicknesses (e.g. Anderson and Anderson, 1974; MacKay, 1963) and breakup and freeze-up progression (e.g. MacKay, 1963; MacKay, 1969).

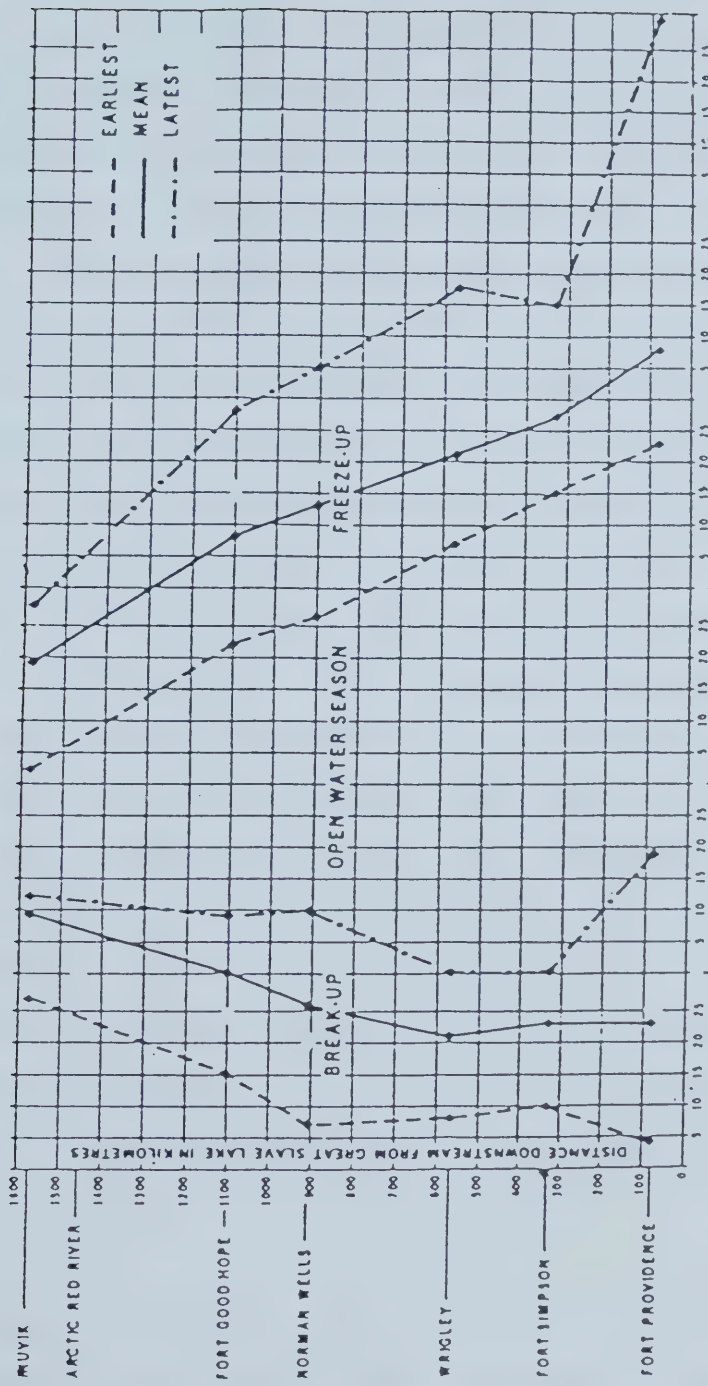

Figure 12. Dates of breakup and freeze-up for Mackenzie River (After Allen, 1977)

3.5.4 Parkinson (1981, 1982)

Parkinson (1981) gives a summary of descriptive field studies that have been carried out during the 1979-80 and 1980-81 winters to define the winter regime in the lower Liard River and in the Mackenzie River from their confluence at Fort Simpson (km 338) to the Beaufort Sea. Two completely different breakup sequences were observed. In 1979-80, there was a very low discharge and the ice melted in situ, with virtually no ice jam development whereas in 1980-81, a heavy rainstorm in the headwaters sent a rapid runoff wave through the whole system, creating near-flood level ice jams.

In a subsequent paper, Parkinson (1982) produced a somewhat more elaborate analysis of the breakup events as observed in 1980 and 1981. Emphasis was put on water temperature measurements along the river during the breakup period. In 1980, due to the lack of sufficient run-off to dynamically remove the jams, the presence of warm water temperatures was reported as being the predominant factor in the ultimate destruction of the successive small ice jams. By contrast, heavy rainstorm in 1981 showed that a significant discharge rise, even of short duration, was capable of removing the entire ice cover with water temperatures still at the freezing level.

3.5.5 Kamphuis and Moir (1983)

Kamphuis and Moir (1983) reported on breakup and ice jamming along the river between Fort Simpson and Fort Good

Hope and provided considerable details for the breakup in 1979, 1980 and 1981. They observed that the ice melting process differs in deep and shallow river channels, the shallow areas being cleared at a faster rate and therefore providing the space to facilitate of ice movement. The ice jamming processes were described, all ice jams along the Mackenzie River being formed by mush ice jamming against intact ice present in the deeper channels downstream. Comparing their observations on the rate of ice breakup progression with the ones reported by MacKay and MacKay (1973a), they noted that a close relationship between stage and breakup rate as proposed by MacKay and MacKay may not be totally appropriate. They suggested that other environmental influences such as candling of the ice prior to breakup (i.e. ice strength), air temperature and refreezing along with the wind effect are possibly more important than river stage for the rate of breakup progression and jam clearing. At Norman Wells (km 905), they pointed out, based on water level records from 1973 to 1981, that ice movement takes place during a rapid rise in water level and at an approximate elevation of 44.5 m. This is about 4.5 m above the chart datum at this location and about 2.5 m above the water level prior to breakup.

3.5.6 Kemp (1983)

Kemp (1983) in an unpublished report, describes the 1982 breakup along the Mackenzie River between Fort Simpson

and Fort Good Hope. Although the same method utilized by Kamphuis and Moir (1983) was used to document the overall large scale breakup progression, more detailed observations are provided in the Norman Wells area (km 905).

3.5.7 Stagg et al (1983)

Stagg et al (1983) analysed the peak water levels at Norman Wells that were measured during breakup for the period 1973 - 1983. The measurements are shown in Table 2. They made a distinction between two types of breakup: "thermal" breakup and "ice jam" breakup. During a thermal breakup, low flow rates in the river permit the ice to melt and gradually disintegrate, thus resulting in lower peak water levels. For an ice-jam type of breakup, higher flow rates produce ice jams downstream, which in turn create higher water levels. Performing a frequency analysis on the available data and noting that, for design purposes, the peak water levels would be the ones resulting from the "ice jam" breakups, they obtained values for long time period which were roughly consistent with levels of ice scarring measured on Bear Island, in front of Norman Wells (km 905).

Year	Elevation (m)	Rank	Probability of Exceedance
1973	48.92	6	6/12
1974	50.13	2	2/12
1975	49.52	4	4/12
1976	49.78	3	3/12
1977	48.99	5	5/12
1978	47.15	8	8/12
1979	46.11	10	10/12
1980	43.60	11	11/12
1981	48.66	7	7/12
1982	50.65	1	1/12
1983	46.70	9	9/12

Table 2. Peak water level measured each year at Norman Wells during spring breakup. Water levels are referred to the Geodetic Survey of Canada (1980 survey) and are in metres above mean sea level (after Stagg et al., 1983).

3.6 Field data collection: techniques and results

3.6.1 General

To collect relevant field data, breakup observations were carried out in 1983 and 1984. The reach of the Mackenzie River covered by the observations extended from Fort Simpson at the Liard River confluence (km 338) to Fort Good Hope (km 1100). General breakup progression and ice jamming events for the two years were monitored from a dedicated Twin Otter aircraft and recorded using 35 mm slides. Vertical air photos were taken of significant ice jams. Visual ground level observations and 35 mm slides were also used to record the local breakup events in the Norman Wells area (km 905). Temporary bench marks were established at several locations along the Norman Wells waterfront to monitor the water level fluctuations during the whole breakup period.

In 1983, close-up aerial 35 mm photos of the ice and water levels near identifiable objects along the bank were taken, to allow for the determination of an approximate ice jam water profile. As described in a subsequent section, the water levels obtained from these photos were later surveyed and referenced to the open water line during the summer of 1983. Finally using the available bench marks along the river between Norman Wells (km 905) and Fort Norman (km 338), complete water profiles for the 1983 ice jam at Norman Wells and for the open water conditions prevailing during

the summer survey were obtained.

The 1984 breakup tended to be a thermal breakup with much of the ice weakening in place. No ice jam formed near Norman Wells and this prevented the intended duplication and verification of the analysis performed for the 1983 jam.

The following sections summarize the field data gathered during the breakup observations in 1983 and 1984 and the open water data collected during the summer of 1983.

3.6.2 1983 breakup

Aerial observations and breakup progression.

As discussed previously, general breakup progression on the Mackenzie River was monitored using a Twin Otter aircraft based in Norman Wells (km 905), where all the flights originated. The observations in 1983 began on May 3 and ended on May 24, one day after the stabilization of an ice jam that formed in the Norman Wells area at 3:07 on May 23. At the beginning of the observation period, flights were conducted every two or three days. Then, as the rate of breakup progression increased, the observation frequency was increased to once, and even twice, a day to document adequately the rapidly changing ice conditions.

During the night of May 1, the ice moved on the Liard River and a jam formed at its confluence with the Mackenzie River (km 338). At the time of first observation (May 3), the accumulation was re-frozen due to colder temperatures and actually rotted in place 4 or 5 days later. This

prevented the formation of a sudden surge of ice and water that would have accelerated the ice clearance process downstream. As shown in Figure 13, the subsequent breakup progression down the Mackenzie was characterized by the formation, release and re-formation of rather minor ice jams. Between May 18 and 20, the Redstone (km 715) and the Keele Rivers (km 738) broke up and triggered formation of a jam in the Old Fort Point area (km 770). Upon release, this accumulation accelerated the breakup progression downstream from that point and on May 22, at 22:30, an important ice movement was reported at Fort Norman (km 828), producing an 80 km long ice jam keyed just upstream of the settlement (Figure 14). The next day, a flight was conducted to Fort Norman to observe the ice conditions at this location from ground level. At about 11:15, the jam released dynamically, causing breakup downstream to Norman Wells (km 905) where the jam analysed in the present study formed. Figures 15 and 16 provide a general view of this jam and a close-up photo of the toe region respectively.

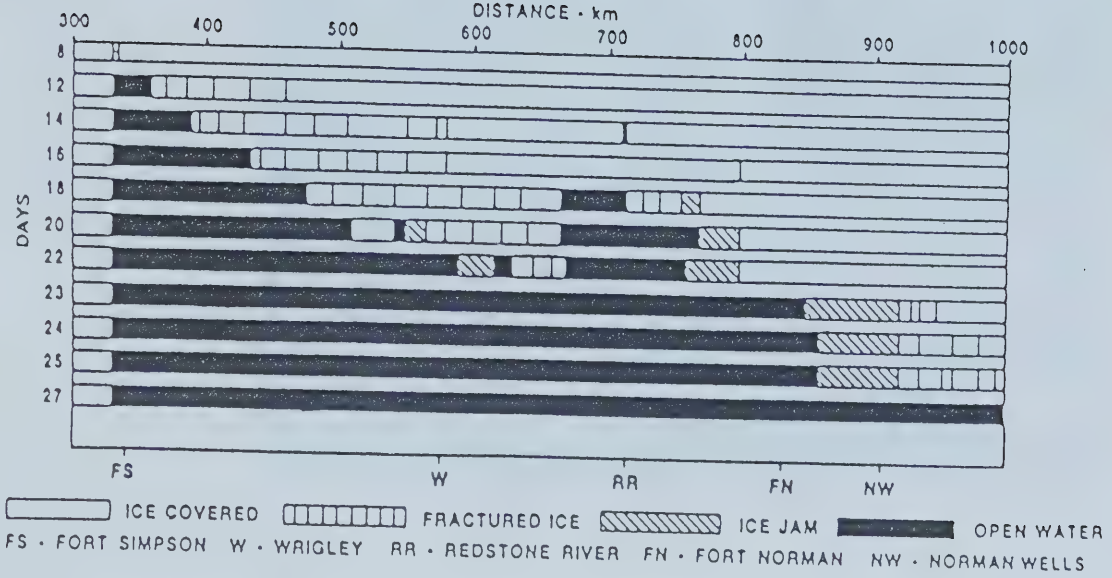

Figure 13. 1983 breakup progression

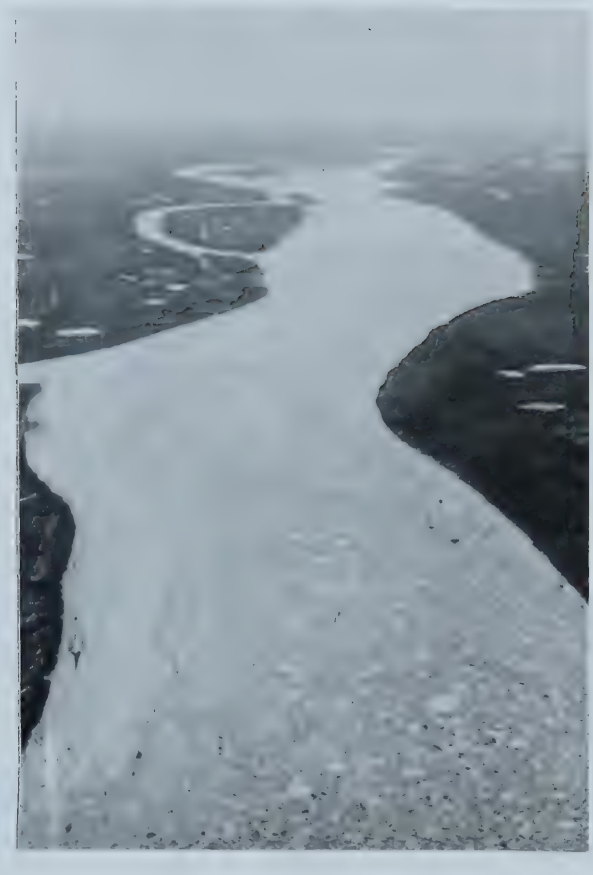

Figure 14. General view of 1983 ice jam at Fort Norman.

Figure 15. General view of the ice jam at Norman Wells, May 23 1983.

Figure 16. Close-up view of the toe region of the ice jam at Norman Wells, May 23, 1983.

Following a technique described by Gerard (1975), oblique photographs of the jam water levels along the river banks were taken from a low-flying aircraft. Special effort was made to photograph locations where easily identifiable objects were present along the banks. The complete reach influenced by the jam, from approximately km 940 (downstream of Norman Wells) to Fort Norman (km 828) was covered using this technique. As discussed later, the water level profile points were then referenced to existing bench marks along the reach during a survey the following summer.

Appendix A provides a more detailed summary of the general aerial observations during the 1983 breakup period.

Ground observations.

The first ice movement in the Fort Norman area (km 828), was reported to have occured on May 22 at 22:30 (RCMP Detachment Officer, Fort Norman). A flight was taken to Fort Norman early on May 23 to observe the ice conditions at this location.

On arrival in Fort Norman at about 10:30, the jam that had formed in front of the village was stable and no ice movement could be noticed from the bank. Some minor ice ride-up had occurred along the shoreline but no appreciable pile-up was observed. The ice which had been pushed onto the bank was generally in good condition, with little candling evident.

At about 11:15, small movements of the ice near the shorelines were noticed and, shortly after, the entire ice jam began to move and the surface appearance of the very fragmented or so-called mush ice could be observed as it was passing by (Figure 17). Judging from Figure 17, the larger roughness elements projections were of the order of 1 m. The ice pieces near the bank were pushed further onto the shoreline, producing some gouging of the banks and much more severe pile-ups. The velocity caused by the ice jam release was estimated to be approximately 10 km/hr.

The ice run (dense 'mush' ice) was still moving past the village at about 12:30, when the observations at Fort Norman were stopped. On return to Norman Wells (km 905), the ice sheet at Norman Wells was still sound: no fracturing could be seen. At 13:20, the surge released by the ice jam movement at Fort Norman produced the first noticeable ice movement at the Off-Site Dock, about 4 km upstream of Norman Wells. Major ice movement at the Government Dock in Norman Wells occurred at 15:07. At about 15:40, ice movement ceased. The ice sheet in front of Norman Wells had moved about 500 m and was left fractured into large floes. Most movement occured well off-shore, along the right side of Bear Island.

The ice push through the Norman Wells area produced many pile-up accumulations along the bank. The largest was on the upstream side of the Off-Site Dock, where the height of the pile-up was estimated to be about 15 m. Two smaller

ridges had formed behind the one in contact with the dock. A smaller accumulation formed at the Government Dock in Norman Wells. Extensive ice pile-ups occurred downstream of the western end of the Esso plant, where the bank is oriented at an angle to the main flow direction. Significant ride-ups were produced for about 800 m or so along the shoreline at this location. No other major pile-up formation was observed along the shoreline in Norman Wells. Figure 18 shows the ice conditions as observed from the ground. Unfortunately the surface appearance of the mush ice could not be seen from the ground at Norman Wells as it had pushed its way in the secondary channel behind Goose Island. It could however be assumed that the surface of this jam was similar to the one observed at Fort Norman.

Figure 17. Surface appearance of running ice pack just after ice jam failure at Fort Norman, May 23 1983.

Figure 18. Ice conditions at Norman Wells after ice movement, as observed from the ground, May 23 1983.

Figure 19. Typical ice sheet composition, Norman Wells, May 23 1983.

Shortly after the ice had stopped moving, the condition of the ice at several locations along the shoreline was documented. The ice sheet was generally composed of a 28 cm layer of snow ice over a layer of columnar ice averaging 90 cm (Figure 19). At some locations (notably at the downstream end of the Esso plant), the columnar ice was well candled, but at other locations there was little evidence of decay.

When ground observations were discontinued on May 26, the ice was still in place in front of Norman Wells and the water levels were decreasing at a slow rate.

Water level measurements.

Water levels at Norman Wells were monitored continuously from April 28 to May 30. Before the W.S.C. stage recorder was put out of order by the ice on May 23 at about 14:30, it provided continuous data on the water levels. After this date, water level variations were monitored at the three locations shown in Figure 20: at the Off-Site Dock (about 4 km upstream of Norman Wells), at the NCPC Dock, and at the On-Site Dock. At each location, a number of rocks were identified to act as temporary bench marks, painted with different colours and tied to a bench mark nearby. Figure 21a combines data obtained from the W.S.C. gauge and data at the NCPC Dock (after May 23) to provide a representative illustration of water level fluctuations at Norman Wells during the entire breakup period.

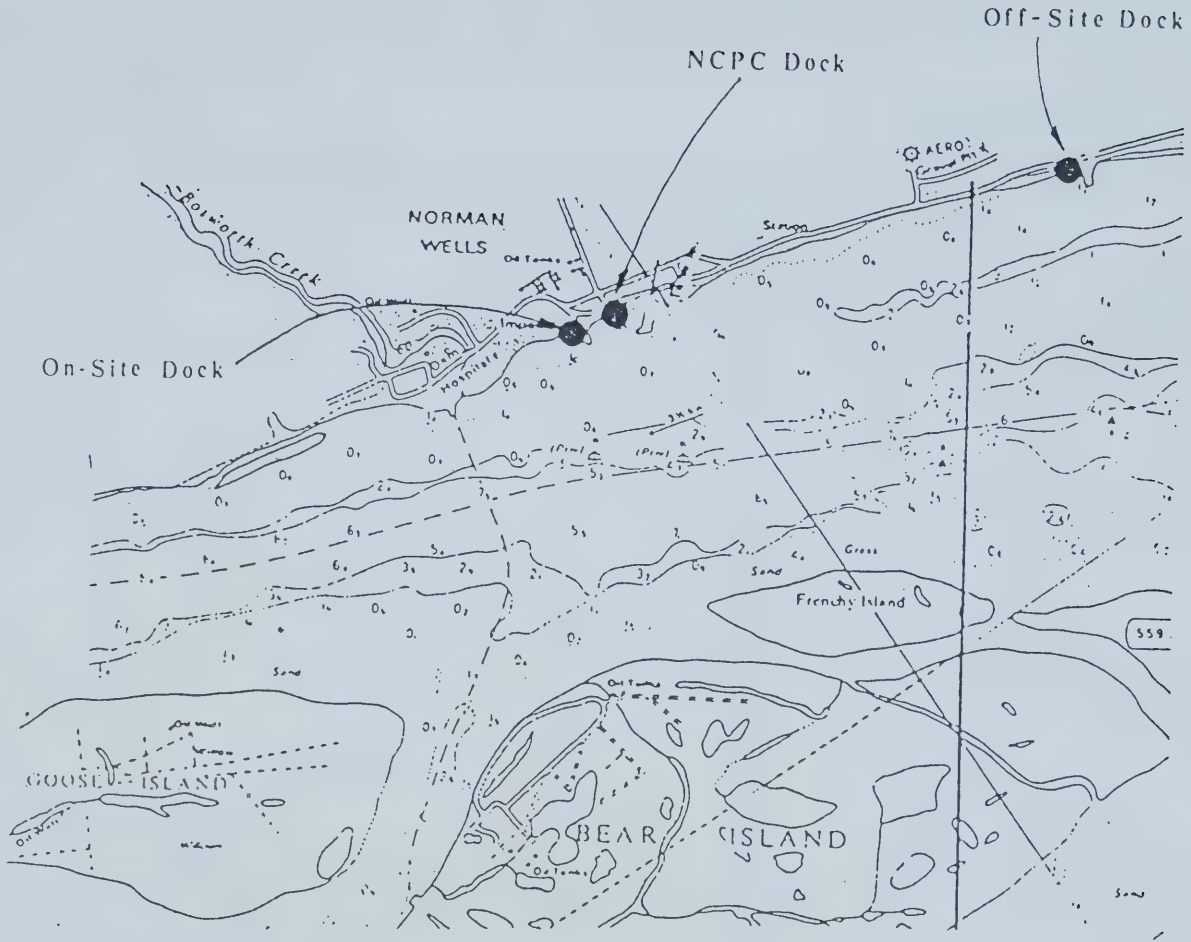

Figure 20. Temporary bench marks locations, Norman Wells.

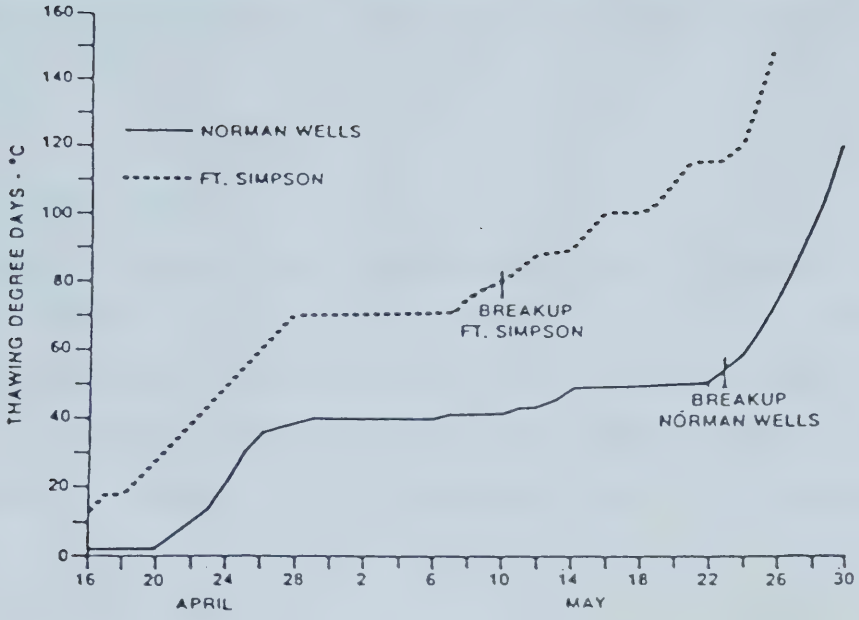

Figure 21b. Thawing degree-days, Norman Wells, 1983

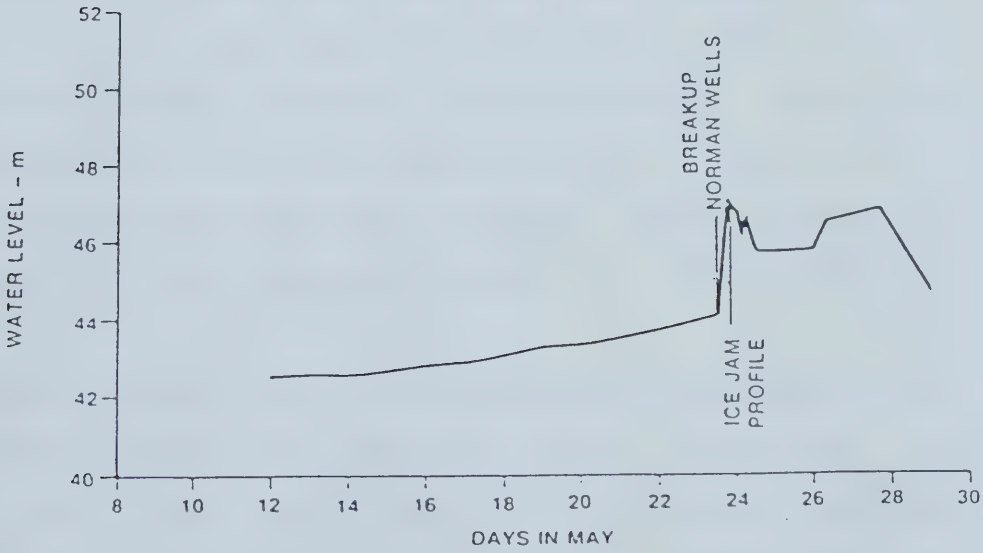

Figure 21a. Water levels during breakup, Norman Wells, 1983

Some water levels were taken by the RCMP officer in Fort Norman and were later tied to the geodetic bench mark 74T060.

Meteorological data.

Figure 21b shows the accumulating thawing degree days obtained from the compilation of AES data at Fort Simpson (km 338) and Norman Wells (km 905). As is apparent from the figure, a cold spell that was well under the seasonal normal prevailed during much of the breakup period. This slowed the breakup progression somewhat. Ice movement occured at Norman Wells after 52 °C days.

3.6.3 Summer 1983 survey

A field trip was conducted during the summer of 1983 to collect data on open water conditions and to survey the ice jam water profile recorded photographically during the breakup period. This survey took four days to complete (from August 17 to August 21) and covered the reach affected by the jam in the Norman Wells area, i.e. from km 828 to km 940.

Eleven bench marks were used along the reach. It must be pointed out that two different geodetic survey lines had been used in the area of interest. The first was completed in 1974 and covers the whole reach of concern with, in general, a group of three geodetic bench marks located at 6

km intervals. In 1980, some of these bench marks in the Norman Wells area were re-surveyed and some elevations were changed quite noticeably (for example, 0.7 m difference for B.M. 74T016). Therefore, to achieve some kind of consistency, all the bench mark elevations used are those determined in the 1974 survey. The detailed measurements are given in Appendix B.

Figure 22 illustrates the open water profile and shows the ice jam profile determined using the 35 mm photos of the river banks taken while the ice jam was in place at Norman Wells. The latter were tied in using the summer open water profile as a reference line. The flight during which the photos were taken was conducted on May 23, at 20:30, about five hours after the ice movement had stopped at Norman Wells (at 15:40). Figures 23 and 24 are examples of the photos. Additional photos were taken the next day at about 17:45 but as the difference in the water elevations between the two flights was small and well within the range of error involved (0.2 to 0.4 m difference), only the photos from the May 23 flight were retained for the analysis. Moreover, an average decrease in stage for the jam, based on the decrease at the gauge, could not be assumed as the difference in stage did not appear, from the photos, to be uniform along the jam.

The reliability of the water levels determined from the photos varied. For example if, on the photo, a tree, rock or other object could be identified near the water line, the

water elevation could be determined within 0.2 to 0.4 m. If, on the other hand, the bank slope was very gentle and there was no easily identifiable object near the water, it is thought that errors up to 0.8 m could occur in the worst cases. For this reason, certain points were rejected while others were used, but with less confidence attached to them. Appendix C presents the detailed data for the ice jam water profile.

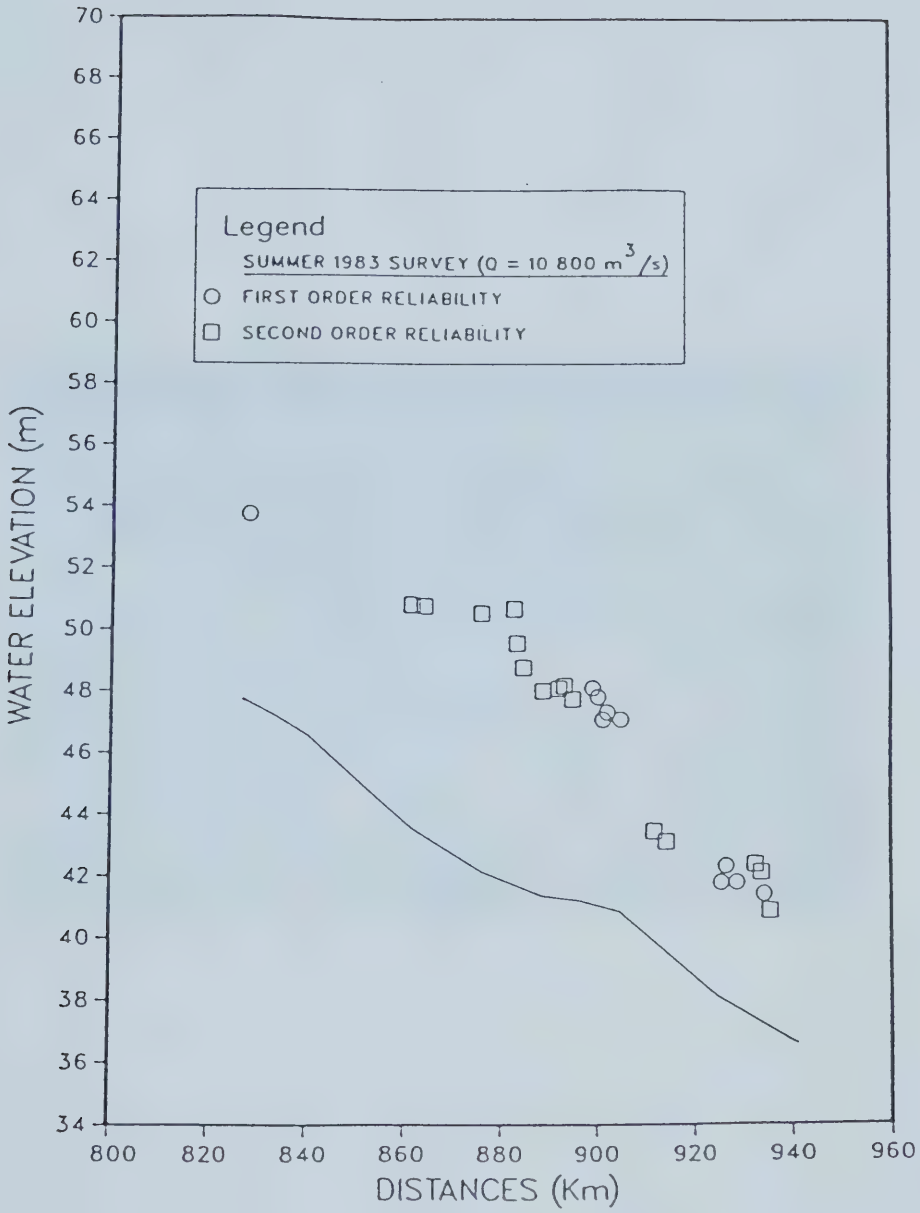

Figure 22. Open water and 1983 ice jam profiles.

Figure 23. Aerial view of the ice conditions at Norman Wells, 1983.

Figure 24. Aerial view of the ice conditions upstream of Norman Wells.

3.6.4 1984 breakup

Aerial observations and breakup progression

Appendix D provides a summary of the salient features observed during the 1984 breakup. The breakup pattern for this year had many similarities with the one observed in 1983. When the flights began on May 1, the Liard River had broken up and an ice jam had formed at its mouth. The jam then released dynamically sometime between May 3 and May 5 and produced a somewhat faster breakup rate progression than in 1983, as shown in Figure 25. Towards May 13, the ice on the Redstone River (km 715) broke up and this accelerated breakup on the Mackenzie River. In the following days, an ice jam formed at Old Fort Point (km 770) (Figure 26) which, upon release, triggered the formation of a jam in the Fort Norman area similar to the one observed in 1983 at this location (Figure 27). Subsequent warm temperatures and radiation input produced such an accelerated melting that the entire jam disappeared in a matter of days. The breakup front then progressed thermally down to the Norman Wells area (km 905) over a period of 3 days. Ice movement at Norman Wells occurred on May 23 and produced only minor pile-up and accumulations on the banks and at the artificial islands built in the river at this location. No ice jam formed this year at Norman Wells.

Water level measurements

As in 1983, water levels were closely monitored in the Norman Wells area during the entire breakup period. The measurements are shown on Figure 28a. It is interesting to note that the ice did not move on May 18, although a surge on that date produced a stage of approximately 44.5 m at Norman Wells. According to Kamphuis and Moir (1983), the ice movement normally takes place at this elevation. A possible cause to this anomaly would be the freeze-up ice jam that formed this year at this location. Although the importance of freeze-up water levels on the breakup is recognized, no reliable data could be obtained from the W.S.C. charts.

In addition to that information, a water profile was surveyed on May 9 while the ice sheet was still intact and before any noticeable deterioration of the ice surface had occurred. The survey covered the Norman Wells area, from km 861.2 to km 924.3. Ground tarps were also installed on the banks and referenced to the available bench marks. Figure 35, presented later, shows the measured water profile, along with the open water profile surveyed during the 1983 summer.

Meteorological data

As pointed out earlier, spring in 1984 was much warmer than in 1983 and, accordingly, the breakup was dominated by thermal processes with minor ice jams. As illustrated in Figure 28b, the ice movement at Norman Wells on May 23 occurred after 180 °C days, more than three times the value

reached in 1983 by breakup at this location.

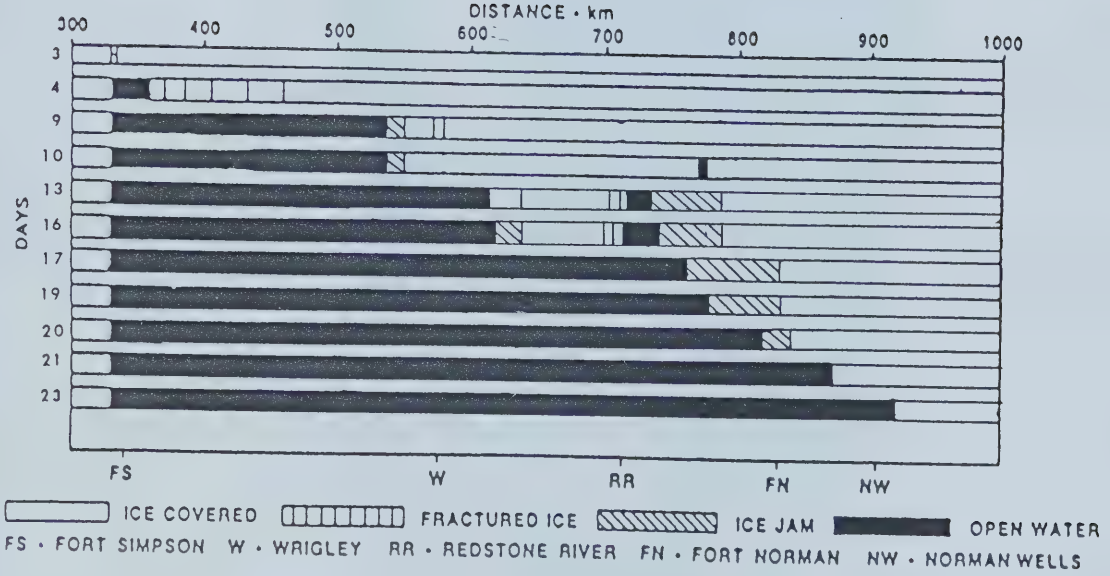

Figure 25. Breakup progression, 1984.

Figure 26. General view of the 1984 ice jam at Old Fort Point (km 770).

Figure 27. General view of the 1984 ice jam at Fort Norman.

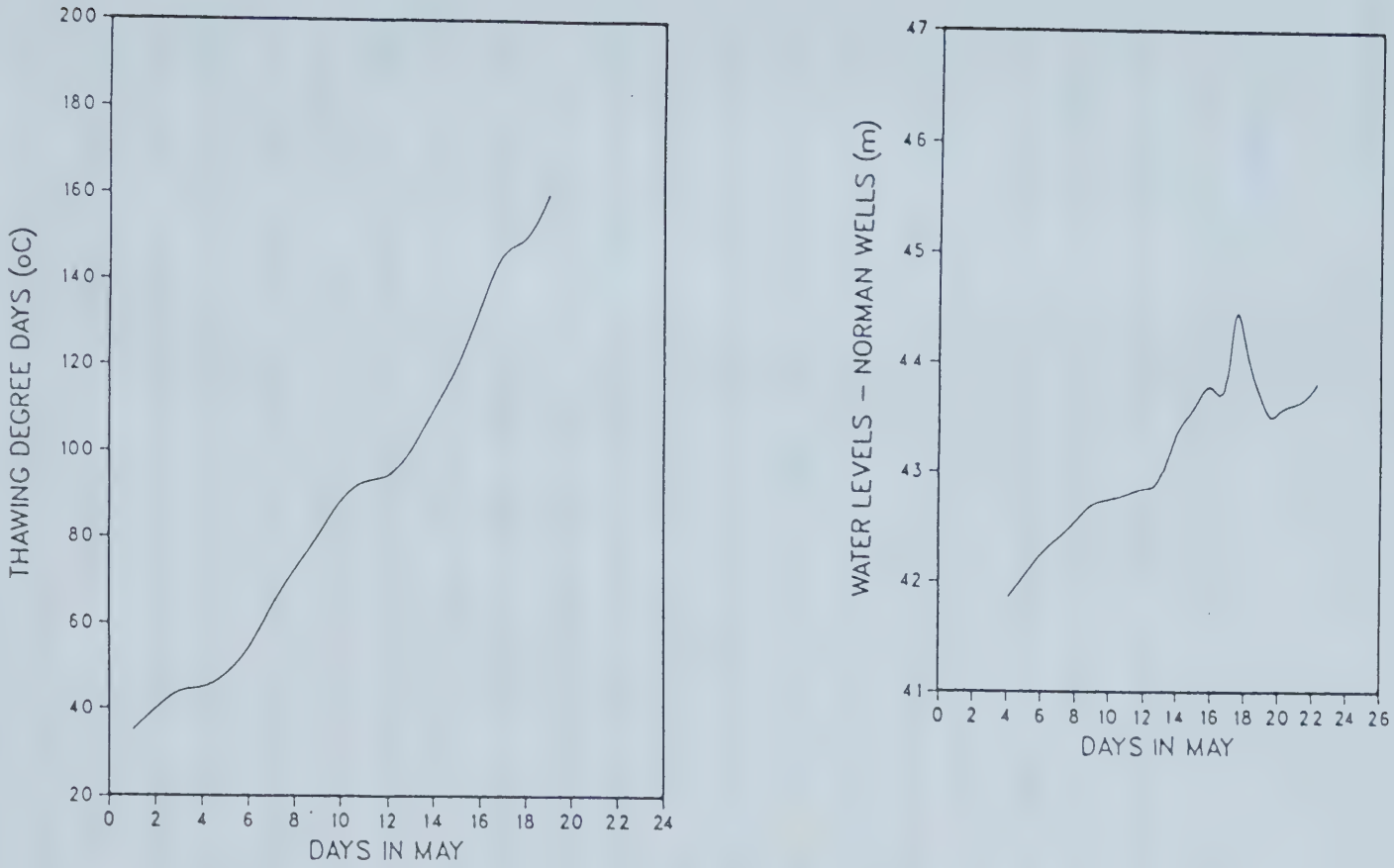

Figure 28. Thawing degree-days and water levels during breakup, Norman Wells, 1984.

4. CASE STUDY: ICE JAM AT NORMAN WELLS

4.1 Method

4.1.1 General

As pointed out earlier, the analysis of a given ice jam involves assumptions that are not often directly verifiable. In most cases, it is impossible to measure the thickness of the accumulation. Different methods have been proposed to obtain an indirect estimate for this parameter. As discussed previously, they all have certain limitations. Moreover, in most of the ice jam analyses reported in the literature, little attention has been given to the longitudinal thickness variation and the special conditions prevailing at the toe. Yet, these two aspects can govern the jam stability and release and have repercussions on ice jam control.

In the present study, the general approach was to use the well-known backwater model HEC-2 to simulate the water profile produced by the documented ice jam. An attempt was made to simulate as accurately as possible the actual configuration of the jam. As a first step, the ice thickness for the entire jam was fixed at various values within the expected range and the roughness subsequently adjusted so that the calculated profile agreed with that measured. This gave a set of pairs of thickness and roughness estimates, any pair of which would give a profile that agreed with the measurements. To choose the most appropriate pair, it was

assumed the underside of the accumulation had roughly the same appearance as the surface and the roughness most appropriate to this surface was selected. Another indirect check was made by using the equilibrium thickness theory. Finally, using the general theory proposed by Uzuner and Kennedy (1976) and the computer model, the analysis was refined to investigate the longitudinal variation of the ice jam and the special conditions prevailing at the toe.

Before presenting the results of these calculations, the following section will briefly describe the HEC-2 model used.

4.1.2 HEC-2 model

The HEC-2 computer program was developed by the Hydrologic Engineering Center of the U.S. Army Corps of Engineers and is intended for calculating water surface profiles for steady gradually varied flow in natural or man-made channels. The computational procedure is based on the solution of the one-dimensional energy equation using the 'Standard Step Method', with losses due to friction evaluated with Manning's equation.

The program has been recently modified to account for the presence of a floating ice cover (See Water Surface Profiles - Users Manual; Calkins et al, 1982). The principal modification takes into account the hydraulic aspects of flow under ice such as reduction in flow area, increased wetted perimeter, and ice roughness. The other ice-related

capability is an ice cover stability criterion.

The analysis of floating ice by HEC-2 has been accomplished through modification of the HEC-2 bridge code. Floating ice is handled by the program code as though it were a floating bridge. The standard techniques used to determine area blocked by a bridge deck and the additional wetted perimeter caused by a submerged low chord are employed for ice analysis. To determine a composite Manning's "n", the program utilizes the Sabaneev formula (Eq. 1). For the ice cover stability criteria, use is made of the dimensionless stability curve given by Pariset et al. (1966).

Program input. Input data requirements are identical to the standard HEC-2 requirements with the addition of an ice cover data card (IC card). This allows the user to specify: ice thickness in the three divisions of a cross-section (i.e. left overbank, right overbank and main channel); "n" value for the underside of the ice which is assumed the same for each division; the specific gravity of the ice; and in fields 6-10 a factor to modify ice thickness or ice "n" value for multiple runs. Ice cover calculations are halted by inputting a value of 0.01 for the specific gravity.

Program output. When ice flow calculations are made, the program will print the following statement: 4478 FLOW UNDER FLOATING ICE, followed in the next line by eight related

variables as shown below

FLOATING ICE COVER, ICE THICKNESS LOB= 5.0 CH= 1.7 ROB= 1.7

SPGR	ICE N	B-S N	C	B	H	T/H	X*K
.916	.0200	.0231	54.	2709.	18.8	.09	0.148

where: LOB = ice thickness in left overbank

CH = ice thickness in main channel

ROB = ice thickness in right overbank

SPGR = specific gravity of ice

ICE N = Manning's n value for ice

B-S N = composite n value

C = Chezy coefficient

B = wetted perimeter of ice

H = depth of flow (the distance from the underside of the cover to the lowest point in the cross-section)

T/H = ratio of ice thickness to depth

X*K = ice stability variable times 1000

Program limitations. The following assumptions are implicit in the analytical expressions used in the program:

(i) Flow is steady.

(ii) Flow is gradually varied.

(iii) Flow is one dimensional (i.e., velocity components in directions other than the direction of flow are not accounted for and, furthermore, the total energy head is assumed the same for all points on a cross section).

(iv) River channels have 'small' slopes, say less than 1:10 (so the pressure head used in the calculations can be represented by the water depth measured vertically).

4.2 Open water calibration

4.2.1 Background

The field survey carried out during the summer of 1983 provided a water profile under open water conditions (see Figure 22). The water level at Norman Wells was 40.8 m during the profile measurements. From the open water rating curve at Norman Wells, given on Figure 33, the discharge was 10 800 m^3/s. Cross-sectional data were obtained from the river bed configuration given by the hydrographic charts previously cited (Government of Canada Fisheries and Oceans, Hydrographic Service). As shown in Figure 29, a total of 26 cross-sections were used to describe the 100 km reach. Appendix E details each cross-section. With regard to the accuracy of the cross-sections thereby obtained, the cross-section at Norman Wells (referred to herein as

cross-section # 9) was compared to cross-section A-A' surveyed by Esso Resources Ltd. at the same location. This is shown on Figure 30. Using a water level of 45.0 m, which was approximately the water level prevailing during the jam event, the difference in the cross-sectional area from the two sections is about 5 per cent.

4.2.2 HEC-2 simulation

The profile obtained from the HEC-2 simulations is shown in Figure 31. The values of 'n' were varied to reflect expected changes in bed roughness as revealed by limited bore hole data available in this reach as shown in Figure 32. In general, low values of 'n', between 0.021 and 0.024, were required to get reasonable agreement with the measured profile. This is consistent with the nature of the river bed in this area.

As is apparent from Figure 31, the calculated profile departs from the measured one at two locations. One is upstream of Norman Wells (from km 898 to km 862). At this location, the discrepancy is probably due to the fact that the cross-sections were based on the depths extracted from the hydrographic charts, which in turn was based on a low water datum dating from 1974. This low water datum may have changed in the past 10 years. The flattening of the slope at Norman Wells is confirmed by the profile carried out in 1984 with an intact ice cover (see Figure 34). The other discrepancy, downstream of Fort Norman, is because there

were no bench marks in this reach so that no point could be surveyed during the summer. The much steeper slope at this location obtained from the low water data seems consistent with the constricted width of the channel at this location.

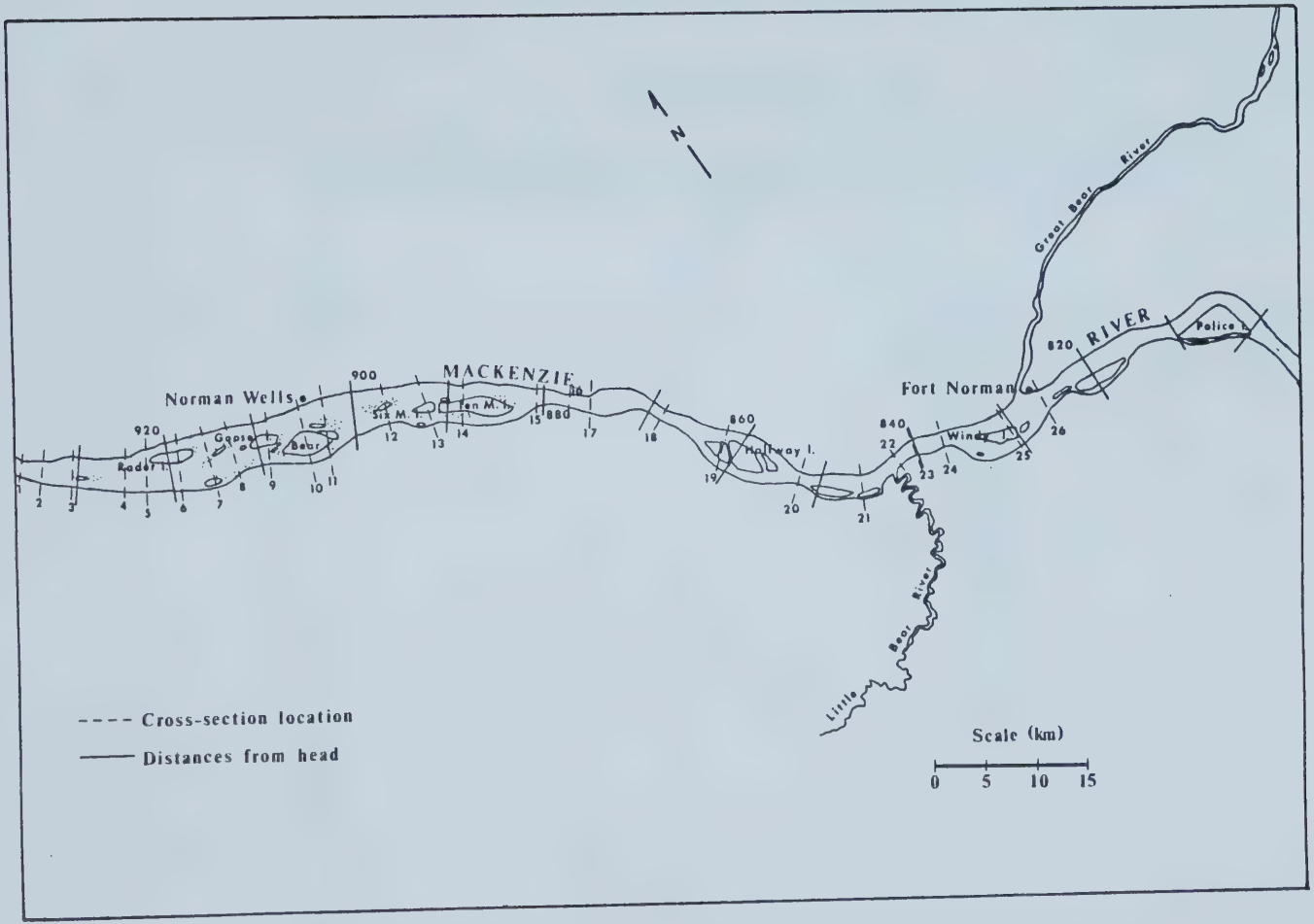

Figure 29. Cross-section locations between Fort Norman (km 828) and km 935.

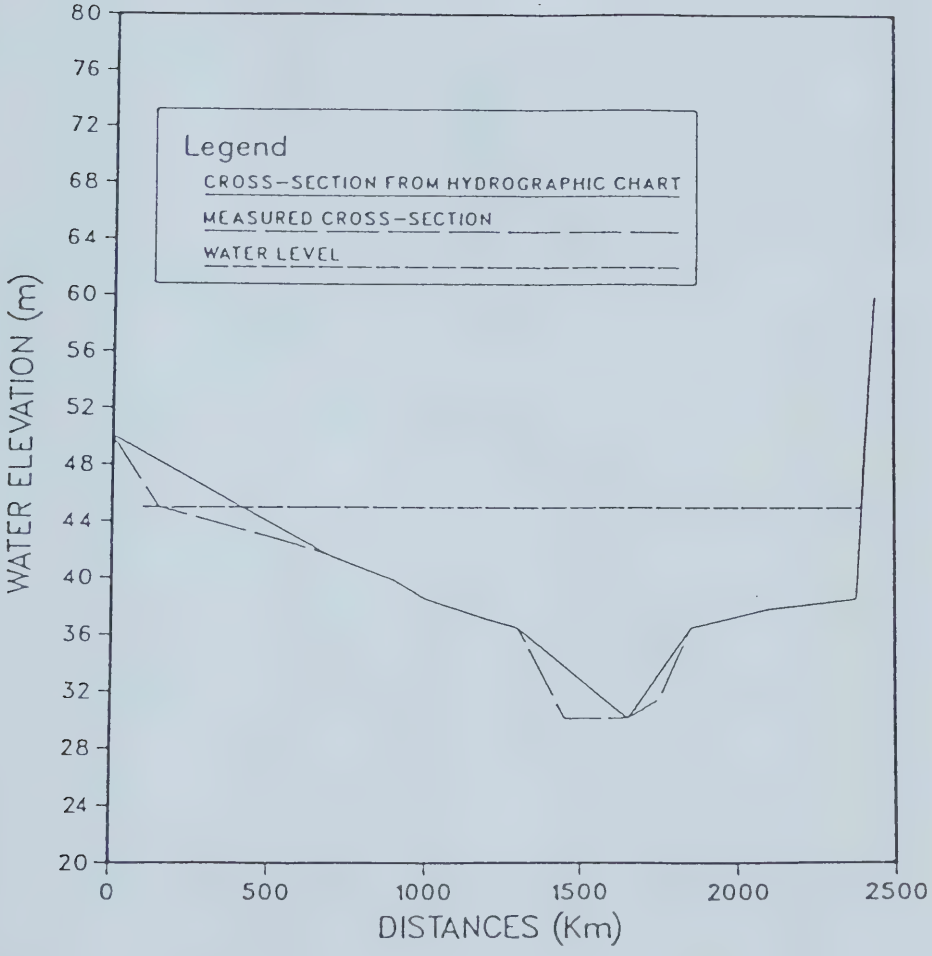

Figure 30. Comparison of measured cross-section and cross-section obtained from the hydrographic charts (km 904)

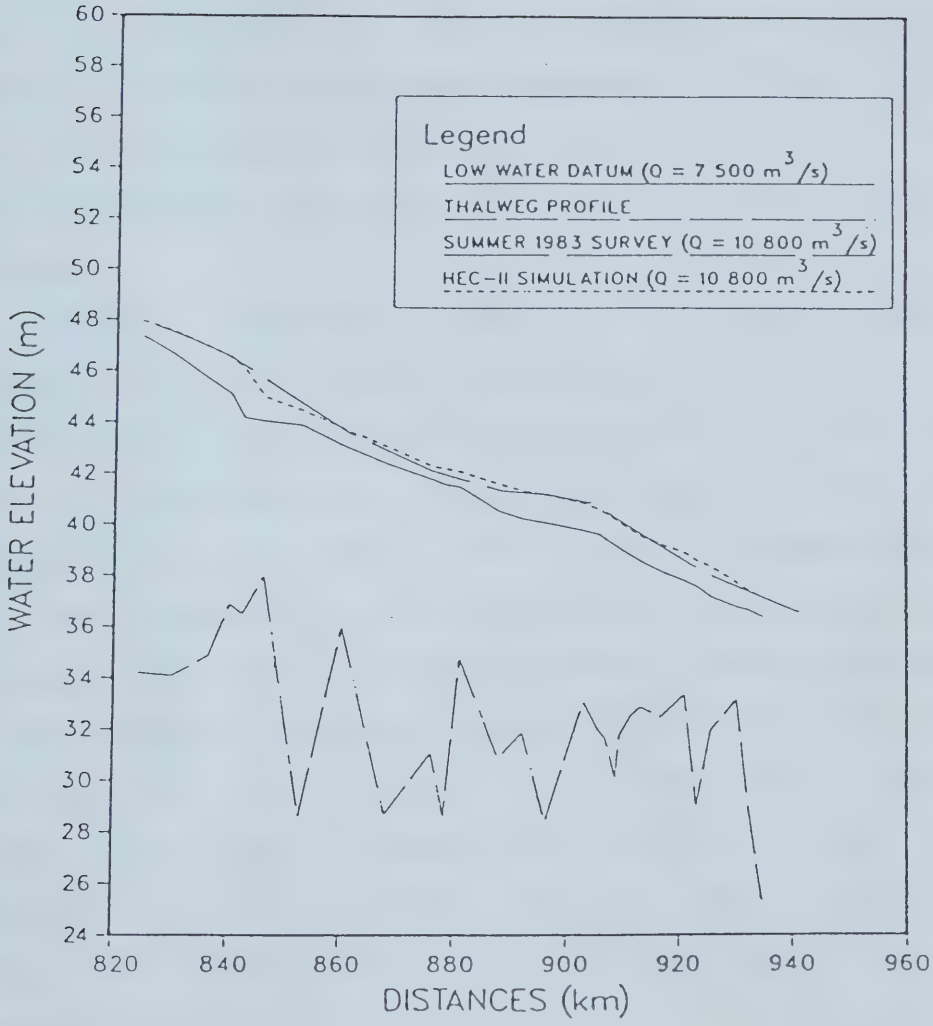

Figure 31. HEC-2 model, open water calibration.

4.3 Ice jam analysis

4.3.1 General background

As discussed earlier, the ice jam in the Norman Wells area was formed when the jam at Fort Norman released early on May 23. The water profile was measured at 20:30, about five hours after the ice movement stopped. At this time the jam was relatively stable and the water level was decreasing slowly.

Referring to Figure 32, the ice jam reach could be divided into four distinct sub-reaches with respect to the ice conditions. Downstream of approximately km 915, the ice sheet could be considered to be intact except for some large cracks. The next sub-reach, from km 915 to approximately 870, was composed of large floes mixed with mush ice at the downstream end, as shown in Figure 15 and, further upstream, of what seemed to be from the air relatively compact mush ice. From there to about km 856 (upstream of Halfway Island), the slush accumulation appeared somewhat less compact. Finally, in the last reach, up to Fort Norman (km 828), ice debris was still flowing toward the ice accumulation.

The ice jam analysis described in the following sections includes: the estimation of the discharge prevailing during the ice jam event; the model simulations with a constant thickness through the entire jam; the calculation of the internal friction parameter as defined by

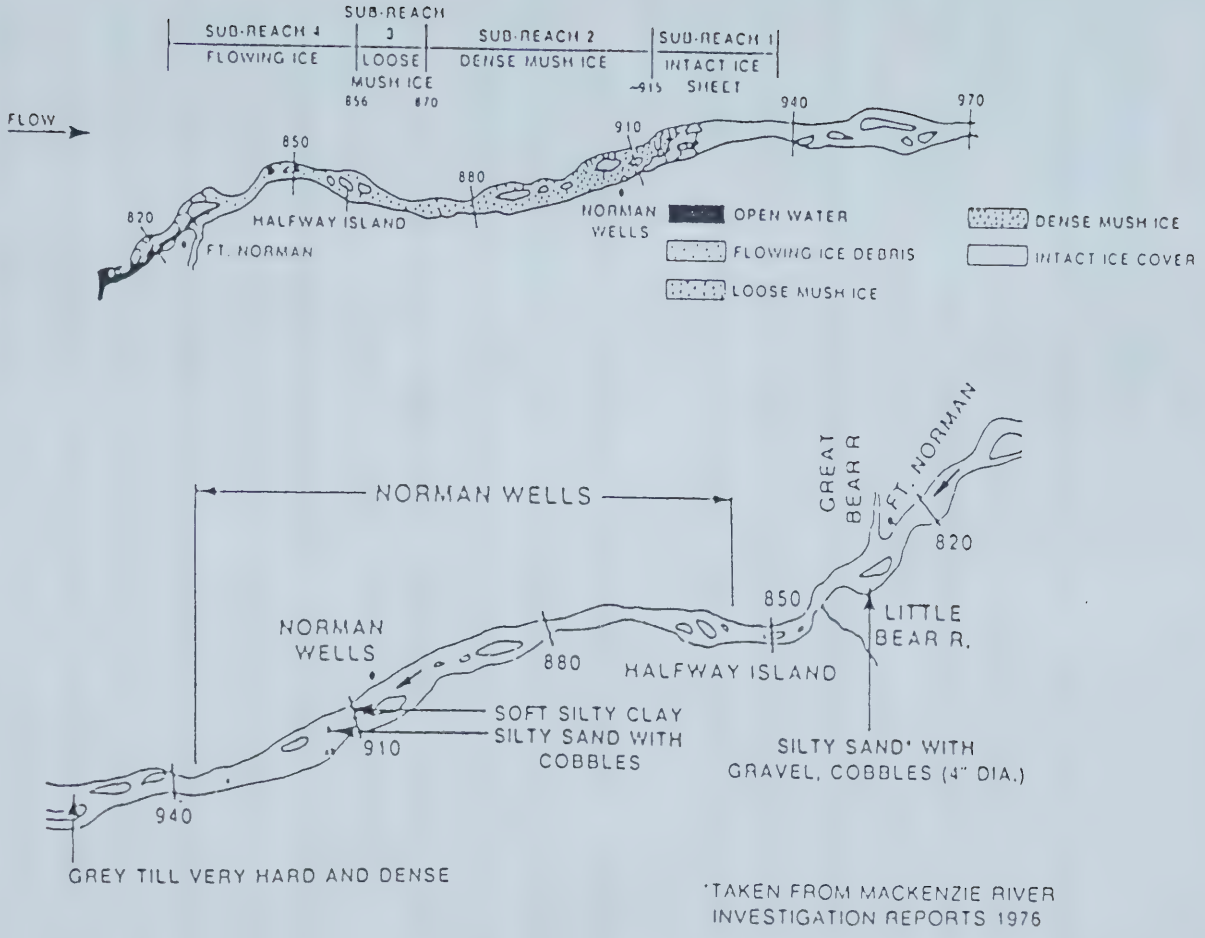

Figure 32. Ice conditions during 1983 ice jam and river bed data.

Pariset et al. (1966); the longitudinal variation of the ice jam thickness; and an investigation of the special conditions prevailing in the toe region of the accumulation.

4.3.2 Discharge estimation

A fundamental requirement for ice jam analysis is knowledge of the discharge while the ice jam is in place. This is very difficult to obtain. Most of the time the usual WSC gauges malfunction and give a poor measurement at breakup. In the present case, the WSC gauge at Norman Wells (# 10KA001) was effectively put out of order at about 14:30 on May 23, 45 minutes before the first noticeable ice movement.

The mean daily discharge at Norman Wells estimated by WSC on May 22 was 22 700 m^3/s. Presumably, this was based on an interpolation of the discharges measured at Fort Simpson (km 338) and Arctic Red River (km 1430) and the use of the open water rating curve adjusted for ice conditions. Other independent estimates are possible. Firstly, using the water level recorded photographically downstream of the ice jam in the "intact" ice sheet region (km 935.5), the discharge was computed using the cross-section data and assumed bed and ice cover roughness. Taking n_b as .024 and n_i as .021 (as confirmed by subsequent simulations), this gave about 10 000 m^3/s. If the error in the water level deduced from the air photos is assumed to be ± 0,3 m, the resulting error in the discharge estimation would be ± 5 % or approximately ± 600

m^3/s. The details of these calculations, along with the ones carried out for the other estimation methods, are given in Appendix F.

A second estimate makes use of the available discharge measurements performed by WSC during winter and spring at Norman Wells. Figure 33 shows the measurements obtained between 1978 and 1980. It is readily apparent from the figure that the measurements for the spring period and the ones for the wintertime form two distinct families of curves. As a first approximation, the points obtained during the spring can be extrapolated. Transposing the water level obtained photographically during the jam event for the still solid ice downstream of the jam to the gauge location at Norman Wells, results in a water level of approximately 44.1 m at the gauge and a discharge of about 13 000 m^3/s. It should be pointed out that this assumes that the Manning's 'n' for the ice does not increase at spring time when radiation input produces a deterioration of the ice sheet. As discussed earlier, a water profile with an intact ice sheet was carried out on May 9 in 1984 when no significant deterioration could be noticed on the surface of the ice. Figure 34 shows the HEC-2 simulations for this condition. The discharge of 9 600 m^3/s prevailing on May 9 was obtained from the rating curve for ice conditions (see Figure 33). The thickness assumed was 1.7 m. The results of the simulations indicate that n_i was about .012 during this period. This is presumably in the same range of values

during the W.S.C. discharge measurements as they were all carried out before May 11. However, subsequent simulations for the 1983 jam indicated that the ice sheet downstream of the jam, in sub-reach 1, was actually much rougher (n_i = .021). This is probably due to the effect of ice candling and the well-documented formation of ripples underneath the ice cover due to warm water and radiation input (Carey, 1966; Larsen, 1966). The discharge of 13 000 m^3/s would therefore be likely high.

Finally, a third estimate was made by using the more reliable water level recorded from the ground at Fort Norman and the cross-section at this location obtained from a previously cited reference (Mackenzie River Investigation Committee, Final report, 1976). At the time of measurement, the reach was in an almost open water condition, with only some ice debris still flowing down toward the head of the jam. The main concern was whether the location was in the backwater region of the jam. Assuming it was not, the discharge was estimated to be 14 700 m^3/s. If it was in the backwater, this estimate would be high.

In view of the above discussion, a compromise value of 12 000 m^3/s was used for the analysis. It is however recognized that the methods used were not very accurate and that the discharge could have been between 10 000 and 15 000 m^3/s. The effect of the discharge estimation on the analysis results will be discussed in a subsequent section.

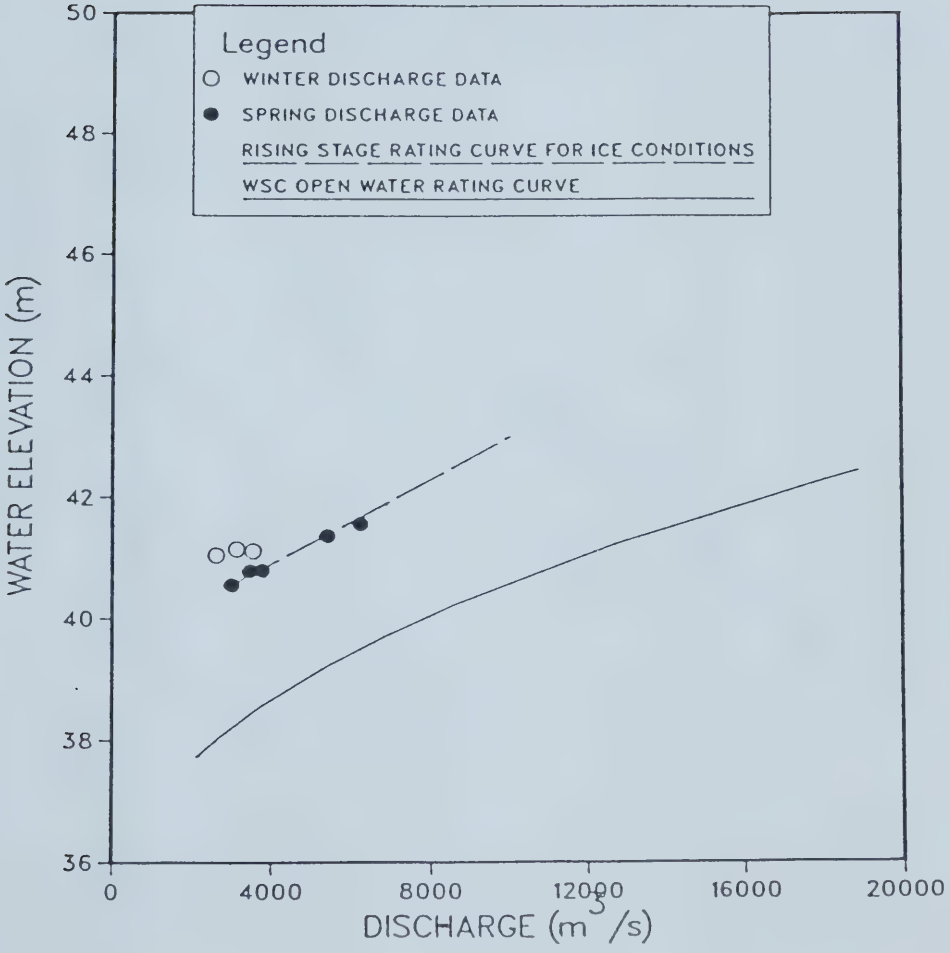

Figure 33. Open water, rising stage and falling stage rating curves at Norman Wells.

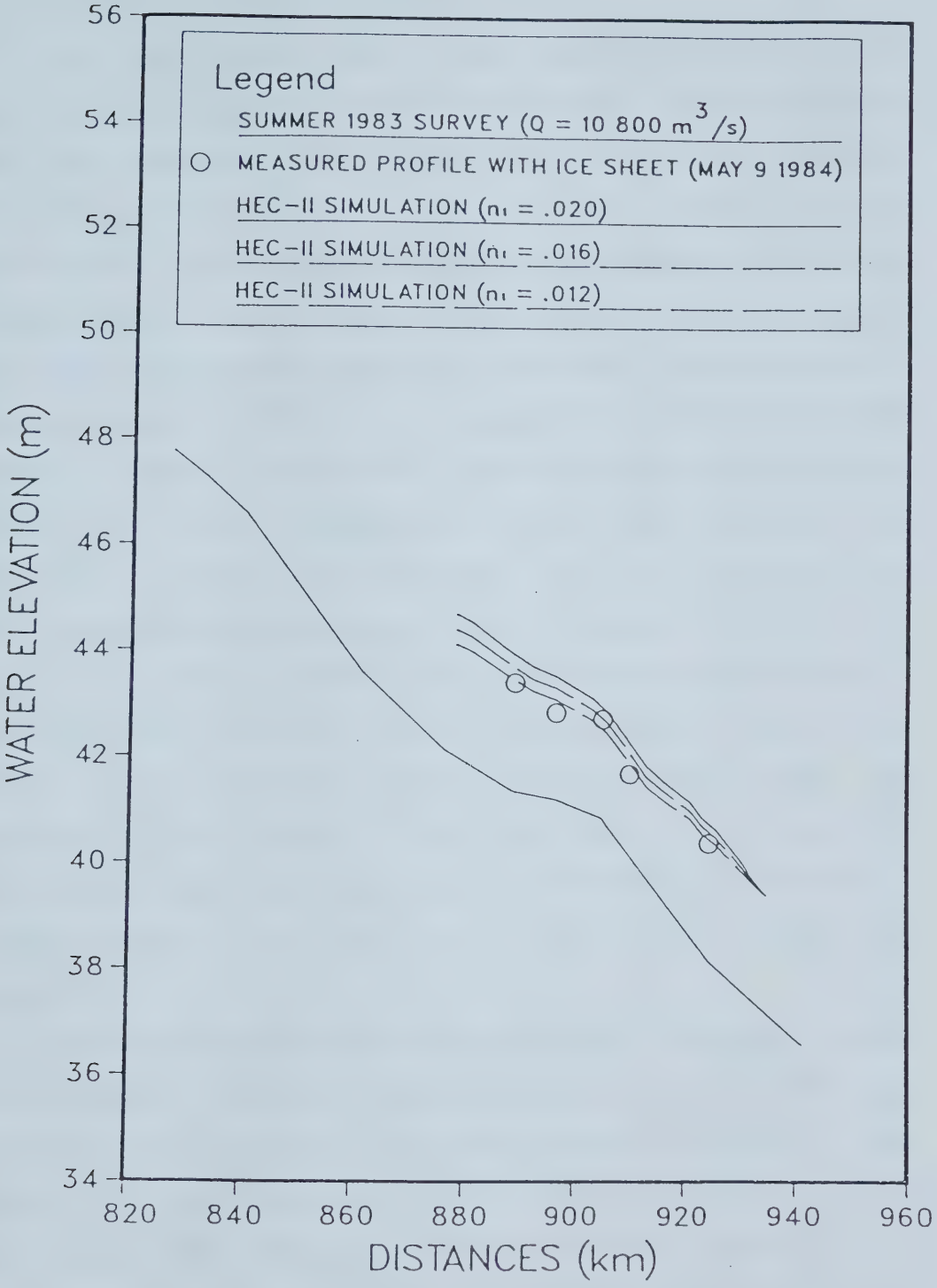

Figure 34. Intact ice sheet roughness.

4.3.3 Constant thickness simulations

The first step in the analysis was to simulate the ice jam, assuming a constant thickness through a good portion of the jam (sub-reach 2) and idealizing the ice configuration prevailing at the toe. As is apparent from Figure 22, the water level profile during the ice jam steepens in the toe region between approximately km 911, where two measurements were obtained photographically, and km 905, where the water levels at Norman Wells were measured directly from the ground. As shown in Figure 35, the ice conditions in the toe region were rather complicated. They were idealized by assuming, as a first approximation, that the accumulation at this location was composed of fairly homogeneous mush ice with its interface with the intact ice sheet in sub-reach 1 at km 914. In terms of the cross-sections defined for this study, the thickness and roughness were varied at cross-section # 8 (km 912). This permitted the calculated profile to pass through the two points at km 914 and to steepen thereafter to reach the higher water levels at Norman Wells.

Roughnesses and thicknesses were then estimated using the backwater model to simulate the water profile. The ice thickness for the intact ice sheet region (sub-reach 1) was taken as 1.68 m as given by a W.S.C. measurement on April 22. The ice sheet Manning's "n" was estimated to be 0.021 from HEC-2 simulations. In sub-reach 2, the toe and main body of the jam, the best-fit roughness was estimated for

assumed thicknesses between 3 and 5 m.

The results obtained for the cross-section at km 881.1 are given in Table 3. Figure 36 shows the ice conditions at this location, which is just upstream of Ten Mile Island, where the channel is undivided. Each pair of thickness and roughness in the first two columns of Table 3 provides a reasonable fit to the measured profile from km 914 to approximately km 870. Upstream of that point a thickness of 1,6 m, with the same roughness as in the previous reach, gave a better fit. In the last sub-reach, from approximately km 856 (upstream of Halfway Island) to Fort Norman, the resistance of the ice cover was ignored as the ice was still flowing toward the head of the jam at the time of measurement. This allowed the profile to pass through the reliable water level measurement at Fort Norman.

After the relation between the thickness and the roughness had been determined, the hydraulic parameters computed by the model were used to calculate the composite roughness in terms of the effective hydraulic roughness "k" instead of Manning's "n". Using the mean depth (approximately equal to 2R or A/B), the slope of the energy line at the given location and the average velocity, the composite roughness was calculated using the semi-logarithmic expression (Table 3, column 3). After this had been done, the ice roughness could be computed. Two approaches were used to determine this parameter. The first method (Table 3, column 4) was to use the Sabaneev equation

rewritten in terms of "k" instead of "n". Based on the open water simulations, the values of k_b in the reach of interest varied from 0,034 to 0,09 m. An average of 0,05 m was used for the present calculations. Any error in this parameter is not very important here as the ice jam roughness is more than one order of magnitude greater than the river bed roughness and therefore contributes to a much larger degree to the overall roughness. The second approach to evaluate the ice roughness (Table 3, column 5) was to use the semi-logarithmic equation applied to the regions associated with each boundary. Assuming that $V = V_b = V_i$, the depth of flow associated with the river bed was first determined from the semi-logarithmic equation applied to that region. Then h_i was determined from $h_j - h_b$ (h_j being the mean flow depth under the jam). Finally, the semi-logarithmic expression was solved to get k_i. Comparing the values obtained from the two approaches, it is apparent that the roughness as calculated from the Sabaneev equation is much larger than that given by the semi-log expression, especially for a very rough boundary. This is not unexpected as the experimental evidence suggests that for high values of R/k the Manning's equation does not apply very well, whereas the semi-log expression is quite rugged (see Figure 3).

TABLE 3

SUMMARY OF HEC-II SIMULATIONS (CONSTANT THICKNESS) ($Q = 12\,000\ m^3/s$)

(Cross section Km 881.11

t_i (m)	n_i*	k_n (m) **	k_i (m) *** (Power expression)	k_i (m) **** (Semi-Log expression)
3.0	.076	3.4	25.4	11.8
3.5	.069	2.6	18.3	9.35
4.0	.06	1.7	10.8	6.05
4.5	.05	0.93	4.6	3.25
5.0	.040	0.40	1.6	1.62

* Calculated so that the calculations fit the measured profile in sub-reach 2 (toe and main body of the jam).

** Calculated from model output using the standard semi-logarithmic expression

$$V/V_* = 2.5\ \ln(R/k_s) + 6.2$$

*** Calculated from the Sabaneev equation expressed in terms of k:

$$k_s = k_i \left((1 + (k_i/k_s)^{-0.25})/2\right)^4$$

**** Calculated from model output using the semi-logarithmic expression with the hydraulic radius associated with the ice.

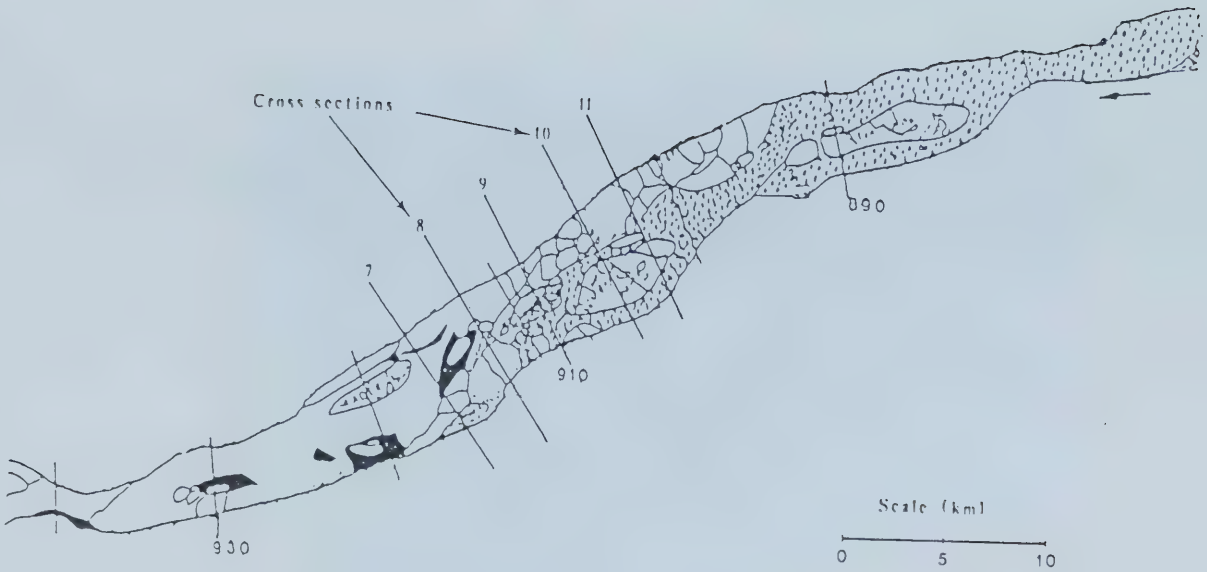

Figure 35. Toe conditions for the 1983 ice jam at Norman Wells.

Figure 36. View of ice accumulation in equilibrium reach.

Based on the results shown in Table 3, the most reasonable pair of roughness and thickness could then be chosen. Although it was impossible to get a close-up view of the mush ice surface appearance for the jam being analysed, it could be assumed that its appearance was not very different from that of the jam in the Fort Norman area. This was shown on Figure 17. Based on this information and noting, as discussed previously, that $\Delta < k < 3\Delta$, the best choice seemed to be $k_i \cong 3.3$ m ($n_i = 0.05$) and $t_i = 4.5$ m.

4.3.4 Equilibrium thickness and internal friction coefficient

The hydraulic parameters calculated by the model were used to evaluate the internal friction coefficient μ. The coefficient was computed using Eq. 10. The approach was to use the semi-logarithmic expression to calculate the depth of flow associated with the river bed, h_b, and then to obtain the depth of flow associated with the ice jam h_i by computing $h_j - h_b$. The shear stress under the accumulation could then be calculated with Eq. 21 and substituted into the equilibrium thickness equation to obtain the internal friction coefficient.

The results are given on Figure 37. The calculations were carried out from cross-section # 9 (km 908.5) to cross-section # 16 (km 878.4) and for thicknesses of 5, 4.5 and 4 m. The reach from cross-section # 12 (km 896.4) to cross-section # 16 (km 878.4) could be considered a

reasonable approximation to an equilibrium reach. For a thickness of 4.5 m, which has been accepted in the previous section as the one representative of equilibrium conditions, the average μ for the equilibrium reach is 1.6.

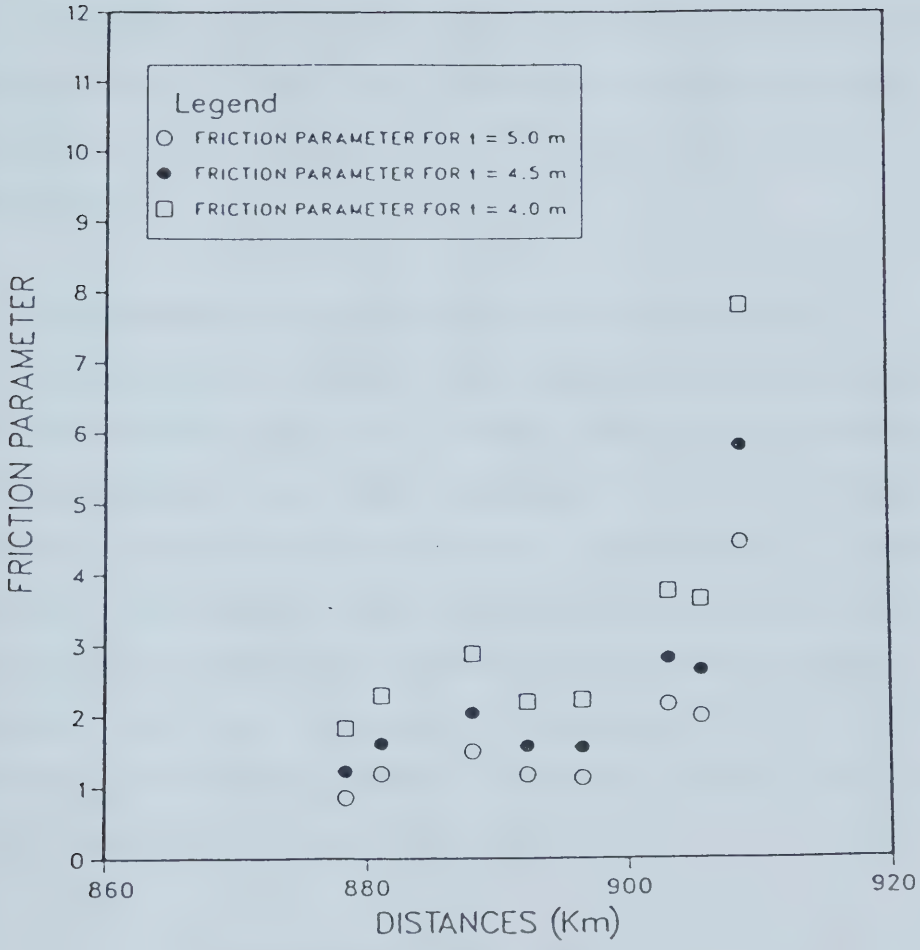

Figure 37. Variation of μ along the 1983 ice jam in the Norman Wells area.

As the energy slope further downstream steepens, this produces a gradual increase in the required value of the coefficient, reaching a maximum of 5.8 at cross-section # 9 (km 908). If we assume the coefficient should be more or less a constant for a particular jam, this increase would indicate an increase of thickness in the toe region. The longitudinal variation of the thickness is discussed in the next section.

4.3.5 Longitudinal variation of ice jam thickness

As pointed out earlier, the general equation derived by Uzuner and Kennedy (Eq. 17) for the stresses involved within an accumulation can be integrated to obtain the ice thickness variation along the jam. The equation, compared with the one describing equilibrium conditions, has an additional term, $(\partial t^2(K\gamma)/\partial x)$, that takes into account the variation of the thickness. To determine a value for the coefficient of passive thrust, K, we can use the definition of the internal friction coefficient:

$$\mu \equiv \tan\phi \, \tan^2(45 + \phi/2) \, (1 - e) \qquad (25)$$

Assuming a porosity of 0,4, this gives an angle ϕ of 35° for μ = 1.6. Consequently, the value used in the present calculations for K was 3.7.

Assuming that μ was constant at 1.6 throughout the jam and that the configuration at the toe was still the

idealized one discussed previously, the ice thickness variation was calculated with a hand-held calculator. The hydraulic parameters obtained from the simulations with constant thickness were used as a basis to compute the thickness profile. The first step in the computations was to assume a trial thickness for the next station and to evaluate the corresponding total mean depth of flow under the jam. The depth of flow associated with the ice could then be computed with the semi-logarithmic expression. The shear stress under the ice jam was then calculated and substituted into equation 16 which was finally solved. If the trial value of the thickness did not satisfy the equation the whole computation was repeated and the solution found by trial and error. The iteration process was completed in two steps. The calculations were first initiated at a cross-section approximately in the middle of the equilibrium reach (km 890) and carried out in the downstream direction. In the second step, the thickness at the leading edge of the jam, at km 860, was assumed to be zero and the calculations were carried out from that point in the downstream direction until the equilibrium thickness was reached.

The calculated ice thickness profile is presented on Figure 38. At the upstream end, the thickness reached equilibrium after approximately 16 km, or about 8 times the average width of the river at this location. In the toe region, thicknesses departed from the equilibrium thickness

where the energy slope began to differ from the uniform open water slope (km 903) and reached 7.7 m at the last cross-section before the intact ice sheet (cross-section # 9, km 908.5). Using these newly calculated thicknesses, the HEC-2 model was again used to simulate the ice jam profile. Supercritical flow was attained in the toe region. This is unlikely to be the situation in the field and simply indicates the initial estimates of the jam thickness variation gives values that are too high near the toe. Also, no allowance was made for the detailed ice configuration near the toe: the same thickness was used across the whole of each section. It was therefore attempted to refine the analysis at the toe to take into account the actual ice conditions at this location.

4.3.6 Special conditions at ice jam toe

As shown in Figures 15 and 16 and schematized on Figure 35, the actual ice conditions prevailing in the toe region were far from the idealized conditions assumed so far in the analysis. The mush ice actually pushed its way to the left side of Six Mile Island (km 892) and into the secondary channel behind Goose and Bear Islands, leaving the main channel covered with a severely cracked but still in place ice cover. It could then be assumed that the accumulation in the left channel, composed exclusively of mush ice, had a thickness and roughness larger than in the ice in the main channel where the ice sheet was severely cracked but still

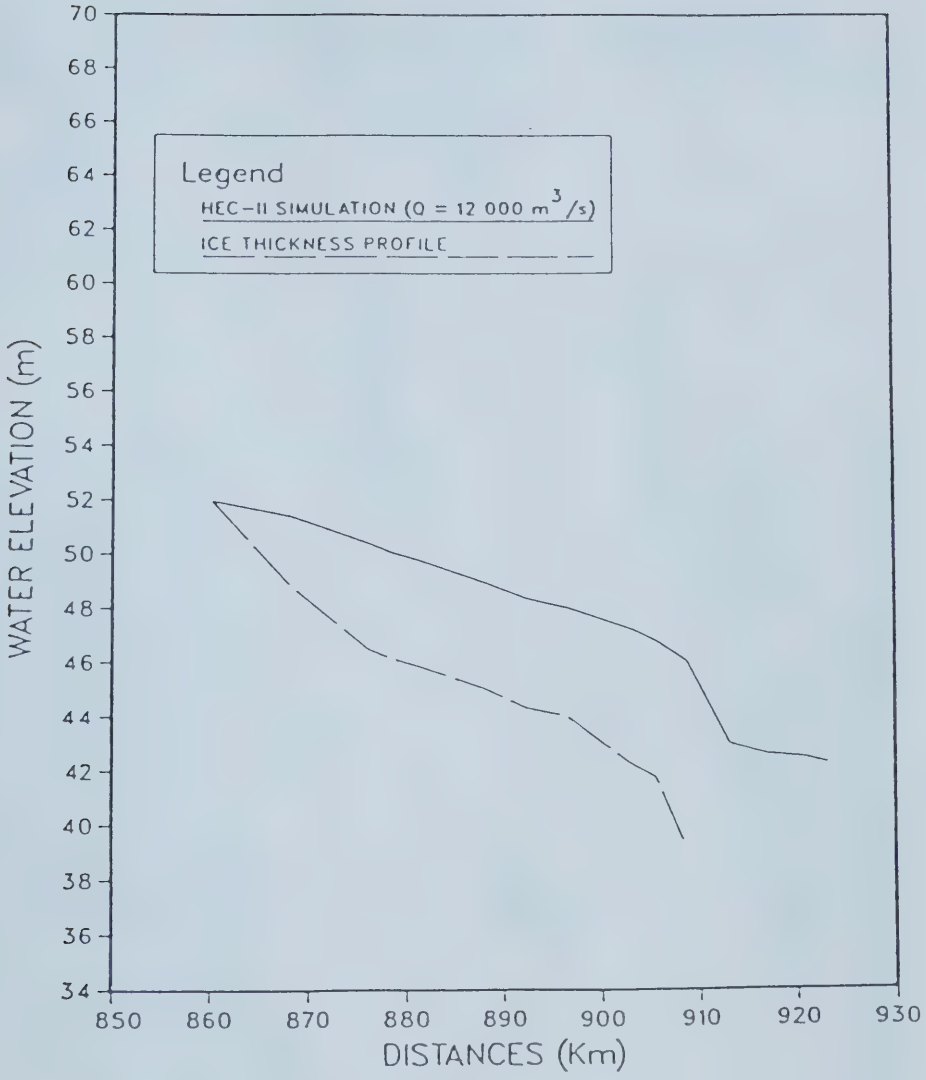

Figure 38. Computed ice thickness profile for the 1983 ice jam.

Figure 39. Bathymetry of the Mackenzie River in the Norman Wells area (Modified from Hydrographic charts, Dept. of Fisheries and Ocean, 1983).

in place. Based on the above observations, the HEC-2 model was tentatively used to allow for the special toe conditions. However, the HEC-2 capabilities for this kind of analysis were found to be limited. Although up to three different ice thicknesses can be specified at one specific cross-section (by specifying the left overbank, the main channel and the right overbank), the model does not allow the ice roughness to vary across the channel. As the normal HEC-2 program, without the ice option, accepts a lateral variation of the Manning's "n" through its optional card NH, it was tried to reverse the two boundaries, i.e. to consider the river bed as the ice undersurface and vice-versa, in order to be able to vary "n". Unfortunately, this procedure did not prove successful as the variations were somehow ignored by the model.

Given these limitations, the analysis was built upon some assumptions based on a careful examination of Figures 15 and 16. As discussed earlier, the cross-sections in the toe region could be divided into two sub-regions: the one in the secondary channel behind Bear and Goose Islands, composed of probably thick mush ice and the one in the main channel, where the ice could be assumed to be in general 1.7 m thick. As apparent from Figure 16, the mush ice pushed its way behind Bear Island and was diverted thereafter to the right and stalled just downstream of Bear Island, at approximately km 912. At this location, a shallow area near the left bank, as revealed by the bathymetry shown on Figure

39, probably acted as an obstruction to the thick ice accumulation moving downstream. As pointed out earlier, the major increase in water level occurs between km 911.5 and Norman Wells at km 905 (see Figure 22). This is the reach where the solid ice cover remained on the thalweg.

The first step was to increase the number of cross-sections in the area of concern to increase the flexibility of the simulations. As shown in Figure 35, two cross-sections (# 81 and # 82 at km 911.5 and 909.4 respectively) were added between cross-sections # 8 (km 913) and 9 (km 908.5). Another section (# 91, km 906.8) was also inserted between cross-section # 9 and # 10 (km 905.5). Each cross-section in what can be considered to be the toe area, from # 8 to # 11, were then divided into two sub-sections, one for the secondary channel and one for the main channel. Given the above observations, the simulations could then be carried out. The ice thickness used for the secondary channel was 5.5 m. This value is between the 4.5 m determined from previous equilibrium calculations and an upper value of 6.5 m which, as revealed by subsequent simulations, would produce a complete blockage of the channel. As the thickness is likely to be greater than the equilibrium thickness because of the dynamic mode of formation, the compromise value of 5.5 m seemed reasonable.

Subsequent simulations showed that the sub-section in the secondary channel did not contribute more than 10 % of the total flow at each of the cross-sections considered, with values as low as 2.6 % for cross-section # 81.

For the sub-region of the main channel, the thickness was set at 1.7 m from cross-section #8 (km 913) to # 11 (km 903) in a first attempt as the ice appeared to be still "in place" in the reach of interest (see Figure 16). Given the above thicknesses, the roughness was then increased so that the simulated profile fitted the measured one in this area. A value for the Manning's "n" of 0.070 was found to be necessary from cross-sections # 8 (km 913) to 91 (km 906.8). At cross-sections # 10 (km 905.5) and # 11 (km 903), which were located upstream of the major increase in water level and which form the transition between the toe and the uniform reach assumed to begin at cross-section # 12 (km 896.4), the thicknesses used were still 1.7 m but the roughness was 0.05.

Subsequently, using the hydraulic parameters computed by the model, the values of the hydraulic roughness at each cross-section were then computed by the method outlined previously, using the semi-log expression applied to each boundary. The values of roughnesses were found to be between 4.9 and 7.4 m. Given this range of values a constant hydraulic roughness of 5 m was assumed and the Manning's "n" for each cross-section in the toe area was then calculated using Eq. 9. The variation in Manning's "n" was then as

shown in Table 4.

Cross-section (location)	Manning's "n"
8 (913)	0.083
81 (911.5)	0.077
82 (904.9)	0.070
9 (908.5)	0.068
91 (908.5)	0.070
10 (905.5)	0.066

Table 4. Computed variation of Manning's "n" at the toe.

These values of "n" were then entered as input and provided a good fit to the measured profile, the increased Manning's "n" at the downstream end of the toe (sections 8 and 81)

compensating for the lower values further upstream. Hence it would appear that the hydraulic roughness of what is apparently a solid in place ice sheet is about 5 m. The formation of localized ridges, as apparent from Figure 18. might be responsible for this roughness increase.

Another possible physical explanation for that anomaly may be that some mush ice had been pushed underneath the ice sheet when the jam was formed. This could have been possible on the right side of Goose and Bear Island. To investigate that, the same kind of analysis as described above was carried out, except that this time the thickness in the main channel was increased to see what effect this would have on the necessary hydraulic roughness. The results are shown on Figure 40. For a probable thickness varying from 1.7 to 3.0 m in the main channel, the necessary constant hydraulic roughness to simulate the profile in the toe area would vary approximately from 5 to 2.6 m. Hence for a thickness of 2 m the necessary roughness falls to the same range of values as the roughness computed for the equilibrium reach (k_i = 3.3 m). It seems, therefore, that the sudden increase in water level at the toe can be quite satisfactorily simulated without appeal to grounding.

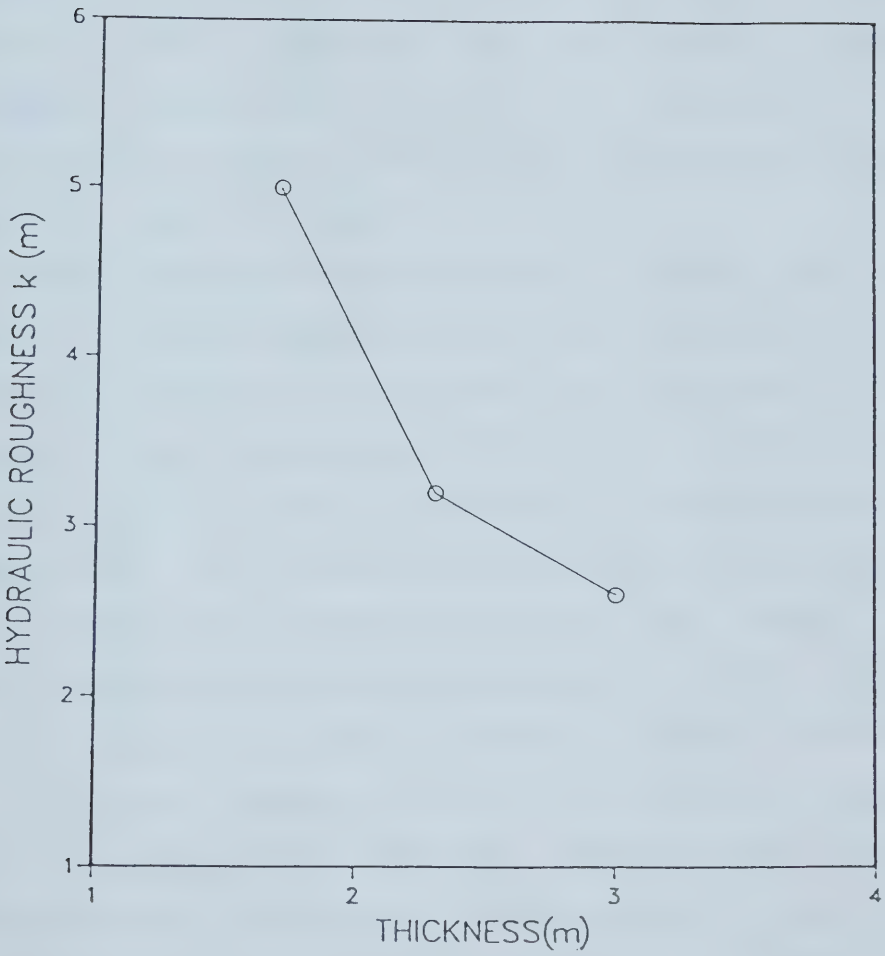

Figure 40. Variation of hydraulic roughness with the thickness at the toe.

4.4 Discussion of 1983 ice jam analysis

4.4.1 Final ice jam simulation

The complete simulated water profile obtained from the analysis described in the preceding sections are shown on Figure 41. As is apparent from the figure, reasonable agreement with the measured points was obtained through the entire reach affected by the jam. The calculated thickness profile is shown in Figure 42.

However the analysis performed to obtain the profile relied on several assumptions as it was not possible to get a direct estimate of the thickness. The following sections appraise these assumptions with respect to their validity and applicability. First, the effect of the discharge on the computed ice jam characteristics and the water levels at Norman Wells will be quantified. Second, the value of the equilibrium thickness, as estimated by the present analysis, and its effect on the related internal friction coefficient and the stage produced by the jam in the equilibrium reach will be discussed. Then the ice thickness and roughness variation along the jam will be compared with existing data. Finally, a review of the basic assumptions involved in the analysis and their inherent limitations will be given.

4.4.2 Effect of discharge

Estimation of the discharge prevailing during the jam event is of primary importance to any ice jam analysis.

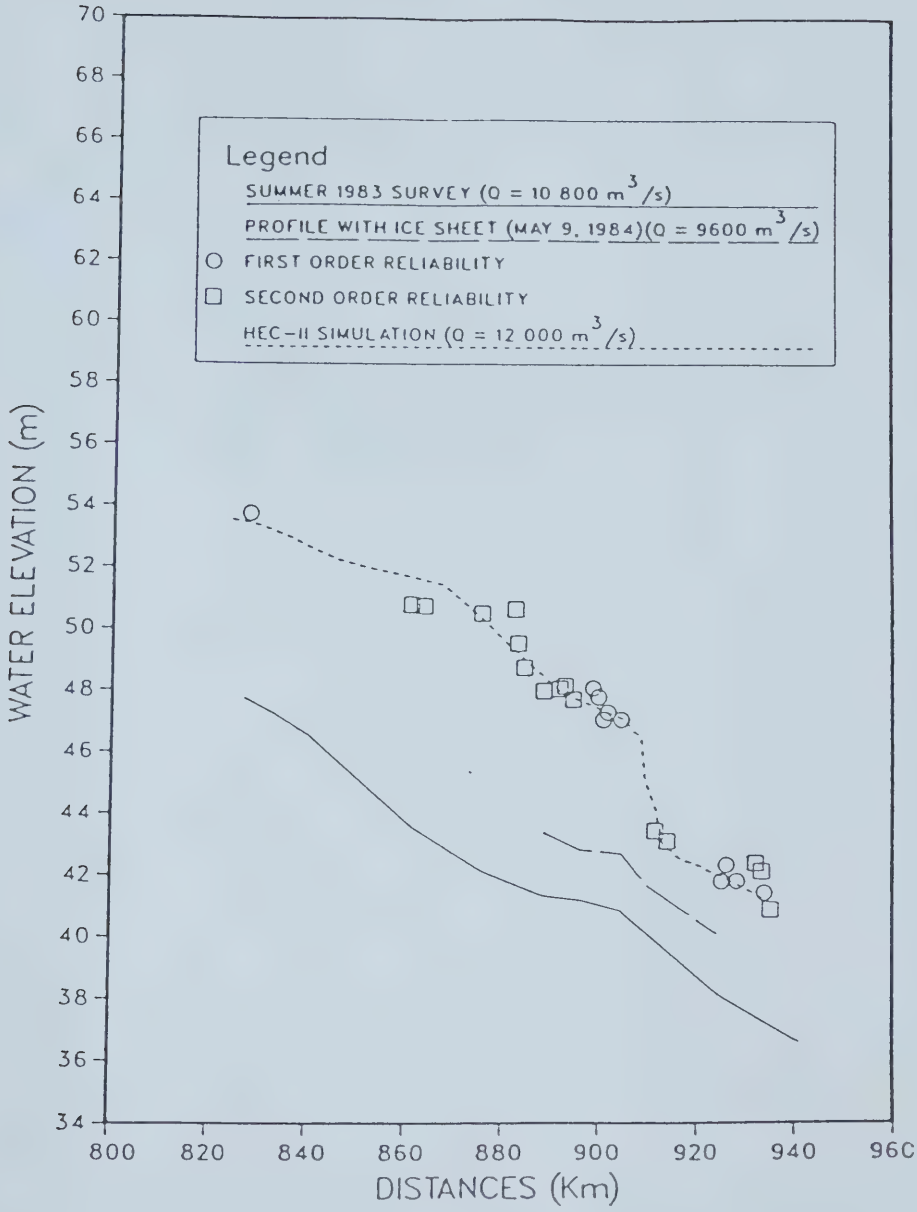

Figure 41. Complete simulated water profile for the ice jam at Norman Wells.

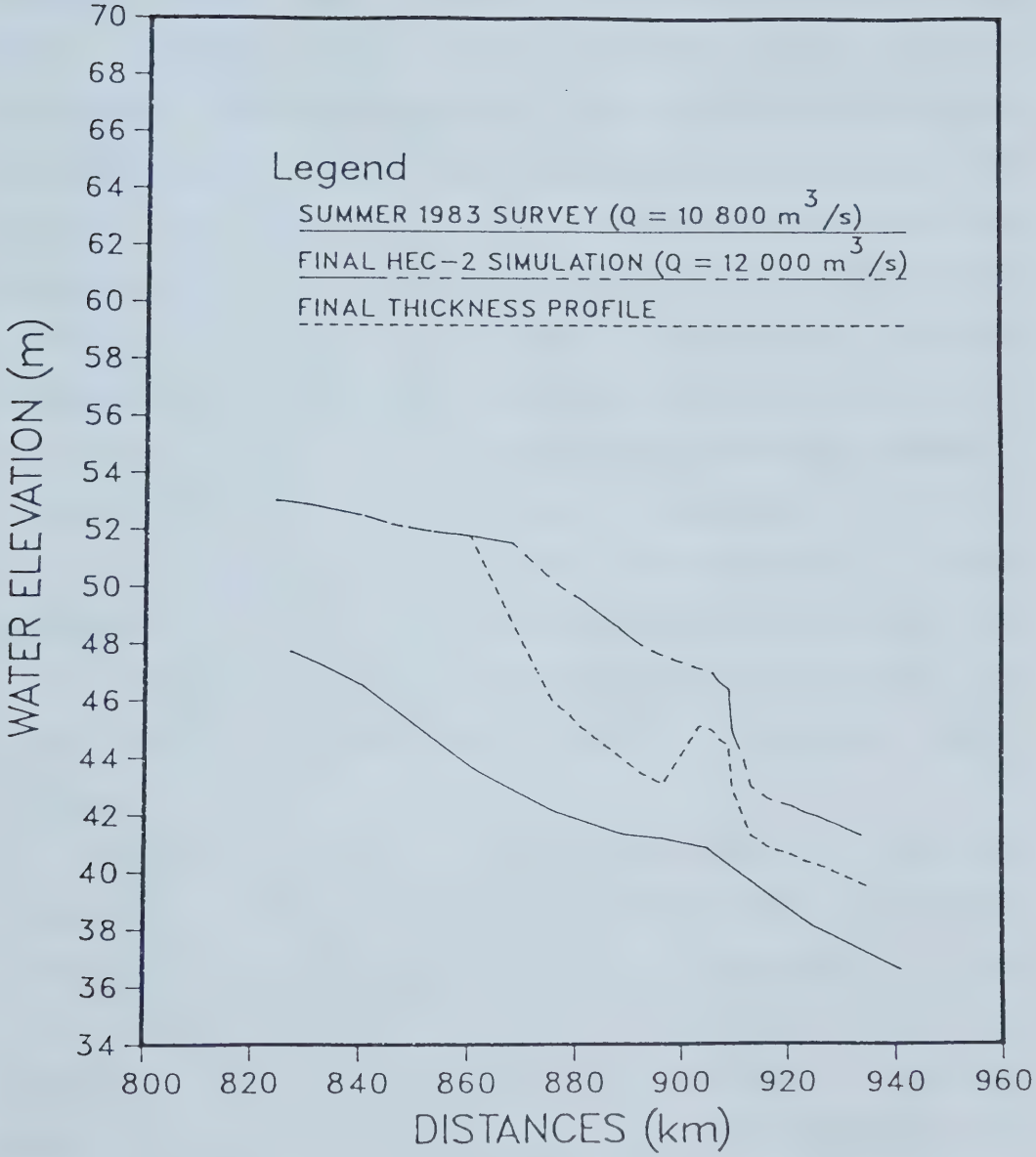

Figure 42. Complete simulated ice thickness profile for the ice jam at Norman Wells.

As described earlier, the estimate used in this analysis was determined from indirect methods having varying degrees of reliability. The assumed value of 12 000 m^3/s could therefore have been in error. A different discharge would have a direct effect on the thickness and roughness estimates. The quantification of the possible effect of the discharge on the analysis was approached from two different angles. The influence of the discharge estimate on the computed jam characteristics, i.e. mainly on the equilibrium thickness and the internal friction coefficient μ, was first investigated by comparing the values previously presented to the ones obtained with a different discharge. Secondly, using the results from the constant thickness simulations, the HEC-2 model was run with a thickness of 4.5 m and a Manning's "n" of 0.05 but for discharges varying from 10 000 to 20 000 m^3/s to investigate the sensitivity of the water levels to different discharges, but for a similar jamming event.

Table 5, which is similar to Table 3 previously presented, gives a summary of the results for the constant thickness simulations carried out with a discharge of 14 700 m^3/s instead of 12 000 m^3/s as used in the detailed analysis, a difference of about 20 %. As shown in Tables 5 and 3, the equilibrium thickness for a discharge of 14 700 m^3/s would fall in the 3.5 to 4.0 m range compared to 4.5 to 5.0 m for the 12 000 m^3/s simulations. As discussed earlier, this choice of thicknesses is suggested by the fact that the

hydraulic roughness, as revealed by field evidence, should be somewhere between 1 and 3 times the equivalent diameter of the larger roughness projections. Using thereafter the hydraulic parameters as computed by the HEC-2 model for the simulation with a thickness of 4.0 m (for a discharge of 14 700 m^3/s), the internal friction was calculated for two sections in the assumed equilibrium reach of the jam. The results are shown in Table 6. The average value of μ was 1.8.

	km 881.1	km 878.4
S	0.000111	0.000119
B	2164	1331
H	8.95	11.6
A	19 366	15 431
V	0.76	0.95
t	4.0	4.0
k_o	0.68	0.67
k_1	0.05	0.05
k_i	3.3	3.2
τ	7.21	10.0
μ	2.0	1.6

Table 6. Computed values of μ in equilibrium reach for Q = 14 700 m^3/s.

TABLE 5

SUMMARY OF HEC-II SIMULATIONS (CONSTANT THICKNESS) ($Q = 14\,700\ m^3/s$)

(Cross section Km 881.1)

t (m)	n_i *	k_0 (m) **	k_i (m) *** (Power expression)	k_i (m) **** (Semi-Log expression)
3.0	.062	2.4	16.5	7.7
3.5	.055	1.35	8.0	4.1
4.0	.045	0.68	3.3	1.85
4.5	.035	0.26	0.85	0.6
5.0	.028	0.11	0.22	0.22

* Calculated so that the calculations fit the measured profile in sub-reach 2 (toe and main body of the jam).

** Calculated from model output using the standard semi-logarithmic expression:

$$V/V_* = 2.5\ \ln(R/k_0) + 6.2$$

*** Calculated from the Sabaneev equation expressed in terms of k:

$$k_0 = k_i \left((1 + (k_i/k_i)^{-0.65})/2\right)^4$$

**** Calculated from model output using the semi-logarithmic expression with the hydraulic radius associated with the ice.

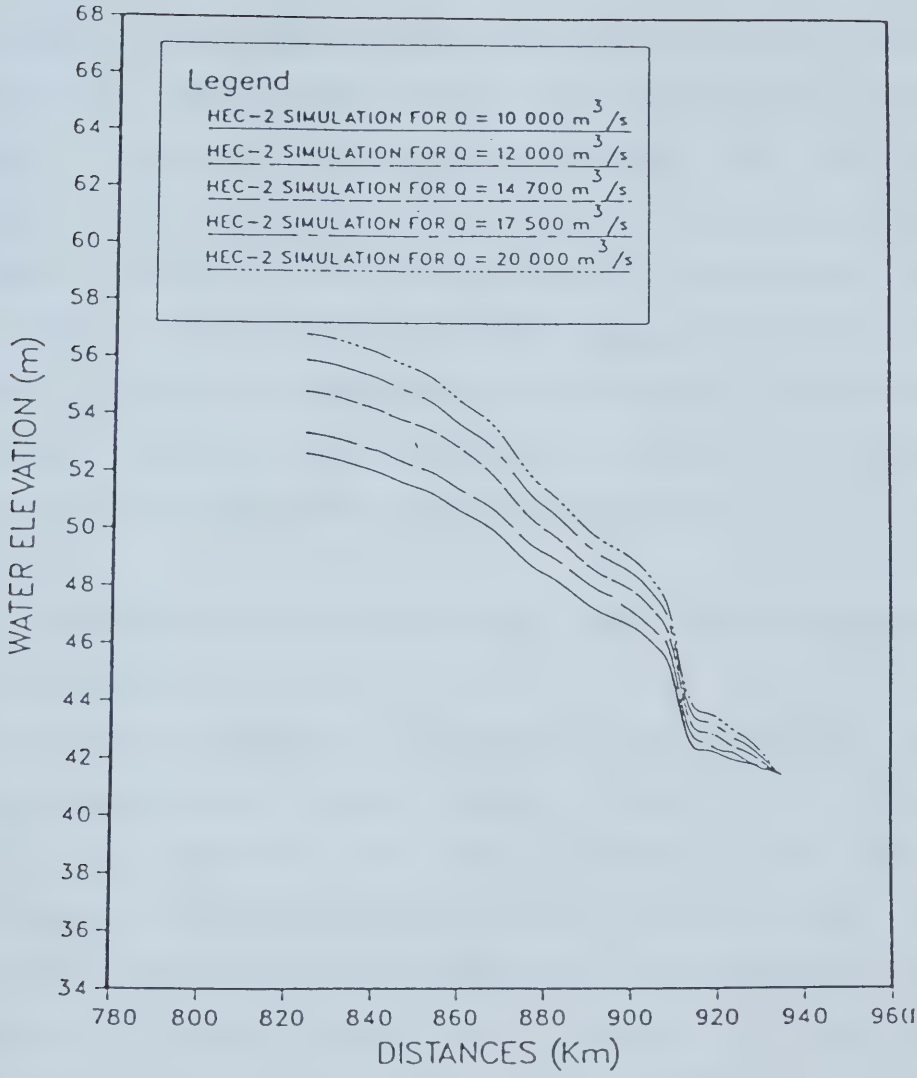

Figure 43. Effect of discharge on water levels at Norman Wells.

The second aspect of the present discussion concerns the effect the discharge could have on the water levels at Norman Wells (km 905), assuming that a jam keying at approximately the same location and having the same general configuration had formed. Using the simulations with a constant thickness of 4.5 m and a roughness of 0.05 for comparison, the resulting profiles for different discharges are shown on Figure 43. For a discharge of 20 000 m^3/s, the water level at Norman Wells would have been about 47.8 m, as compared to 46.3 for a discharge of 12 000 m^3/s. Obviously, the above discussion is relative as a different discharge would have also changed the computed thickness.

4.4.3 Internal friction coefficient, equilibrium thickness, and stage

As it is impossible to measure the jam thickness, some indirect approach has to be used to solve the closure problem and determine the stage caused by an ice jam in equilibrium. As described earlier, the three unknowns are the ice jam roughness, the thickness of the accumulation and the internal friction coefficient. Needless to say, the three parameters are closely related. The ice roughness affects the depth of flow associated with the ice boundary which in turn is used to compute the shear stress underneath the accumulation. This value is finally necessary in the equilibrium expression to obtain the friction coefficient. Given the scarce information available on these parameters

and their interdependence, it is then necessary to discuss which parameter should be determined indirectly in order to be able to compute the other two.

As was evident from the section presenting the literature review, very little is known about ice jam resistance. The only related information is the data provided by Nezhikhovskyi (1964). Major weaknesses in the application of this information to ice jams were identified. Concerning the thickness, some prototype data were collected in at least two cases by Calkins (1982, 1983). The information was obtained from the remaining ice jam shear wall along with actual measurements of the ice thickness when the jam being documented froze in place. The measured thicknesseses could then be compared with the ones computed with the equilibrium theory. Obviously, these documentations were possible only under special circumstances which were not reproduced during the present study. Finally, the internal friction coefficient μ has been evaluated by Pariset et al. (1966) to be 1.28 from prototype measurements. Beltaos (1982) concluded from his case studies that $\mu = 1.2$ for the majority of the rivers he studied and suggested the use of this value. None of these involved direct measurements of μ.

Considering the above, the trend in ice jam analysis in practical applications (see, for example, Vogel and Root, 1981; Calkins, 1983) has been to consider μ to be a constant having a value close to 1.3 and to then evaluate the other

parameters to complete the analysis. However, the use of a constant value for this parameter has yet to be validated. It should be pointed out first that Beltaos' average value was obtained by using Nezhikhovskyi's data to estimate the ice roughness. This approach has serious shortcomings, as it recognized by the author himself. A recent paper by Andres and Doyle (1984) suggests, on the other hand, that μ may in fact vary from 0.8 to as high as 2.7, with an average of 1.6. As discussed earlier, Andres and Doyle were able to document two water profiles of the same jam, but with different discharges. This provided the opportunity to independently determine the roughness of the underside of the jam and to thereby compute the friction coefficient. As pointed out earlier, their technique, except for the direct measurement of the ice thickness possible in exceptional circumstances (Calkins, 1981), is the most reliable to date to evaluate the different parameters as it involves less uncertainties .

The above discussion therefore suggests that the use of a constant value of μ for all jams in any given region should be applied with reserve. Considering the definition of the coefficient (Eq. 19) and assuming that the porosity of the accumulation is a known constant, it can be seen that μ depends solely on the angle of friction of the mass of ice floes. It is unlikely that this angle would be constant for any given ice jam conditions, as the types and dimensions of ice floes forming a jam could vary widely. Past studies

could therefore provide only an indication of the range of values possible for μ. To suggest with the current understanding that it should be almost a constant seems premature. As shown by Andres and Doyle (1984), even a small variation in μ is important as it can produce a significant change in the computed stage.

In view of the foregoing discussion, the present analysis has used an approach different from the ones described above to evaluate the internal friction coefficient. Making use of the standard semi-log expression and field data suggesting that $\Delta < k < 3\Delta$, the roughness of the accumulation was first estimated. The corresponding thickness was then accepted as the equilibrium thickness and μ was computed using the hydraulic parameters determined by the backwater model. Using this method, a value of 1.6 was obtained for the friction coefficient. This is encouraging as it is the same as the average value reported by Andres and Doyle (1984). Considering that the average and maximum ice floe thicknesses of the jam documented by these authors (0.9 and 1.5 m respectively) and that the surface appearance of the jam they studied were similar to the situation analysed herein, it seems that the present approach provides a good alternative to evaluate μ when the more rigorous method described by Andres and Doyle is not applicable.

Regarding the evaluation of the equilibrium thickness, the results obtained could be compared with another indirect approach. A rough estimation of the total thickness of an

accumulation was possible on two occasions during the breakup observations when, in 1984, two jams formed while the intact ice sheet was still in place at some location upstream. The first case is the jam at Old Fort Point (km 770). This was shown on Figure 26. Considering the fact that the river was open from km 768 to 734 and assuming a thickness of 1.7 m for the intact ice sheet, the bulk volume of ice composing the jam could be computed. Using a porosity of 0.4 and obtaining the surface area actually occupied by the jam from the topographic maps, the thickness thereby obtained was 6 m. The other jam documented was the one at Birch Island (km 700). In this case the computed thickness was approximately 5.5 m. It should be pointed out that this simple analysis neglected the ice lost on the banks in the area of open water and any melting. Moreover, the general slope in the reaches associated with the above jams was 0.0002 as compared to 0.00006 in the equilibrium reach of the jam documented in the present study. The values obtained above should therefore represent an upper bound for the thicknesses.

The results obtained could also be compared with a different presentation of ice jam stability as given by Beltaos (1983). This simplified presentation, which was given in Figure 9, allows direct determination of the stage caused by an ice jam in equilibrium, given the channel geometry and flow discharge. The river can be replaced by a very wide rectangular channel of equivalent average

dimensions and the flow is assumed to be "uniform" in a reach-average sense. The simulations performed in the present analysis could be used to estimate the parameters η and ξ as defined by Beltaos. Table 7 summarizes the data obtained at cross-sections within the equilibrium reach. Using average values, the calculated values of η and ξ were 75.2 and 193.6 respectively. It can be seen from Figure 9 that these values fall close to the average line proposed by Beltaos.

	km 881.1	km 878.4
S	0.000105	0.000109
B	2135	1322
h_j	8.47	11.07
t	4.5	4.5
H	12.61	15.21
η		75.2
ξ		193.6

Table 7. Computed hydraulic parameters in equilibrium reach ($Q = 12\ 000\ m^3/s$).

Finally, we can compare the roughness value obtained for the equilibrium reach with the values obtained by different investigators. Pariset et al. reported values of 0.05 to 0.06 for the roughness of ice jams on the St-Lawrence River. In the recent paper already cited, Andres and Doyle (1984), found a value of 0.072, which is slightly larger than the value reported herein. It is interesting to note that their approach to evaluate this parameter was more direct than the one used in the present study and that the type of floes composing the jam and the surface appearance was similar to the jam analysed herein. Although other factors such as the depths and the configuration of the river could have an effect on the results, this is certainly an indication that the method outlined here could provide reasonable estimate of the roughness if the approach used by Andres and Doyle can't be used. It should also be pointed out that when compared with other roughness measurements,the value obtained for the present jam (0.05) can be considered to be low. For example, if the data provided by Nezhikhovskyi, as shown in Table 1, had been used to estimate the roughness, it can be seen that the estimated value would have been around 0.1.

4.4.4 Thickness and roughness variation along and across the jam

The analysis presented in this study went beyond the constant thickness simulations and simple equilibrium

calculations to investigate the thickness and roughness variations, both longitudinaly and transversely.

The calculations for the longitudinal variation of the ice thickness assumed that the internal friction coefficient μ was constant along the entire jam and equal to 1.6. In reality, this may or may not be the case. In a study quoted by Uzuner and Kennedy (1976), Merino (1974) found the parameters C_o and K to be strain-rate dependent. This would suggest that K and C_o are not constant along the jam. Nevertheless, considering the present state of understanding in the variation of these parameters, they were treated as constants. Using therefore a constant value of 1.6 for μ gives the angle of friction ϕ as 35°. This compares favorably with the values deduced from the data provided by at least one investigator (Berdennikov (1964)) and is a reasonable value for a granular mass with good interlocking characteristics.

Finally, the use of the semi-log expression to analyse the situation in the toe region has allowed a tentative definition of the "roughness variation" at this location. Other studies (Calkins, 1981) have noted an increase of the Manning's "n" in the toe region. This is in fact a direct result of the increasingly shallower depths characterizing this location and provides another example of the inadequacy of the Manning's "n" when dealing with extremely rough boundaries. As pointed out earlier, the Manning's "n" could vary significantly when the roughness elements becomes of

the same order of magnitude as the depth of flow. The use instead of a constant roughness expressed in terms of k is however more logical and, as described in a previous section, provided a more rigorous mean to examine the special conditions at this location.

4.4.5 Limitations of analysis

Despite the encouraging results obtained, the analysis reported in the present study has some limitations. Beyond the assumption involved in applying the equilibrium theory, the validity and the applicability of the method presented herein could be affected by various factors that have been assumed negligible. They are briefly reviewed in the following.

First of all, there were limitations to the gradually varied flow model used to perform the analysis. A fundamental assumption was that the flow was steady. Obviously, the flow during an ice jam event is basically of an unsteady nature. The case studied herein was no exception. However, it is evident from Figure 21 that there were different degrees of unsteadiness. When the first ice movement occurred, there was a very dynamic change in the water level ($\cong$ 0.48 m/h). When the water profile was measured 5 hours later, the water levels were decreasing at a much slower rate ($\cong$ 0.07 m/h). It was therefore felt reasonable to treat this as a "quasi-steady" situation, i.e. one for which an assumed steady state is a close

approximation. Another point worth considering is the presence of islands in the reach. This produced divided flow for more than three consecutive cross-sections at some locations. The recommendation of the HEC-2 Users Manual in this case is to run separate profiles for each leg of the divided flow as the water surface elevations are not necessarily identical at each cross-section. However, to allow for this was thought to be a secondary refinement and it was neglected in the present study.

Other limitations come from the techniques used to collect the data. First of all, the basic information concerning the cross-sections was not obtained by direct measurements but from hydrographic charts, which in turn were based on data from 1974. Although a reasonable agreement was obtained when a measured cross-section in the Norman Wells area was compared to the one obtained from the charts, it is possible that the error involved at other cross-sections is more considerable. Another point, evident from Figure 22, is the scatter in the measurements of water levels along the jam. This was due mainly to the high altitude from which the photos were taken. Obviously, a compromise must be reached on this point as the photo must be taken high enough to provide a general view of where the photo was taken and still provide a reasonable view of identifiable objects on the banks. It should also be pointed out that more points should have been identified in the toe region to obtain a more precise picture of the water level

change at this location. Finally, the methods used to estimate the discharge were admittedly inaccurate but the fact that the Mackenzie River is such a large river helped minimize the possible error attributable to this factor. It is worth noting that the assumed discharge of 12 000 m^3/s is almost half that given by WSC one day before the jam event (22 700 m^3/s).

Finally, the approach used to analyse the ice jam had some limitations of its own. The fundamental concept was the use of the semi-log expression and the description of the roughness in terms of the hydraulic boundary roughness k_i. This approach assumes that the velocity profile under the ice cover follows a semi-logarithmic equation and that the shape of the profile is well defined, consistent and a function of k_i only. However the velocity profile is likely to be extremely complex. It is however thought that despite its limitations, the use of k instead of the Manning's "n" is a much preferable approach for an ice jam analysis as there is at least some indication that the semi-log expression describes more appropriately the flow against very rough boundaries and because k can be estimated directly by visual observations. The analyses presented herein should however be duplicated in other studies to provide more background to the use of k.

4.5 General implications for analysis of ice jams at Norman Wells

Considering the results obtained and the observations presented in the present study, certain general implications for the analysis of ice jams at Norman Wells could be identified. First of all, based on the breakup data accumulated over the years, it seems that the ice movement at Norman Wells (km 905) is very often preceded by the formation of an ice jam at Fort Norman (km 828). This latter location has been identified by MacKay and MacKay (1973) as an area where a jam frequently forms. The formation of a jam at Fort Norman is not however an indication of a dramatic breakup and severe ice jamming at Norman Wells. In 1984, as discussed earlier, an ice jam similar to the one observed in 1983 formed at Fort Norman. However, due to very warm weather, the entire jam, about 70 km long, melted in place in a matter of days. Hence even given the formation of a jam at Fort Norman, it must still be known how and when the jam will release and how meteorological parameters can influence the process.

To put the 1983 jam into a broader context, Figure 44 shows the probability distribution of the peak water levels at Norman Wells, for the period from 1973 to 1983, as given by Stagg et al. (1983). The water level produced by the 1983 ice jam was 46.7 m. As apparent from the figure, two different kind of breakups, thermal and dynamic, produced jams of varying severity. Although the 1983 breakup at

Norman Wells had a dynamic nature, it did not produce a very significant increase in water levels. On the other hand, record water levels were attained in 1982 when an ice jam formed very dynamically and keyed at about km 928. Although the discharge in 1982 is not available, the difference in water elevation could be explained by the location where each jam keyed. In 1982, the ice accumulation also seemed to be very dense and much shorter than in 1983 and was keying at approximately km 928. Also worth noting is that there was open water downstream of the jam, as compared to the 1983, jam which keyed on the intact ice sheet. It would therefore seem that the worst condition for the water level reached at Norman Wells would be when the ice sheet downstream of Goose and Bear Islands is weak and does not offer much resistance to the ice run and when a strong surge, produced by the release of a jam at Fort Norman or further upstream comes down the river. In these conditions, the jam would key in the vicinity of km 928. This would place the toe region, where most of the head losses are produced, over a reach characterized by shallow depths and a sinuous thalweg, especially between Rader Island (km 915) and Bear Island (km 906). The combination of all those elements would probably produce the worst possible conditions and is likely to have been responsible for the record water levels in 1982. It should however be pointed out that 1982 was characterized by special conditions as the failure of another jam further upstream of the jam in place at Norman Wells might have

aggravated the situation.(Kemp, 1983).

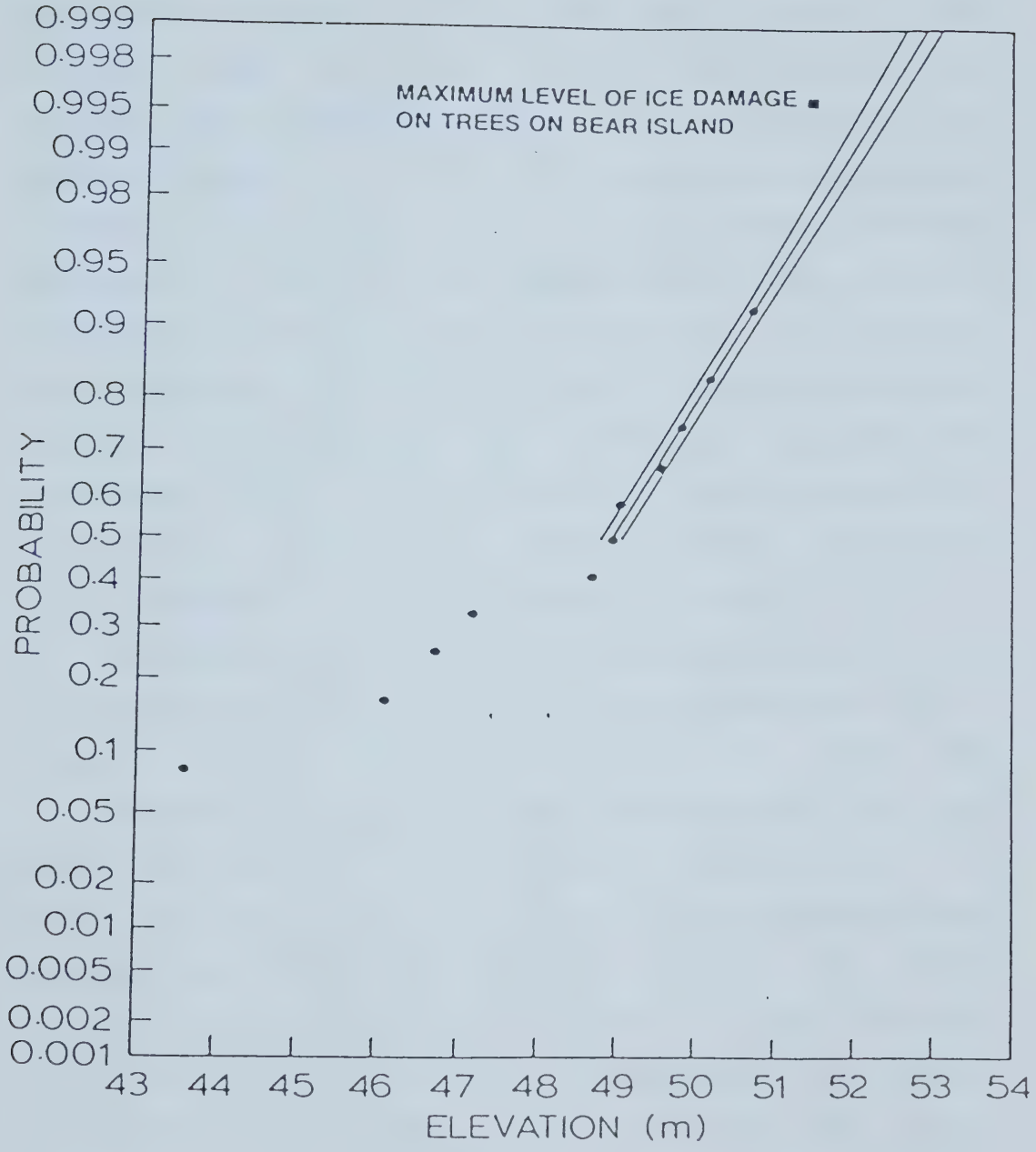

Figure 44. Probability distribution of peak water levels at Norman Wells,]973-]983 (Stagg et al.,]983).

5. CONCLUSIONS

This study has described the field documentation and presented an analysis of the ice jam that formed in the Mackenzie River at Norman Wells in 1983. Unlike past analyses, that concentrated on the equilibrium section, the present analysis used gradually varied flow calculations, coupled with the theory for floating jams formed by internal collapse, to simulate the complete water level profile. A fundamental concept was the use of the standard semi-logarithmic expression, instead of the usual Manning's equation, to describe the flow under the ice jam. The expression of the ice jam roughness in terms of an absolute roughness k_i, rather than n_i, provided a simple and direct way to estimate the actual roughness of the jam.

The results obtained in this investigation showed that the water profile caused by the ice jam documented could be simulated entirely using standard gradually varied flow calculations and the equations describing the ice jam mechanics. The water level increase of approximately 3 m within 6 km at the toe was satisfactorily simulated without assuming grounding. The criteria suggested by field evidence, that the hydraulic roughness k_i could be between one to three times the larger roughness projections, appears to provide a reasonable basis to estimate the actual roughness of the jam. The use of the semi-log expression with an absolute hydraulic roughness k_i rather than the usual Manning's "n_i" is a preferable approach for an ice jam

analysis as the latter is known to describe poorly the flow against very rough boundaries whereas the former is more rugged.

The average coefficient of internal friction μ was found to be 1.6. This value compares favorably with at least one other investigation with similar ice conditions and in which this parameter was determined with a more reliable method than the one used herein. Although this value is within the range of values reported by other investigators, it should be pointed out that it is higher than the value of 1.2 that have been suggested in the literature for practical applications. Judgement must therefore be exercised in the selection of this parameter in the absence of field data.

6. RECOMMENDATIONS

The aim of the study was to simulate completely the water level profile produced by an ice jam and to investigate the ice thickness and roughness variations. The encouraging results indicated the proposed approach could be a viable one to analyse satisfactorily the water levels caused by a floating ice jam. Similar analyses and other studies on a number of related topics would nevertheless be welcomed.

Recommendations for further study are as follows:

1. Although the approximate technique used to determine the water level profile from air photos was found satisfactory in general, the number of points documented in the toe region was not sufficient. Future investigations should attempt to obtain more water level points at this location to properly define the sudden water level changes. The use of a helicopter would also greatly increase the precision of the measurements.

2. The present analysis used simple equilibrium calculations to obtain the ice jam characteristics. A general program that would incorporate gradually varied flow and the equation describing more completely the mechanics of the jam should be developed. The HEC-2 model was found to be limited for the analysis of the toe:

although 3 different thicknesses could be specified at each cross-section, the roughness could not be varied.

3. Future studies dealing with ice jams should investigate the use of k as outlined in the present thesis to perform the analysis. If similar results are obtained, the approach could be considered a good alternative to more rigorous methods such as direct ice thickness measurements and documentation of two profiles for different discharges.

4. The general factors governing the breakup and its progression should be further investigated as they may be relevant to the configuration, severity, and consequences of ice jams. Notably, study of the transient aspects of ice jamming, such as how, why, and when jams release , should be encouraged to identify the governing factors.

5. Finally, as the whole approach presented herein was developed because of the present inability to measure the accumulation thickness, development of remote sensing instrumentation capable of measuring this parameter directly would give a very strong impetus to ice research.

List of references

Allen, W.T.R. (1977). "Freeze-up, Break-up and Ice Thickness in Canada", Canada Department of Fisheries and the Environment, Atmospheric Environment Service, CLI-1-77, Downsview, Ontario, 185 pp.

Andres, D.D. (1980). "The Breakup Process and the Documentation of the 1978 Ice Jams on the Athabasca River at Ft. McMurray", Proc. Workshop on Hydraulic Resistance of River Ice, Canada Centre for Inland Waters, Burlington, Ontario, Sept., pp. 143-161.

Andres, D.D. and Doyle, P.F. (1984). "Analysis of breakup and ice jams on the Athabasca River at Fort McMurray, Alberta", Canadian Journal of Civil Engineering, Vol. 11, number 3, September, pp. 444-458.

Ashton, G.D. (1978). "River Ice", Annual Review of Fluid Mechanics, Vol. 10.

Atkinson, C.H. (1973). "Problems and Economic Importance of Ice Jams in Canada", Seminar on Ice Jams in Canada, Univ. of Alberta, NRC Technical Memorandum No. 107.

Barnes, H.T. (1928). "Ice Engineering", Renouf Publishing Co., Montreal, 364 p.

Barnes, H.H. Jr. (1967). "Roughness Characteristics of Natural Channels", USGS Water Supply Paper 1849.

Bayazit, M. (1976). "Free Surface Flow in a Channel of Large Relative Roughness", J. Hyd. Res., 15, No. 2.

Beltaos, S. (1978). "Field Investigations of Ice Jams", IAHR, Lulea, Sweden, pp. 357-371.

Beltaos, S. (1979). "Flow Resistance of Fragmented Ice Covers (ice jams)", Proc. Canadian Hydrology Symposium:79, Vancouver, May, pp. 93-126.

Beltaos, S. (1983). "River Ice Jams: Theory, Case Studies and Applications", Journal of the Hydraulics Division, ASCE, October, paper 18308.

Beltaos, S. and Krishnappan, B.G. (1981)."Surges from Ice Jam Release: a Case Study", Proc. 5th Canadian Hydrotechnical Conference, Fredericton, May, pp. 663-681.

Bolsenga, S.J. (1968). "River Ice Jams - A Literature Review", Research report 5-5, U.S. Corps of Engineers, Lake Survey District.

Brown, R.J.E. (1957). "Observations on Breakup in the Mackenzie River and its Delta in 1954", Reprinted from Journal of Glaciology, October, Vol. 3, pp. 133-141.

Calkins, D.J. (1978). "Physical Measurements of river Ice Jams", Water Resources Research, Vol. 4, No. 4, Aug., pp. 693-695.

Calkins, D.J., Deck, D.S. and Martinson, C.R., (1982). "Resistance Coefficients from Velocity Profiles in Ice-Covered Shallow Streams", Canadian Journal of Civil Engineering, Vol. 9, pp. 236-247.

Calkins, D.J. and Ashton, G.D. (1975). "Arching of Fragmented Ice Covers", Special Report 222, CRREL, Hanover, New Hampshire.

Calkins, D.J., Hayes, R., Daly, S.F. and Montalvo, A., (1982). "Application of HEC-2 For Ice-Covered Waterways", Journal of the Technical Councils of ASCE, Proceedings of the ASCE, Vol. 108, No. TC2, November.

Calkins, D.J. (1983). "Ice Jams in Shallow Rivers with Floodplain Flow", Canadian Journal of Civil Engineering, Vol. 10, No. 3, pp. 538-548.

Carey, K.L. (1967). "The Underside of River Ice, St. Croix River, Wisconsin", U.S. Geological Survey Professional Paper 575-C, pp. 195-199.

Department of Public Works (1976). "Final Report on the Mackenzie River Investigation", volume 2 and 3.

Doyle, P.F. (1977). "1977 Breakup and Subsequent Ice Jam at Fort McMurray", Alberta Research Council, Transportation and Surface Water Engineering Division, Report SWE/77/01, 25 p.

Doyle, P.F. and Andres, D.D. (1979). "1979 Spring Breakup and Ice Jamming on the Athabasca River near Fort McMurray", Alberta Research Council, Transportation and Surface Water Engineering Division, Report SWE/79/05, 32 p.

Ferrick, M.G. (1984). "Analysis of Rapidly Varying Flow in Ice-Covered Rivers", Proceedings of IAHR International Ice Symposium, Hamburg, pp. 359-368.

Ferrick, M.G. and Lemieux, G.E. (1983). "Unsteady River Flow Beneath an Ice Cover", Proceedings of the Conference on Frontiers in Hydraulic Engineering, Hydraulics Division of the ASCE, MIT, Massachusetts.

Ferrick, M.G., (1984). "On River Waves", CRREL Report 329, U.S. Army Cold Regions Research and Engineering Laboratory, Hanover, New Hampshire.

Frankenstein, G. and Assur, A. (1972). "Israel River Ice Jam", IAHR, Leningrad, U.S.S.R., pp. 153-157.

Gerard, R. (1975). "Preliminary Observations of Spring Ice Jams in Alberta", IAHR, Hanover, New Hampshire, pp. 261-277.

Gerard, R. (1984). Discussion of "River ice jams: theory, case studies and applications", by S. Beltaos, Journal of the Hydraulics Division, ASCE, November.

Henderson, F.M. and Gerard, R. (1981). "Flood Waves Caused by Ice Jam Formation and Failure", Proc. of the IAHR Ice Symposium, Quebec City, Vol. 1, p. 209.

Joliffe, I. and Gerard, R. (1982). "Surges Released by Ice Jams", Proceedings of the Workshop on Hydraulics of Ice-Covered Rivers, University of Alberta, Edmonton.

Kamphuis, J.W. and J.R. Moir. (1983). "Ice Breakup and Jamming Observations Along the Mackenzie River", Canadian Journal of Civil Engineering, Vol. 10, No. 1.

Keefe, J. (1910). "A Reconnaissance Across the Mackenzie Mountains on the Pelly, Ross, and Gravel Rivers, Yukon and Northwest Territories", Geol. Survey Branch, Dept. of Mines, Ottawa, p. 20.

Kemp, T.S. (1982). "Mackenzie River Norman Wells 1982 Breakup", Esso Resources Canada Limited, Internal Report IPRT.ME.83.30.

Kennedy, J.F. (1975). "Ice-Jam Mechanics", Proceedings of the Third International Symposium on Ice Problems, IAHR, Hanover, New Hampshire, pp. 143-163.

Kindle, E.M. (1920). "Arrival and Departure of Winter Conditions in the Mackenzie River Basin", The Geological Review, Vol. 10, pp. 388-399.

Kennedy, R.J. (1958). "Forces Involved in Pulpwood Holding Grounds", Engineering Journal, Vol. 41, January, pp. 58-68.

Larsen, P.A. (1969). "Head Losses Caused by an Ice Cover on Open Channels", J. Boston Soc. Civ. Engineers, Vol. 56, No. 1.

Limerinos, J.T. (1970). "Determination of the Manning Coefficient from Measured Bed Roughness in Natural Channels", USGS Water Supply Paper 1898-B, Washington.

MacKay, J.R. (1961). "Freeze-up and Break-up of the Lower Mackenzie River, Northwest Territories", Proceedings, 1st International Symposium on Arctic Geology, University of Toronto, Vol. 2, pp. 119-134.

MacKay, D.K. (1965). "Breakup on the Mackenzie River and its Delta, 1964", Geographical Bulletin, Vol. 7, No. 2, pp. 117-128.

Mackay, D.K and Mackay, J.R. (1973a). "Breakup and Ice Jamming on the Mackenzie River, N.W.T.", Report on Hydraulic Aspects of Northern Development, Glaciology Division, Water Resources Branch, Environment Canada, Ottawa, pp. 227-236.

Mackay, D.K and Mackay, J.R. (1973b). "Location of Spring Ice Jamming on the Mackenzie River, N.W.T.", Technical Report No. 8, Glaciology Division, Water Resources Branch, Environment Canada, Ottawa.

Mackenzie River Basin Committee (1981). "Spring Breakup", Mackenzie River Basin Study, Report Supplement 3.

Mathieu, B. and Michel, B. (1967). "Formation of Dry Ice Jams", Proc. of the 12th Congress of IAHR, Vol. 4, pp. 283-287.

Mercer, A.G. and Cooper, R.H. (1977). "River Bed Scour Related to the Growth of a Major Ice Jam", Proc. 3rd National Hydrotechnical Conference, Canadian Society for Civil Engineering, Laval University, Quebec City.

Merino, M.P. (1974). "Internal Shear Strength of Floating, Fragmented Ice", thesis presented to the University of Iowa, at Iowa City, in partial fulfillment of the requirements for the degree of Master of Science.

Michel, B. (1965). "Static Equilibrium of an Ice Jam at Breakup", Proc. 11th Congress of IAHR, Vol. 5, pp. 37-48.

Michel, B. (1966). "Ice Covers in Rivers", Proc. of Conference on Ice Pressures against Structures, Laval University, NRC Technical Memorandum No. 92.

Michel, B. (1971). "Winter Regime of Rivers and Lakes", CRREL Monograph 111-B1a, 130 p.

Michel, B. (1973). "Theory and Simulation of Ice Jams at Breakup", Proceedings of Seminar on Ice Jams in Canada, University of Alberta, NRC Technical Memorandum No. 107.

Michel, B. (1980). "Interpretation of Alberta Ice Jams Data", Report GCS-80-03, Dept. of Civil Engineering, Laval University, July.

Nezhikhovskyi, R.A. (1964). "Coefficient of Roughness of Bottom Surface of Slush Ice Cover", Soviet Hydrology, No. 2, pp. 127-150.

Pariset, E. and Hausser, R. (1961). "Formation and Evolution of Ice Covers on Rivers", Transactions of the Engineering Institute of Canada, Vol. 5, No. 1, pp. 40-49.

Pariset, E., Hausser, R. and Gagnon, A. (1966). "Formation of Ice Covers and Ice Jams in Rivers", Journal of the Hydraulics Division, ASCE, Vol. 92, No. HY6, pp. 1-24.

Parkinson, F.E. (1982). "Water Temperature Observations During Breakup on the Liard, Mackenzie River System", Proceedings of Workshop on Hydraulics of Ice Covered Rivers, University of Alberta, Edmonton, Alberta.

Pratte, B.D., (1979). "Review of Flow Resistance of Consolidated, Smooth and Rough Ice Covered Waters", Proceedings, Canadian Hydrology Symposium: 79 Vancouver, B.C., Canada, pp. 52-59.

Sabaneev, A.A. (1948). "On the Computation of a Uniform Flow in a Channel with Non-Uniform Walls", (text in Russian). Transactions, Leningrad Polytechnical Institute, no. 5.

Shulyakovskii, L.G. (1964). Manual of Forecasting Ice Formation for Rivers and Inland Lakes", Manual of Hydrological Forecasting No. 4, Israel Program for Sientific Translations, Jerusalem, 1966, 245 p.

Stagg, P.W., Kemp, T.S. and Moir, J.R., (1983). "Analysis of Peak Water Levels in the Mackenzie River at Breakup", Proceedings of the Symposium on Science and Arctic Hydrocarbon, Exploration: the Beaufort Experience, Whitehorse, Yukon.

Tatinclaux, J.C. (1977). "Equilibrium Thickness of Ice Jams", Journal of Hydraulics Division, Proc. ASCE, Vol. 103, No. HY9, Proc. Paper 13170, Sept., pp. 959-974.

Tatinclaux, J.C. and Cheng, S.T. (1978). "Characteristics of River Ice Jams", IAHR, Lulea, Sweden, pp. 461-475.

Tatinclaux, J.C. and Gogus, M. (1983). "Asymmetric Plane Flow with Application to Ice Jams", Journal of Hydraulic Engineering, Proc. ASCE, Vol. 109, No. 11, pp. 1540-1554.

Uzuner, M.A. (1975). "The Composite Roughness of Ice-Covered Streams", J. Hydraulic Research, 13, No. 1.

Uzuner, M.S. and Kennedy, J.F. (1974). "Hydraulics and Mechanics of River Ice Jams", Iowa Institute of Hydraulic research, Report No. 161, The University of Iowa, Iowa City, Iowa, May.

Uzuner, M.S. and Kennedy, J.F. (1976). "Theoretical Model of River Ice Jams", Journal of Hydraulics Division, ASCE, Vol. 102, No. HY9, pp. 1365-1383.

Vogel, R.M. and Root, (1981). "The Effects of Floating Ice Jams on the Magnitude and Frequency of Floods along the Missisquoi River in Northern Vermont", Proceedings of the IAHR, International Symposium on Ice, Quebec City, pp. 347-360.

Water Surface Profiles - Users Manual, U.S. Army Corps of Engineers, Hydrologic Research Center, HEC-2, September 1982.

Williams, G.P. and Mackay, D.K. (1973). "The Characteristics of Ice Jams", Proceedings of Seminar on Ice Jams in Canada, University of Alberta, NRC Technical Memorandum No. 107.

APPENDIX A

Summary of aerial observations, 1983 breakup

TABLE A-1

1983 FLIGHTS SUMMARY

SALIENT OBSERVED FEATURES

Date	Time	Reach (Km)	Breakup duration	Observed features
May 3	11:00	905-700	2.5	Ice jam at Liard-Mackenzie confluence. Ice firm along whole reach.
May 4	14:15	905-338	3.5	No change. Except for the Wrigley river, all tributaries frozen over.
May 8	19:00	905-715	7.5	Ice movement at km 770 and upstream of Keele river confluence (km 730).
May 9	14:00	905-665	8.5	Reconnaissance of the Redstone River basin: no sign of breakup.
May 11	09:00	905-570	10.5	Flooded areas along shorelines generalized. Secondary channels at Old Fort Point (km 770) almost clear of ice. Melting features at tributaries confluences.
May 12	14:00	905-338	11.5	Mush ice accumulation upstream of Wrigley river confluence (km 580). Numerous cracks (km 450 to 360). Ice jam at Fort Simpson melted in place.
May 14	14:00	905-338	13.5	Significant ice movements at Old Fort Point due to landslide (km 773). Open water at most tributaries confluences.

May 16	13:00	905-338	15.5	Large open water areas around islands in N.W. area. Extensive open water areas in reach between Keele and Redstone Rivers (km 738-715). Major ice movements near many tributaries confluences.
May 17	14:30	905-1100	16.5	Ice sheet still solid downstream of Norman Wells.
May 18	08:40	905-572	17.5	Numerous cracks around Police Island. Two newly formed ice jams (km 768-790 and 760-761) at Old Fort Point. Essentially no ice (except for ice debris) from km 760 to 710. Further ice movements at river confluences.
May 19	19:00	905-575	18.5	Small ice jam from km 670 to 666. A 10 Km long mush ice accumulation (moving downstream) at km 675.
May 20	14:20	905-510	19.5	Small ice jams at km 790 and 550. Open water from km 715 to 676 and from 550 to 541.
May 21	15:00	905-738 905-1015	20.5	Open water around Rader Island. Open water area (1 km long) at Sans Sault Rapids (km 1015).
May 22	09:30	905-590	21.5	Further instability at tributaries confluences. Open water areas: km 758 to 665, 650 to 630. Large broken ice accumulation moving downstream at km 616. Ice sheet intact from km 610 to 590.

May 23	09:40	905-828	22.5	Important ice movement on May 22 at 22:20 produced large ice jam from km 830 to 760. Open water at Little Bear River confluence (1 km). Ice jam release at 11:30.
May 23	20:00	905-900	22.5	Reconnaissance after ice movement in Norman Wells. Photos for water profile.
May 24	10:00	905-1100	23.5	Ice sheet cracked at Rader Island. Many cracks but no important ice movement. Open water at Sans Sault Rapids (2 km). Open water (2 km) in front of Fort Good Hope.

APPENDIX B

Bench marks locations and open water profile between Ft. Norman (km 828) and km 935

TABLE B-1

CHANNEL SLOPES - FORT NORMAN (Km 828) TO DOWNSTREAM OF NORMAN WELLS (Km 905)

B.M. #	B.M. ELEVATION (m)	WATER STAGE (m)	REACH SLOPE
74T060 (Km 826.8)	71.194	47.789	
74T065 (Km 832.9)	56.981	47.259	8.689E-5
P23A3 (Km 840)	60.614	46.569	9.718E-5
74T071 (Km 861.2)	54.616	43.468	1.462E-4
74T004 (Km 876.1)	53.937	42.028	9.664E-5
74T007 (Km 888.95)	58.234	41.255	6.016E-5
74T012 (Km 896.4)	56.936	41.100	2.081E-5
74T016 (Km 904.8)	60.928	40.805	1.229E-4
ESSO4 (Km 905.6)	52.150	40.730	9.375E-5
74T018 (Km 910)	54.204	39.756	2.21E-4
74T021 (Km 924.3)	51.921	38.125	1.141E-4
74T076 (Km 941)	52.710	36.539	9.497E-5

APPENDIX C

1983 ice jam water level profile

The last column in the following table indicates first the degree of reliability attached to a particular point (varying arbitrarily from 1 for a vey good measurement to 3 for a poor and not very reliable one) and whether the point was included or not in the plot shown on Figure 22. Three additional points taken from the ground in Norman Wells and in Fort Norman are also given.

TABLE C-1

ICE JAM PROFILE

Location (km)	Water level (m)	Comments
832.4	55.34	3 - no
843.6	54.45	3 - no
853.3	50.20	3 - no
857.1	49.93	3 - no
861.4	50.81	2 - yes
864.0	50.76	2 - yes
864.0	50.76	2 - yes
867	47.94	3 - no
876	50.52	2 - yes
882.8	50.67	2 - yes
883.4	49.55	2 - yes
884.7	48.76	2 - yes
886.8	47.27	2 - yes
888.7	48.01	2 - yes
889.3	51.16	3 - no
892	48.08	2 - yes
893.1	48.17	2 - yes
894.8	47.73	2 - yes
898.9	48.09	1 - yes
900	47.79	1 - yes
901	47.50	1 - yes

901.9	47.63	1 - yes
911.5	43.46	2 - yes
914	43.02	2 - yes
919.5	42.33	2 - yes
919.3	42.33	2 - no
925.3	42.78	1 - yes
925.3	41.69	2 - no
926.3	42.34	1 - yes
926.8	42.55	2 - yes
927.6	41.50	2 - no
928.5	41.81	1 - yes
932.3	42.40	2 - yes
933.5	42.14	2 - yes
934.1	41.44	1 - yes
935.4	40.89	2 - yes

Additional points:

LOCATION	TIME	ELEVATION (m)	COMMENTS
NCPC dock (Km 904.6)	20:17	47.065	1 - yes
Off-site dock (Km 900)	20:32	47.057	1 - yes
Fort Norman (Km 828)	19:15	53.75	1 - yes

APPENDIX D

Summary of aerial observations, 1984 breakup

TABLE D-1

1984 FLIGHTS SUMMARY

SALIENT OBSERVED FEATURES

Date	Time	Reach (Km)	Breakup duration	Observed features
May 3	14:00	905-338	1.0	Mackenzie River broke up upstream of Fort Simpson. Jam at the Liard River confluence.
May 4	14:15	905-338	2.0	Mackenzie River free of ice down to km 340. Minor jam keyed at km 370.
May 5	11:00	905-450	3.0	Increase in breakup rate progression. Breakup front at km 470 with a 33 km long ice jam at km 430 and a 20 km long ice jam at km 454.
May 6	14:00	905-500	4.0	Breakup front at km 520 with an ice jam keyed at km 510. Ice between the Keele and Redstone Rivers deteriorating fast with numerous open water patches.
May 7	09:00	905-550	5.0	No major change. Jam at km 510 still in place but 15 km shorter.
May 9	14:00	905-520	7.0	Breakup front now at km 540. 13 km jam keyed at km 538; 20 km jam keyed at km 510.
May 10	11:00	905-520	8.0	Open water just downstream of Old Fort Point (km 770). Minor jams at km 550 and 537. Breakup front at km 550.
May 12	13:00	905-620	10.0	Weather prevented the observation of the breakup front.

May 13	14:30	905-750	11.0	Breakup front at Seagull Island (km 750). Major jam at km 790 just upstream of Police Island.
May 14	09:40	905-790	12.0	Ice jam formation at Seagull Island (km 790). Major jam at km 625.
May 15	19:00	905-790	13.0	No change from the previous flight.
May 16	14:20	905-630	14.0	Ice jam at Old Fort Point (km 800). Determination of approximate volume of ice possible as ice still present upstream. Jam near Birch Island released. Ice jam at km 630.
May 17	15:00	905-650	15.0	Breakup at Fort Norman (km 828). Ice jam at km 630 has released; ice debris flowing towards the jam near Police Island.
May 18	10:30	905-828	16.0	Ice jam at Fort Norman still in place. Open water stretch downstream of jam (at km 840) preventing the major ice jam from putting a force on the ice sheet downstream.
May 19	15:00	905-828	17.0	Ice jam at Fort Norman has decreased in length by 20 %. Water levels dropping at Norman Wells (km 905).
May 20	15:00	905-828	18.0	Jam at Fort Norman melting in place due to very warm temperatures. Only 30 % of the original length.
May 21	18:00	905-860	19.0	Breakup front now at Halfway Island. No ice jam: the ice sheet simply disintegrating thermally. Breakup has occured downstream of Norman Wells from km 990 to the Rampart at km 1090. Fracturing of ice sheet is occuring in Norman Wells area.

May 22	18:00	905-900	20.0	Breakup upstream of Norman Wells (km 900) at 13:30 with an ice movement of approximately 100 m.
May 23	15:00	905-900	21.0	Breakup at Norman Wells (km 905). No ice jam formation.

APPENDIX E

Mackenzie River cross-sections between Fort Norman (km 828) and km 935

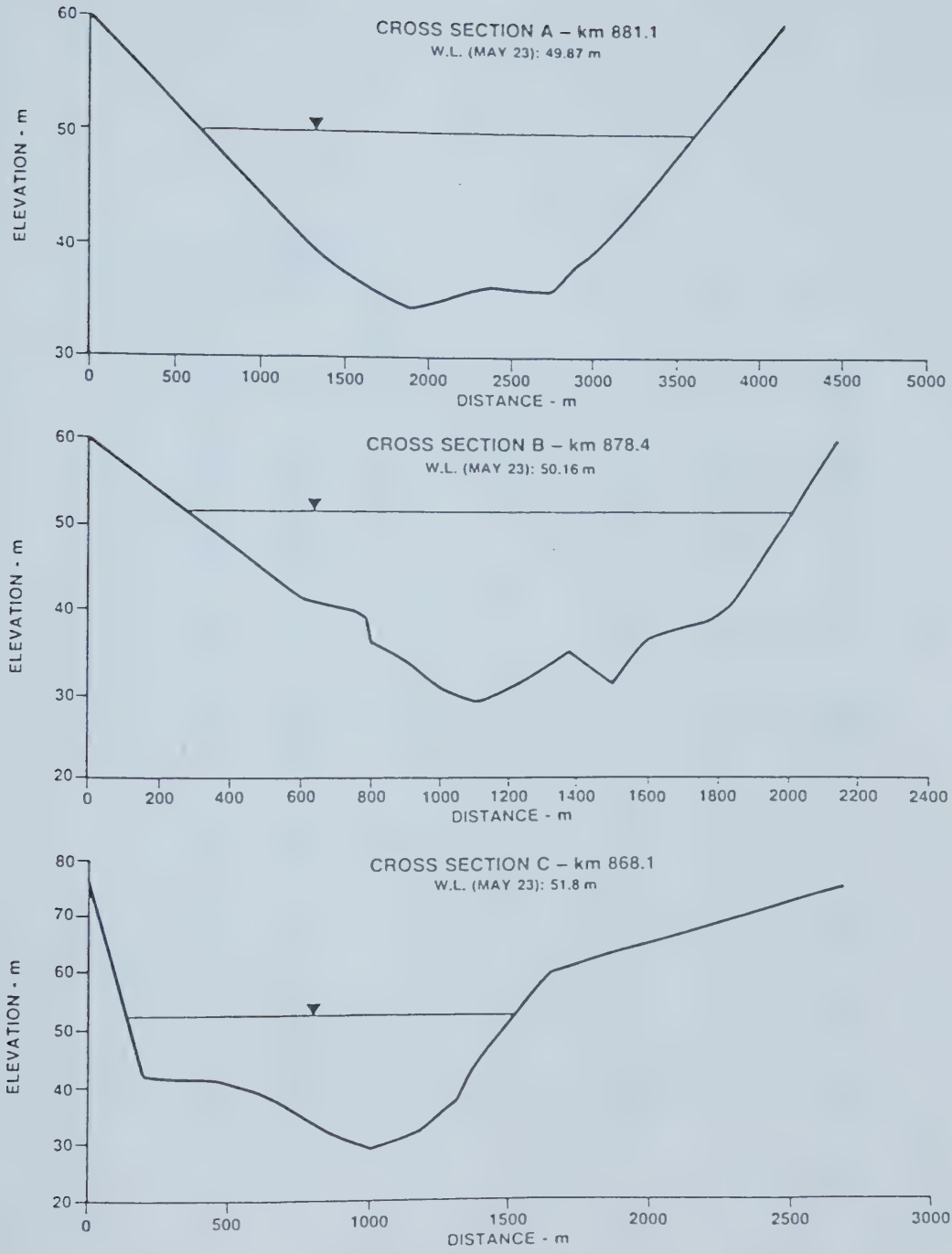

Figure E-1. Typical cross-sections.

1	T1	CROSS-SECTIONS									
2	T2	km 935 to km 826									
3	T3	MACKENZIE RIVER, N.W.T.									
4	J1	-0	-0	-0	-0	-0	1	-0	12000	41.20	
5	J2	1	-0	-1							
6	J3	38	43	1	26	8	64	65			
7	NC			021							
8	IC			1.68	.022						
9	X1	1	15	180	2330						
10	GR	60.0	0	45.0	180	35.7	230	35.6	480	36.6	780
11	GR	34.6	1040	33.5	1280	30.7	1510	25.3	1700	25.3	1830
12	GR	30.7	1940	33.7	2030	35.7	2280	45.0	2330	60.0	2475
13	X1	2	25	20	2620	2500	2500	2500			
14	GR	60.0	0	45.0	20	34.0	125	32.5	300	34.0	375
15	GR	35.2	500	35.8	800	34.0	980	34.0	1120	34.9	1220
16	GR	34.0	1275	36.0	1475	35.4	1500	32.8	1700	31.0	1800
17	GR	29.0	1900	31.0	2040	34.0	2100	34.6	2150	34.0	2250
18	GR	33.9	2400	34.0	2480	36.0	2525	45.0	2620	60.0	3000
19	X1	3	17	20	3400	2100	2100	2100			
20	GR	60.0	0	45.0	20	34.1	110	33.9	340	34.1	410
21	GR	34.9	460	36.1	510	41.6	1310	36.1	1660	34.1	2060
22	GR	33.2	2160	33.3	2460	34.1	2710	34.3	3040	36.1	3340
23	GR	45.0	3400	60.0	3450						
24	X1	4	23	20	3620	4600	4600	4600			
25	GR	60.0	0	45.0	20	34.5	150	32.0	250	34.5	320
26	GR	36.5	420	37.8	530	36.5	620	34.5	650	34.5	800
27	GR	36.5	1200	36.8	1350	36.5	1500	35.4	1780	34.5	1980
28	GR	34.5	2100	34.7	2380	34.4	2700	33.5	2900	34.5	3070
29	GR	35.1	3350	36.5	3580	45.0	3620	60.0	3820		
30	NC			.024							
31	X1	5	28	0	4450	2375	2375	2375			
32	GR	60.0	0	45.0	20	34.9	125	34.2	200	34.9	280
33	GR	35.3	340	34.9	400	34.6	500	34.9	550	36.9	625
34	GR	36.9	1325	34.9	1350	31.3	1400	29.0	1500	31.9	1680
35	GR	34.9	1780	35.7	1820	36.9	1975	36.9	2160	36.4	2400
36	GR	34.9	2500	33.8	2650	33.8	2875	34.9	3000	36.9	3100
37	GR	36.9	3400	37.5	4150	60.0	4450				
38	X1	6	25	0	5380	3050	3050	3050			
39	GR	60.0	0	35.1	100	34.6	200	34.2	480	35.1	550
40	GR	37.1	690	38.8	720	40.1	1120	37.1	1450	35.1	1620
41	GR	33.4	1830	34.1	2200	35.1	2480	36.6	2530	34.5	2800
42	GR	37.1	3000	38.8	3030	50.0	3080	60.0	3200	50.0	4150
43	GR	37.1	4230	36.9	4420	36.8	5000	37.1	5180	60.0	5380
44	X1	7	25	0	5700	3075	3075	3075			
45	GR	60.0	0	37.5	1100	35.5	1150	34.5	1200	32.5	1400
46	GR	35.5	1625	36.6	1800	37.5	1850	40.5	2200	37.5	3150
47	GR	35.7	3250	35.5	3375	35.2	3700	35.5	3750	36.3	4150
48	GR	35.5	4500	35.2	4650	35.5	4900	37.2	4975	35.5	5050
49	GR	34.7	5175	35.5	5300	37.5	5325	40.0	5450	60.0	5700
50	IC	5.50	2.30	2.30	.069						
51	X1	8	17	3260	5380	2925	2925	2925			
52	GR	60.0	0	39.7	1500	37.9	1730	35.9	1750	35.4	2030
53	GR	35.9	2250	36.2	2730	37.9	2830	39.6	3260	37.9	3920
54	GR	35.3	4200	32.9	4400	33.9	4800	35.9	5000	37.9	5160
55	GR	39.2	5200	60.0	5380						
56	IC	5.50	2.30	2.30	.065						
57	X1	81	17	3200	5000	1400	1400	1400			
58	GR	60.0	0	38.8	1300	37.4	1600	38.8	2250	40.5	2650
59	GR	38.8	2800	38.0	3000	38.8	3200	38.3	3500	36.8	3800
60	GR	33.8	4200	32.6	4350	33.8	4600	36.8	4700	38.3	4800

61	GR	38.8	4900	60.0	5000						
62	IC	5.50	2.30	2.30	.060						
63	X1	82	20	3450	4775	1950	1950	1950			
64	GR	60.0	0	40.5	950	39.0	1100	37.0	1125	34.7	1300
65	GR	37.0	1500	39.0	1600	41.6	1750	48.0	2500	40.4	3450
66	GR	39.0	3525	37.0	3560	34.0	3660	32.6	3800	31.8	4125
67	GR	34.0	4350	37.0	4400	38.1	4450	39.0	4650	60.0	4775
68	IC	5.50	2.30	2.30	.058						
69	X1	9	19	3600	4740	4430	4430	4430			
70	GR	60.0	0	42.1	400	38.5	580	36.1	650	36.5	800
71	GR	39.1	1000	38.5	1210	41.5	1400	50.0	2300	41.5	3000
72	GR	39.8	3200	38.5	3300	37.1	3500	36.5	3600	30.1	3950
73	GR	36.5	4150	37.8	4400	38.5	4680	60.0	4740		
74	IC	5.50	2.30	2.30	.060						
75	X1	91	18	3300	5750	1100	1100	1100			
76	GR	60.0	0	35.5	125	37.4	275	40.9	375	50.0	950
77	GR	50.0	2800	39.4	3050	38.3	3300	37.4	3500	37.4	3900
78	GR	34.4	4150	31.7	4550	34.4	4700	37.4	4750	38.7	4850
79	GR	39.4	5050	40.8	5150	60.0	5750				
80	IC	5.50	2.10	2.10	.057						
81	X1	10	15	3840	6000	3000	3000	3000			
82	GR	60.0	0	36.7	300	39.0	340	40.7	700	50.0	900
83	GR	50.0	3340	40.2	3600	39.0	3840	35.8	4000	32.0	4200
84	GR	33.5	4780	37.0	5080	38.3	5480	39.0	5780	60.0	6000
85	NC			.024							
86	IC	5.00	2.50	2.50	.050						
87	X1	11	19	3900	6440	2420	2420	2420			
88	GR	60.0	0	40.5	1100	39.1	1280	37.1	1400	39.1	1500
89	GR	57.7	1600	57.7	3120	39.1	3800	38.5	3900	37.1	4680
90	GR	33.1	4800	33.8	4950	34.1	5050	36.3	5200	38.4	5550
91	GR	36.5	5800	38.3	6200	39.1	6400	60.0	6440		
92	NC			.021							
93	IC			4.50	.050						
94	X1	12	22	100	4280	6000	6000	6000			
95	GR	75.0	0	60.0	100	39.4	140	37.4	200	34.7	240
96	GR	30.4	340	28.4	500	34.4	680	37.4	850	38.2	1050
97	GR	37.4	1275	39.4	1420	52.7	1500	52.7	2250	39.4	2700
98	GR	36.8	3050	35.4	3380	34.4	3500	38.2	3600	39.4	3900
99	GR	60.0	4280	75.0	5450						
100	NC			.021							
101	IC			4.50	.050						
102	X1	13	28	0	5050	3500	3500	3500			
103	GR	60.0	0	39.5	1050	38.9	1150	37.5	1375	34.5	1400
104	GR	32.1	1480	34.5	1525	37.5	1580	39.5	1600	52.3	1650
105	GR	52.3	2525	39.5	2575	37.5	2600	34.5	2650	31.9	2700
106	GR	34.5	3030	36.4	3120	37.5	3300	37.9	3350	39.5	3600
107	GR	38.9	3700	39.5	4150	34.9	4300	36.9	4550	37.5	4610
108	GR	38.1	4700	39.5	4980	60.0	5050				
109	IC			4.50	.050						
110	X1	14	24	175	4900	4900	4900	4900			
111	GR	75.0	0	60.0	175	39.4	280	37.9	300	31.1	400
112	GR	34.9	500	39.9	620	43.5	875	52.3	1400	52.7	2600
113	GR	39.9	2700	38.3	2800	39.9	2900	41.7	3000	39.9	3125
114	GR	38.1	3250	34.9	3500	32.9	3600	30.9	3900	37.9	4000
115	GR	39.5	4100	39.9	4200	60.0	4900	75.0	6000		
116	NC			.021							
117	IC			4.50	.050						
118	X1	15	12	0	4180	7230	7230	7230			
119	GR	60.0	0	40.8	1240	38.8	1340	35.8	1700	34.8	1850
120	GR	35.8	2180	36.2	2350	35.8	2750	38.2	2875	38.8	2950

121	GR	40 8	3100	60 0	4180						
122	IC			4 50	.050						
123	X1	16	16	0	2150	2600	2600	2600			
124	GR	60 0	0	40 9	600	39 5	750	38 9	780	35 9	800
125	GR	33 4	900	30 9	1000	28 9	1100	30 9	1220	34 5	1380
126	GR	30 9	1500	36 9	1600	38 1	1725	38 9	1775	40 9	1840
127	GR	60 0	2150								
128	NC			023							
129	IC			4 50	.050						
130	X1	17	10	0	2120	2300	2300	2300			
131	GR	60.0	0	45.0	500	41.1	850	39.1	1100	36.1	1180
132	GR	32.6	1380	31 1	1530	31.1	1720	41.1	1800	60.0	2120
133	IC			4 50	.050						
134	X1	18	15	0	2700	8100	8100	8100			
135	GR	75 0	0	42 1	200	41 7	250	41.3	450	39 7	600
136	GR	36 7	700	31 7	850	28 7	1000	31 7	1180	35 1	1250
137	GR	36 7	1300	39.7	1340	41 7	1350	60.0	1650	75.0	2700
138	IC			0.02	.023						
139	X1	19	21	0	4100	6770	6770	6770			
140	GR	60 0	0	44 1	200	41 0	320	40 4	375	37.4	500
141	GR	37.4	680	40 4	720	42.4	800	44.2	920	60.0	1300
142	GR	60.0	2550	42.4	2950	40.4	3075	40 0	3150	37.4	3200
143	GR	36.0	3300	37 4	3550	40 4	3680	40 9	3850	42.4	4020
144	GR	60 0	4100								
145	NC			023							
146	IC			1 68	020						
147	X1	20	11	0	1920	8200	8200	8200			
148	GR	60 0	0	43 2	940	41 2	980	40 6	1050	38 2	1100
149	GR	33.2	1180	28 6	1500	33 2	1580	38.2	1675	43 2	1775
150	GR	60 0	1920								
151	IC			1 68	020						
152	X1	21	11	0	2430	5950	5950	5950			
153	GR	60 0	0	43 4	880	42 8	1050	43.4	1100	41 4	1200
154	GR	38 0	1580	38 4	1700	41 4	1900	42 9	2150	43 4	2360
155	GR	60.0	2430								
156	NC			.025							
157	IC			1.68	.020						
158	X1	22	13	0	1680	4100	4100	4100			
159	GR	60.0	0	43 5	350	41 5	480	36.5	600	38 5	720
160	GR	41 5	800	41 9	1000	41.5	1320	41 3	1400	39.9	1480
161	GR	41.5	1540	43 5	1580	60 0	1680				
162	X1	23	16	0	1600	2400	2400	2400			
163	GR	60 0	0	44 4	60	42 4	160	42 4	220	37 8	400
164	GR	39.4	580	42 0	650	42.0	1000	42 4	1120	42.4	1180
165	GR	41.2	1300	39.4	1380	36.9	1400	39.4	1450	44.4	1520
166	GR	60.0	1600								
167	IC			1 68	.020						
168	X1	24	13	0	1520	3220	3220	3220			
169	GR	60.0	0	44 9	50	42.9	120	40 1	320	42 9	380
170	GR	34.9	650	39 9	880	42.4	1050	39 9	1200	37 4	1250
171	GR	39.9	1300	44 9	1460	60 0	1520				
172	X1	25	22	0	3800	6800	6800	6800			
173	GR	60 0	0	45 9	100	34 1	250	40.9	450	43.9	500
174	GR	45 9	550	60.0	1400	60.0	1650	45 9	1920	43 9	2000
175	GR	43.9	2200	45 9	2350	45 9	2540	45 3	2700	43.9	2850
176	GR	45.9	2920	46.3	3200	40.9	3300	37 4	3400	40.9	3575
177	GR	43.9	3700	60 0	3800						
178	X1	26	11	0	2700	3850	3850	3850			
179	GR	60.0	0	46 6	780	44.6	975	41.6	1000	40 6	1350
180	GR	41 6	1700	43 4	2150	44 6	2450	45 8	2520	46.6	2650

APPENDIX F

Calculations for discharge estimates

1. Discharge estimate from hydraulics downstream of ice jam

From open water calibration, n_o = 0.024

From subsequent simulation with intact ice cover, n_i = 0.021. Combining both using the Sabaneev equation, n_o = 0.022.

From oblique air photo, the water level at km 935.5, about 20 kilometers downstream of the ice jam toe, was 41.2 m. Using an ice thickness of 1.68 m, the cross-section shown on Figure F-1 results. The slope in this area, from the open water survey, was 0.0000949.

Using the hydraulic parameters calculated from Figure F-1 and the Manning's equation, a discharge of about 9300 m^3/s can be computed.

2. Discharge estimate from cross-section at Fort Norman (km 828)

Using drawing no. P30E-4 147 from the Mackenzie River Investigation, Final Report, DPW, 1976 and a water level of 53.75 m as measured at this location from the ground, results in an area of 14 512 m^2 and a wetted perimeter of 3438 m. With a Manning's "n" of 0.024 for the river bed, as deduced from open water simulation, and assuming that the ice still moving at the surface had a minor influence on the flow, the computed discharge was about 14 700 m^3/s.

3. Discharge estimate from past discharge measurements

Taking an average slope between km 935.5 and Norman Wells (km 905) of 0.000096, the water level at km 935.5 obtained from air photo (41.2 m) could be transposed at Norman Wells to give approximately 44.1. Using the available winter discharge measurements available at Norman Wells as given on Figure 33, the range of discharge possibly prevailing during the jamming event could be roughly evaluated as being between 13 000 and 14 000 m^3/s.

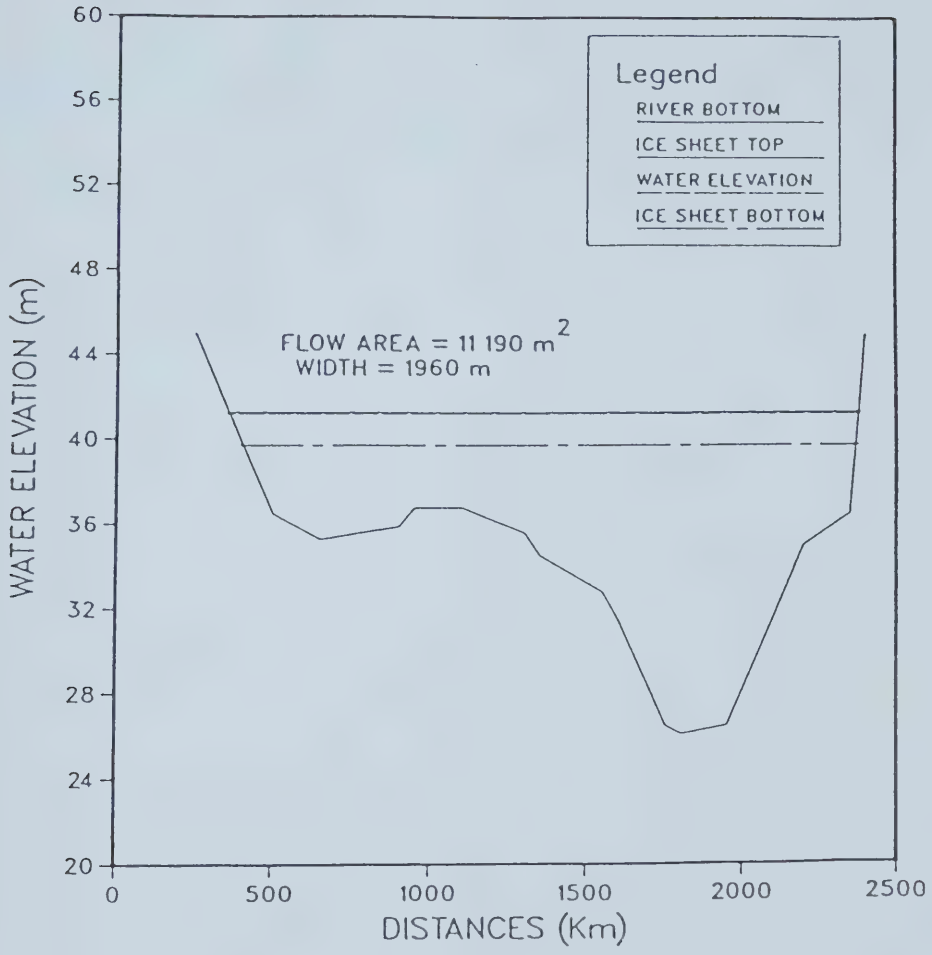

Figure F-1. Cross-section downstream of ice jam at km 935.5.

APPENDIX G

Surge induced by a jam: literature review and partial field documentation

1.General

Although it was not the main objective of the present thesis to look at the problem of surges created by the sudden release of an ice jam, some data have been collected during the 1983 breakup observations. The following sections will first briefly review the past work carried out on jam release and then describe the information obtained during the observations.

2. Literature review

2.1 Early attempts

Some of the earliest studies dealing with the interaction of ice and a surge coming down a river are those reported by Cooper (1966) and Liland (1971). The purpose of their investigations was mainly to determine the effect a solid and continuous ice cover would have on the characteristics of a surge in an open channel. Both reached the conclusion that a radical change in the profile and propagation velocity of a surge is observed with the addition of an ice cover in a channel.

2.2 Henderson and Gerard (1981)

Ten years later, Henderson and Gerard addressed more specifically the question of flood waves caused by ice jam formation and failure. Their approach was to use the classic dam break theory to present analytical solutions describing events following sudden failure and re-formation of relatively "steep" jams on a large river. It was assumed

that the formation of an ice jam is equivalent to the sudden insertion of a resistant baffle (of zero volume) into the river, and that its breakup is equivalent to the sudden (instantaneous) removal of the baffle. The effect of bed slope and resistance were neglected. It was shown that, under the conditions assumed, the surge which forms downstream as a result of the sudden failure of an ice jam cannot have a height greater than one half of the difference in water levels across the original jam, but that subsequent re-formation of the jam may produce water levels behind the new jam which exceed the surge level by up to six times the height of the surge (for the case where the new jam amounts to a complete blockage of the river channel), resulting in a water level higher than that behind the original jam. The surge attenuation by the reflection of the negative waves from the backwater curve behind the original jam was also discussed: it was shown that it increases in direct proportion to the slope of the river channel bed. The authors finally compared the implications of the theory with a partially documented ice jam release (Doyle and Andres, 1979). Although the depths observed were reasonably well explained by the theory, a serious discrepancy was found between the observed surge velocity (4 m/s) and the theory prediction (11 m/s). More work on the effect of resistance on surge attenuation was suggested.

In a discussion of the above paper, Beltaos (1981) suggested that the discrepancy between the observed surge

velocity (4 m/s) and the calculated value (11 m/s) could be explained first by the presence of an undisturbed ice cover below the jam prior to release and secondly by the assumption of initial step-like change in stage across the jam whereas the observed stage profile showed a gradual, though very steep relative to S_o, decline of stage at the downstream end of the jam.

In another discussion of the Henderson's paper, Calkins (1981) reported on field measurements on the transients set up by ice jams on the Ottauquechee River, a rather small steep river in Central Vermont. Surge velocities of 4-5 m/s were measured as well as water level rises of 0.6 m in 20 s.

2.3 Beltaos and Krishnappan (1981)

Beltaos and Krishnappan used more detailed numerical methods to simulate the failure of the ice jam documented by Doyle and Andres (1979) and analysed by Henderson and Gerard (1981). The approach used was to formulate the one-dimensional differential equations for the ice-water flow that occurs subsequent to the release of an ice jam. Like Henderson and Gerard, the effect of the fragmented ice released by the jam failure was neglected. The presence of an undisturbed ice cover downstream of the ice jam and its effect on the surge retardation was accounted for by an increased friction factor or a reduced ratio V/V_*. The value $V/V_* = 9$ (compared to a value of 16 for open water and 5 for a solid ice sheet) was found to adequately reproduce available stage and velocity estimates at a downstream

location. Effect of the jam length on the surge was also discussed: it was found that jams of the same maximum depth as that of, but longer than, the actual jam would have resulted in increased peak stages and durations of surging velocities.

2.4 Joliffe and Gerard (1982)

As a direct continuation of the above studies, Joliffe and Gerard (1982) examined specific problems that were left unanswered by the previous investigations. More specifically, they reported on a laboratory study to investigate whether the ice released with the surge modifies the surge characteristics and a numerical study to assess the possible influence of jam length, stream slope and resistance on the surge. The main conclusions were that in the absence of large friction at the banks, the ice in an ice jam has little influence on flow behaviour following sudden jam failure and that the simple dam break analysis (as used by Henderson and Gerard, 1981) should only be relied on when the jam conditions approximate the assumptions involved in the analysis, i.e. small channel slope and frictional resistance and a steep jam toe. They also point out that the simple dam break analysis established a lower bound for flow depths and an upper bound for velocities.

2.5 Ferrick (1983,1984)

Ferrick (1983) re-analysed existing data on unsteady flow beneath an ice cover. He first suggests a definition of wave types based on the measured wave celerity. Diffusion waves occur in free-flowing ice-free rivers and propagate at a speed that is only slightly greater than the flow velocity. Dynamic waves propagate significantly faster than diffusion waves ($c = v + \sqrt{gy}$). Finally, pressure waves occur in closed conduit flow and propagate even faster, at a speed influenced by the rigidity of the conduit. Pressure waves can occur in ice-covered rivers if the buoyant response of the cover is not rapid enough to accomodate changing flow conditions. From his analysis of a case study, Ferrick (1983) observes that in the presence of a fragmented (jammed) stationary floating ice cover, the waves propagated as dynamic waves that may have been affected by overpressure. He also suggested that the presence of a floating ice cover transforms diffusion waves to dynamic waves and proposed that the ice may produce upstream wave reflection and wave movement, thereby altering the wave behaviour.

In a more recent paper, Ferrick (1984) studied river waves in laboratory experiments and re-analysed the case study described by Doyle and Andres (1979) to determine the effects of the ice cover upon these waves and to identify the physical processes that produce these effects. He identified a group of dimensionless parameters of the St-Venant equations that quantify the relative importance of

the effects of friction, inertia and pressure gradient upon river waves. For waves in ice-covered rivers, he proposed the use of a friction scaling parameter F, which represents the friction/inertia balance:

$$F = (2V_1^2/C_*^2 C_m^2)\ (k\Delta x/y_1) \qquad (1)$$

where V_1 and y_1 are the mean velocity and depth in the river reach during passage of the wave, c_m is the measured wave velocity, C_* is the mean dimensionless Chezy conveyance coefficient, Δx is half the wavelength or half the propagation distance of the wave, whichever is smaller, and $k = 1$ for open water and 2 for ice-covered conditions. The friction parameter provides a mean to determine wave types. According to Ferrick, laboratory experiments indicate that $F >> 10$ is characteristic of bulk waves dominated by friction and that important dynamic wave effects occur at $F < 10$. These laboratory experiments also indicates that the addition of an ice cover increased wave celerity and slowed wave recession relative to an identical sequence of open water rapidly varying flow waves. The evaluation of the friction parameter indicated dynamic wave behaviour in all laboratory tests. In the Athabasca River case study, the parameter revealed that the documented wave was dominated by friction, which corresponds to a bulk wave. Ferrick (1984) finally notes that although the governing equations for the bulk waves can be obtained as a simplification of the dynamic wave equations, models based upon the dynamic wave

equation frequently do not provide accurate simulation of bulk waves.

3. Case study: release of Fort Norman jam.

The breakup observations carried out in 1983 on the Mackenzie River provided the opportunity to partially document the release of an ice jam and the behaviour of the wave thereby created. On May 22, at approximately 22:30, an important jam formed in the Fort Norman area. The accumulation was keyed at km 830 and extended upstream for about 70 km with its pans-'mush' ice interface at km 816 (see Figure 14). At about 11:15 on May 23, the jam released dynamically. At this time, the ice sheet downstream was still sound. At 13:20, the surge created by the ice jam release produced the first noticeable ice movement at the Off-Site Dock, about 4 km upstream of Norman Wells. Major ice movement at the Government Dock in Norman Wells (km 904) occurred at 15:07. Ice movement ceased at about 15:40. The ice sheet in front of Norman Wells moved about 500 m and was left fractured into large floes.

The conditions prevailing before the jam release in Fort Norman can be reconstructed with the HEC-2 model. A water level of 55.62 m was measured at Fort Norman at 12:13, just at the mouth of the Bear River. This is 38 minutes after the actual jam failure. Considering the very dynamic nature of the event, it is thought that a difference in water elevation of at least 0.4 m (it could be more) could be expected. Therefore, it can be assumed that the water

level at Fort Norman before the jam release was approximately 56.0 m. At this time, the water level at Norman Wells was 44.15 m. Using an average ice thickness of 1.7 m for the reach between Fort Norman and Norman Wells, a Manning's n of 0.021 for the ice and of .024 for the bed and a discharge of 12 000 m^3/s, the water level profile was simulated with HEC-2. The results are shown in Figure G-1. Also shown on the figure is the water level induced by the jam then in place at Fort Norman. The difference in elevation is about 4.7 m. From the plot of the water level variation at Norman Wells, the height of the surge that arrived at this location was approximately 3.0 m high.

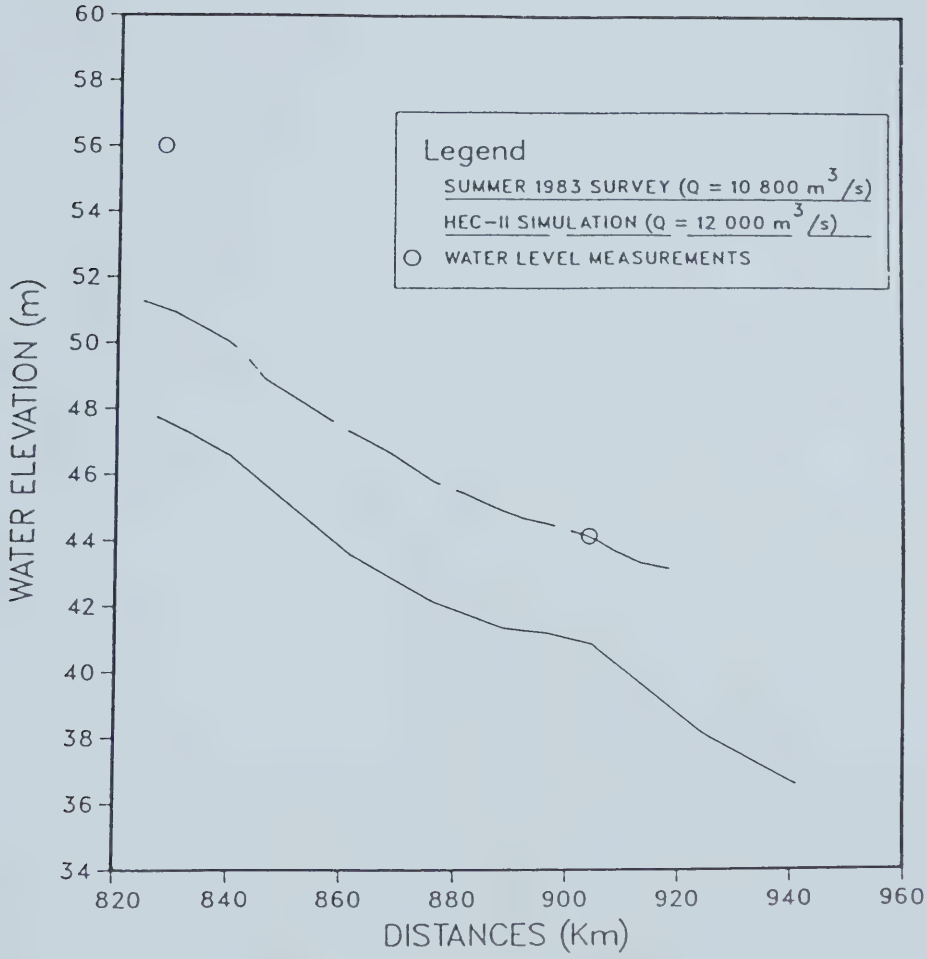

Figure G-1. Simulation of ice conditions before the ice jam release at Fort Norman.

University of Alberta Library
0 1620 0567 9616

B34325